Oral presentations

CH-1

Alveolar growth abnormalities: not just BPD Zeyad Metwalli, Robert Guillerman, Claire Langston Texas Children's Hospital, Houston (United States)

Purpose: Alveolar growth abnormalities are characterized by lobular simplification with enlarged alveoli with deficient septation, and are most commonly observed in premature infants with bronchopulmonary dysplasia (BPD). In infants and children without BPD, radiologists and pathologists can misdiagnose alveolar growth abnormalities as emphysema. To promote appropriate recognition, we present the imaging findings of the largest known series of alveolar growth abnormalities in infants and children without a history of BPD.

Materials and methods: All patients with alveolar growth abnormalities over a 9-year period (2000-2009) at a tertiary children's hospital were identified from a pathology database. The chest CT exams and clinical charts were retrospectively reviewed. Preterm patients with BPD were excluded from analysis.

Results: Alveolar growth abnormalities were diagnosed in 12 near- or full-term patients (age 6 days-4 years) by lung biopsy or following lung transplant. Associated abnormalities included trisomy 21 in 2 (17%), pulmonary interstitial glycogenosis in 2 (17%) and filamin A gene mutations in 2 (17%). All but one patient (92%) had structural cardiac abnormalities. CT findings included lobular architectural distortion in 7 (58%), intralobular hyperlucency in 6 (50%), ground glass opacities in 6 (50%), and coarse perilobular interstitial thickening in 4 (33%). Additional findings of multilobar hyperinflation were noted in 2 patients with filamin A gene mutations and subpleural cysts in 2 patients with trisomy 21. Pulmonary hypertension was present in 10 patients (83%), but not always associated with pulmonary artery enlargement on CT. Three patients were lost to follow-up, and 7 of the remaining 9 developed refractory respiratory insufficiency (2 requiring lung transplantation). Conclusion: Alveolar growth abnormalities can occur in near- and full-term patients as a primary idiopathic disorder or in association with congenital heart disease and certain genetic conditions. Appropriate recognition is important due to the high morbidity including pulmonary hypertension and refractory respiratory insufficiency that may require lung transplantation.

CH-2

Evaluation of infant respiratory distress syndrome and surfactant therapy effects using lung ultrasonography

Jovan Lovrenski¹, Erich Sorantin², Sanja Stojanović³ ¹Institute for Children and Youth Health Care of Vojvodina, Novi Sad (Serbia), Medical University Graz (Austria), ³Institute of Radiology, Clinical Center of Vojvodina, Novi Sad, (Serbia)

Purpose: To present the accuracy of a new, ultrasound-based grading system for infant respiratory distress syndrome (IRDS) and its applicability in evaluation of the surfactant replacement therapy effects.

Materials and methods: A prospective study included 120 preterm infants with clinical signs of IRDS. Ninety-nine chest X-rays (CXR) and lung US findings were compared. CXR findings served as control, and US findings of the same children the study group. CXR included 3 subsamples of I, II and III grades of RDS (CXR-1, CXR-2, CXR-3). For statistical reasons I and II grade comprised one subsample (CXR-1,2). US findings at each examined lung area were graded from 1 (normal) to 6 (subpleural consolidation). Grades 2 to 5 represented different amounts of B lines. MANOVA and discriminant analysis defined the difference between the groups, their characteristics and homogeneity. The changes in US findings before and within 24 h after surfactant administration were also evaluated.

Results: The high homogeneity of US findings in CXR-1,2 and CXR-3 group (93.33% and 100% respectively) enabled defining of the border equation. The conversion of of the US grade from each lung area into an equation makes prediction of IRDS grade possible for any US finding. Thus, if the result of the equation is less than zero, it can be expected, with 100% confidence, that a certain US finding belongs to the IRDS of III grade. In IRDS grade III, a sum of US findings greater than 34 indicated the possibility of prediction with 91.67% certainty, while a sum lower than 22 excluded grade III. During the first hour after surfactant administration, the US findings at individual lung areas improved up to three, and within the first 24 h up to four grades in relation to initial examination before surfactant therapy.

Conclusion: Lung US allows for the differentiation between the lower (I and II) and higher (III) grades of IRDS. It enables an early detection of surfactant therapy effects in the lungs. Lung US has the potential to greatly reduce the number of CXR in preterm infants.

CH-3

Role of transabdominal sonography of lung bases (TASL) in the diagnosis and follow-up of hvaline membrane disease (HMD) in premature neonates with respiratory distress soon after birth.

Akshay Saxena, Chirag Ahuja, Kushaljit Sodhi, Praveen Kumar, Niranian Khandelwal

Post Graduate Institute of Medical Education and Research. Chandigarh, (India)

Purpose: To evaluate the role of transabdominal sonography of lung bases (TASL) in diagnosis and follow up of hyaline membrane disease (HMD) in premature neonates with respiratory distress soon after birth

Materials and methods: Eighty eight patients with gestational age <32 weeks having respiratory distress within 6 h of birth were enrolled. The diagnosis of HMD was made if the patient had either positive shake test or suggestive chest radiograph (showing either poor expansion with air bronchogram or reticulogranular pattern or ground glass opacity). TASL was done in all eighty-eight patients using broadband curvilinear probe within first 24 h of life and biweekly subsequently. Sonogram was interpreted as normal (if there were no retrodiaphragmatic hyperechogenicity with normal dia-



phragm echo complex); as HMD pattern (consisting of diffuse retrodiaphragmatic hyperechogenicity replacing completely the normal diaphragm complex) or broncho-pulmonary dysplasia (BPD) pattern (corresponding to the same hyperechogenicity as that of the HMD pattern but less diffuse and less homogeneous). Biweekly follow up was done for patients showing HMD pattern to normalization, BPD, death or discharge from the hospital.

Results: Diagnosis of HMD was made in 38 patients. TASL had 85.7% sensitivity, 75% specificity, 88.88% positive predictive value and 69.2% negative predictive value for the diagnosis of HMD. During follow up TASL, 26/27(96.2%) of patients who showed HMD pattern initially and did not develop bronchopulmonary dysplasia (BPD) showed complete resolution on the 14th day. All patients who showed BPD pattern on the 17th day developed clinical BPD at day 28 of life. Day 14 appears to be the earliest day at which abnormal sonographic pattern (HMD or BPD pattern) was predictive of clinical BPD on day 28

Conclusion: TASL is a useful adjunct to chest X ray in the diagnosis of HMD. It can also be used in the follow up of HMD to (i) predict BPD early and (ii) decrease the cumulative radiation dose administered to neonates.

CH-4

Prediction of bronchopulmonary dysplasia using lung ultrasonography within the first 24 h of life

Jovan Lovrenski¹, Erich Sorantin², Sanja Stojanović³
¹Institute for Children and Youth Health Care of Vojvodina, Novi Sad (Serbia), Medical University Graz (Austria), ³Institute of Radiology, Clinical Center of Vojvodina, Novi Sad (Serbia)

Purpose: To present a new grading system for lung ultrasonography (US) findings and its application in early prediction of bronchopulmonary dysplasia (BPD).

Materials and methods: Lung US was performed within the first 24 h of life in 120 preterm infants with clinical signs of respiratory distress syndrome (RDS). Thirty of them developed BPD, all below 31 gestational week, weighing less than 1,500 g. The control group was formed based on these criteria. US findings at each examined lung area were graded from 1 (normal) to 6 (subpleural consolidation). Grades 2–5 represented different amounts of B lines. Prediction possibilities of BPD development and its mild and severe forms (type 1 and 2), both clinical and radiographic, were evaluated. MANOVA and discriminant analysis defined the difference between the groups, their characteristics and homogeneity.

Results: Statistically significant difference was verified between US findings of the study and the control group at each lung area. Homogeneity of the study and the control group was 83.33% and 94.12% respectively. Groups of BPD clinical types 1 and 2 had a homogeneity of 91.7% and 88.9%, while for radiographic types 1 and 2 homogeneity was 93.75% and 92.86% respectively. The high homogeneity enabled defining of border equations for the each data set. The implementation of the US grade from each examined lung area into equation makes prediction of BPD development, as well as its clinical and radiographic type, possible for any preterm infant with US finding within the first 24 h of life. Thus, if the result of the border equation for the first data set is less than zero, the confidence that the patient will not develop BPD is 94.12%. Pleural thickness also showed statistically significant difference between the study (confidence interval (CI) 1.74-2.02 mm) and the control (CI 1.40-1.63 mm)

Conclusion: Lung ultrasonography findings might enable an early prediction of BPD. Their association with clinical parameters should be considered in studies to come.

CH-5

Volumetric inspiratory/expiratory chest computed tomography (CT) findings in bronchopulmonary dysplasia (BPD)

Frederick Long¹, Yuchung Yan², Robert Castile¹
¹Nationwide Children's Hospital, Columbus (United States), ²Beijing Childrens Hospital, Beijing (China)

Purpose: to describe volumetric inspiratory/expiratory high resolution CT (HRCT) findings in infants with moderate to severe new BPD using a comprehensive scoring system and examine associations with lung function and clinical severity.

Materials and methods: 55 infants with clinically refractory BPD (age 45±34 wks, birth weights 775±256 g) underwent volumetric controlled ventilation CT and infant pulmonary function tests (PFTs). CT (GE lightspeed VCT at 80–100 kVp, 15 mAs, 1.25 mm, Edose 2–3 mSv) was performed using controlled ventilation at 25 and 0 cm H20 pressure. CT was scored by lobe by two "blinded" radiologists using a 0–3 Likert scale for: triangular subpleural (TO) and linear (LO) opacities, architectural distortion (AD), atelectasis (ATX), air trapping (AT), bulla (B), emphysema (E), ground glass (G), bronchiectasis (BE) and bronchial wall thickening (BT). CT findings were correlated with FEV0.5, FEF25-75 and clinical severity score (ventilator mean airway pressure x FiO2 at 36 wks post conceptual age).

Results: Mean CT scores (\pm SD) were: TO-10.1 \pm 4.3, LO-8.5 \pm 4.7, AD-6.5 \pm 4.0, ATX-6.1 \pm 2.9, AT-5.0 \pm 3.9, B-2.1 \pm 3.6, E-0.3 \pm 0.7, BT-0.3 \pm 0.7, BE-0.2 \pm 0.9, and G-0.2 \pm 09. FEV0.5, FEF25-75 correlated significantly (p<.05) with AT (r= -0.51, -0.64), AD (r= -0.45, -0.63), and ATX (r= -0.27, -0.34), respectively. Severity score correlated significantly with AD (r=0.55), TO (r=0.37), LO (r=0.36), and AT (r=0.31). CT findings were equally distributed throughout the lungs.

Conclusion: Interstitial/fibrotic changes (TO, LO, AD), ATX and AT were the most frequent CT findings in patients with difficult to treat BPD. All the frequent CT score abnormalities correlated significantly with lung function and/or clinical severity.

CH-6

Usefulness of Doppler US in the diagnosis of pulmonary pathology in children

Gloria del Pozo Garcia, Carmen Gallego, Julio Arevalo, David Coca, Miguel Rasero, Gabino Gonzalez de Orbe Hospital Universitario, Madrid (Spain)

Purpose: To determine the value of spectral and color Doppler US to differentiate lung lesions in children.

Materials and methods: US findings of 37 lung lesions were prospectively analyzed. Localization, size, echotexture, visualization of air bronchograms and cystic changes, presence of color Doppler flow (low, moderate, increased) and its spectral doppler pattern (quadriphasic high RI, low RI) was assessed. US findings were compared to the initial radiographs taken at the time of diagnosis and at follow up, and with available CTs and clinical evolution.

Results: Ultrasound showed 14 cases with sparce air bronchograms and decreased vascularity corresponding to pneumonias (11 with homogeneous echotexture, 3 with heterogeneous parenchyma, having a complicated course); 17 homogeneous consolidations with air bronchogram and moderate or increased vascularity corresponding to resolving pneumonias; 5 homogeneous consolidations with increased vascularity and crowding of the vessels corresponding to atelectasis; and 1 consolidationn with cystic changes changes and a lower IR in spectral Doppler US corresponding to a cystic adenomatous malformation (CCAM). A high IR spectral pattern was detected in all lesions with the exception of the CCAM.



Conclusion: Color Doppler US may be used to differentiate atelectasis from pneumonia (relative number of vessels) and to evaluate for pneumonia resolution (homogeneous, increased air bronchograms and highly vascularized). Spectral Doppler US was useful in differentiating inflammatory from other lung pathologies. Spectral Doppler US however was not useful to differentiate atelectasis from pneumonia.

CH-7

Preoperative multi-detector computed tomograpy (MDCT) evaluation of congenital lung anomalies in children: comparison of axial, multiplanar, and 3D images

Edward Lee¹, Donald Tracy¹, Soran Mahmood¹, Christopher Weldon¹, David Zurakowski¹, Phillip Boiselle²

¹Children's Hospital Boston and Harvard Medical School, Boston, ²Beth Israel Deaconess Medical Center and Harvard Medical School, Boston, (United States)

Purpose: To compare the preoperative diagnostic accuracy of axial, multiplanar and 3D MDCT images for evaluating congenital lung anomalies in pediatric patients, and to assess the potential added diagnostic value of multiplanar and 3D MDCT images in this setting.

Materials and methods: We used our hospital information system to identify all consecutive pediatric patients who had both a preoperative MDCT angiography examination and a pathologically proven congenital lung anomaly between June 2005 and February 2010. Each MDCT examination was reviewed independently by two experienced pediatric radiologists for the types, location, associated mass effect, and associated anomalous vessels of congenital lung anomalies on axial, multiplanar, and 3D MDCT images. Final diagnosis was determined by surgical and pathological findings. Diagnostic accuracy, confidence level of diagnosis (scale 1–3, 1 = highest and 3 = lowest), perceived added diagnostic value of multiplanar or 3D MDCT images (scale 1–5, 5 = highest and 1 = lowest), and interobserver kappa agreement were evaluated.

Results: The final study cohort consisted of 46 children (28 males and 18 females; mean age 5.6 months±6 months). Histopathological diagnoses included congenital pulmonary airway malformation (n=19; 41%), sequestration (n=15; 33%), congenital lobar emphysema (n=7; 15%); and bronchogenic cyst (n=5; 11%). Both independent reviewers correctly diagnosed types, location, associated mass effect, and associated anomalous arteries of all congenital lung anomalies with high accuracy (100%) and confidence level (mean confidence level <1.2) on each type of image display. However, for the detection of anomalous veins, multiplanar and 3D images were associated with greater diagnostic accuracy and higher confidence level than axial images. Specifically, diagnostic accuracy for detection of anomalous veins (n= 15; 33%) was 60% (9 of 15 cases) for axial MDCT images, 80% (12 of 15 cases) for multiplanar MDCT images, and 100% (15 of 15 cases) for 3D MDCT images (Friedman test, p=0.011). Confidence levels for detection of anomalous veins was significantly higher with 3D MDCT images (mean level =1.0) and multiplanar MDCT images (mean level = 1.5) compared to axial MDCT images (mean level = 2.6) (Friedman test, p < 0.01). Both multiplanar and 3D MDCT images were found to provide added diagnostic value for accurately detecting anomalous veins associated with congenial lung anomalies (paired t-tests, p < .0012).

Conclusion: Axial MDCT images allow for an accurate diagnosis of types, location, associated mass effect, and anomalous arteries of congenital lung anomalies, but supplemental multiplanar and 3D MDCT images add diagnostic value for the evaluation of congenital lung lesions associated with anomalous veins.

CH-8

Diagnosis of tracheobronchomalacia — At last a reliable, noninvasive four-dimensional technique

Zhi Yie Judith Tan¹, Michael Ditchfield², Ramsden Andrew², Marcus Crossett¹

¹Southern Health, Clayton, ²Monash Childrens'Hospital (Australia)

Background: Tracheobronchomalacia in children, especially neonates and infants, is an important cause of respiratory difficulties but is non-specific in its clinical presentation. It is commonly associated with prolonged intubation and congenital heart disease. Previous means of assessing the airway include bronchography, bronchoscopy and more recently CT. These all have issues with reliability, need for intubation and contrast administration. Single-level conventional multi-slice CT has the issue of respiratory movement out of the plane of interest.

Purpose: To report our experience with a new technique of assessment of tracheobronchomalacia in infants using a 320-detector row CT with 16 cm of volumetric coverage.

Materials and methods: Six infants (age 2 weeks to 8 months, 3/6 male) at a tertiary paediatric centre with complex respiratory disease whose airways were assessed for tracheobronchomalacia using a volumetric 320-detector row CT. The entire lung volume (three-dimensions) was examined over one respiratory cycle (<1 s). In one patient intravenous contrast was administered for assessment of possible vascular airway compression. The patients were free breathing at atmospheric pressure, one was intubated. The studies were assessed by a paediatric radiologist and senior radiology registrar for: i) visualisation of the trachea, major and tertiary bronchi for fixed and dynamic airway narrowing; ii) assessment of the lung parenchyma; iii) assessment of vascular structures; iv) radiation dose.

Results: In all cases the main airway and lung parenchyma and vascular structures (double aortic arch, pulmonary arterial sling) were well demonstrated. The pathologies identified were: diffuse trache-obronchomalacia in association with severe bronchopulmonary dysplasia (2 cases), focal tracheomalacia in isolation (1 case) and associated with vascular anomalies (2 cases). One study was normal, excluding tracheobronchomalacia as a cause of the respiratory difficulties. The mean radiation dose was 1.89 mSv (range 0.58–2.98 mSv).

Conclusion: Volumetric 320-detector row CT enables threedimensional imaging over an entire respiratory cycle without intubation and at low radiation dose compared to the other modalities previously used in its assessment. It provides comprehensive assessment for tracheobronchomalacia and its associations.

CH-9

Evaluation of the baseline pre-HAART chest x-ray in pediatric patients

Nasreen Mahomed, Mbaliso MBAKAZA University of Witwatersrand, Johannesburg (South Africa)

Background: Approximately 60,000 pediatric patients are infected with HIV in South Africa annually. Subsequent to having the world's largest HIV epidemic, South Africa also has the largest antiretroviral therapy programme in the world.

Purpose: To evaluate the baseline pre-haart chest, X-ray, HAART subjectively and to subcategorize the radiographic pattern according to CD4 class

Materials and methods: A total of 57 paediatric patients eligible to start antiretroviral therapy were included. Parameters evaluated on baseline pre-haart chest, X-ray, HAART included hilar and Mediastinal lymphadenopathy, Air space disease, Parenchymal

(interstitual) disease, Bronchiectasis, Cavities, Lobar collapses, Pleural reactions and cardiomegaly

Results: 50/57 (87.7%) had an abnormal chest X-ray (CXR); 48/57 (84%) had hilar nodes; 7/57 (12.3%) had mediastinal nodes, Interstitial parenchymal disease; 6/57 (10.5%) had miliary infiltrate (<2 mm), 16/57 (28%) had a reticular nodular infiltrate (nodular >2 mm); 12/57 (21%) had airspace consolidation, chronic lung disease assessed by bronchiectasis and cavities; 3/57 (5,3%) had bronchiectasis; 7/57 (12.3%) had cavities; 1/57 (1.8%) had lobar collapses; 3/57 (5.3%) had pleural reactions; 2/57 (3.5%) had cardiomegaly; 22/24 (91.7%) of patients with CD4 less than 15% had abnormal CXR; 18/20 (90%) of patients with CD4 between 15 and 24% had abnormal CXR; 10/13 (76.9%) of patients with CD4 greater than 25% had abnormal CXR.

Conclusion: This study demonstrates that radiological abnormalities on pre-HAART chest X-ray are very common with 87.7% of patients having an abnormal chest X-ray. Hilar nodes were the commonest finding, followed by a reticular nodular infiltrate. Despite the high prevalence of hilar nodes, lobar collapses was only demonstrated in 1.8% of patients. Features of chronic lung disease were low. Pleural and pericardial effusions were uncommon. Sub-categorization of patients according to CD4 counts demonstrated that patients with the lowest CD4 counts had the highest incidence of abnormal chest X-Ray with hilar nodes and reticular nodular infiltrate having the highest prevalence.

CH-10

Serial evaluation of children following lung transplantation for bronchiolitis obliterans: comparison of high resolution computed tomography with detailed lung function assessment including lung clearance index.

Jim Carmichael, Alister Calder, Helen Spencer Great Ormond Street Hospital, London (United Kingdom)

Purpose: 1) To evaluate longitudinal changes in lung structure and function in children following lung transplantation using both inspiratory/expiratory computed tomography (CT) and detailed lung function indices including lung clearance index by multiple breath washouts (LCI-MBW), a sensitive global measure of lung function. 2) To determine whether CT or LCI-MBW are earlier indicators of development of bronchiolitis obliterans syndrome (BOS) than spirometry.

Materials and methods: We evaluated all CT studies in a cohort of 42 children following lung transplantation. We included all CT studies performed more than one year following lung transplantation. We excluded CT studies performed for acute indications, and those studies performed without expiratory sections. The CT scans were scored by two radiologists, blinded to the clinical details and lung function data, using an established scoring system. We evaluated bronchial wall thickening, bronchial dilatation, mosaic attenuation and air trapping in standardised areas. Kappa statistics were used to assess interobserver agreement. CT findings will be compared with findings from serial lung function evaluations including LCI. Results: 147 scans in 42 children met inclusion criteria. In an initial assessment of 37 studies in 10 children by the two observers, CT scores demonstrated good intra-observer correlation: (k=0.7) for bronchial wall thickening/dilatation/mosaic attenuation. Good correlation was also found between observers for air trapping (k=0.65). Lung function data will be made available for comparison once CT scoring is complete to maintain blinding.

Conclusion: This study will show the evolution over time of lung structural and functional changes in children following lung transplantation. We will be able to demonstrate the relative merits of CT versus LCI, a more sensitive test of lung function than spirometry, in the early identification of children with BOS.

CH-11

Limited, fast-MRI as an alternative to CT for preoperative evaluation of pectus excavatum

Krista Birkemeier, Daniel Podberesky

Cincinnati Children's Hospital Medical Center, Cincinnati (United States)

Purpose: The purpose of this work is to propose magnetic resonance imaging (MRI) as a feasible, rapid, and ionizing radiation free alternative to CT for the preoperative evaluation of pectus excavatum.

Materials and methods: Forty-seven patients, ranging in age from 8 to 36 (mean 14.8) years, referred for preoperative imaging of pectus excavatum underwent limited, axial balanced steady-state free precession magnetic resonance imaging (MRI) of the chest, with a limited patient charge, at full inspiration (I), end expiration (E), and stop quiet breathing (QB). This provided a quick and lower cost protocol. A pediatric radiology fellow and staff independently performed a blinded retrospective review with calculation of Haller index (HI) and asymmetry index (AI) at the level of greatest anterior-posterior chest narrowing, and measurement of the greatest degree of sternal tilt (ST) at each phase of respiration. The intraclass correlation coefficient (ICC) was used to determine inter-rater reliability. Qualitative measure of right heart compression (RH C) at I and E was documented and analyzed with a weighted Cohen's Kappa coefficient. Additionally, HI's of 3 patients that underwent MR and CT within the same year are reported for comparison. Exam time was also determined.

Results: ICC reliability was almost perfect (0.81–1) for HI_I (0.98), HI_E (0.93), HI_QB (0.89), AI_I (0.88), AI_E (0.89), and ST_E (0.82). ICC reliability indicated substantial agreement (0.61–0.8) for AI_QB (0.73), ST_I (0.75), and ST_QB (0.79). RH_C_I (kappa 0.4681, p=0.0410) and RH_C_E (kappa 0.4156, p=0.0559) showed moderate (0.41–0.60) inter-reader agreement with a wide confidence interval (0.0742, 0.8620). CT/MR HI in three patients with both studies measured 3.1/3.2, 4.6/4.9, and 2.4/2.4. Mean exam time was 10 min. Conclusion: Limited MRI is a reliable and cost-effective alternative to CT for preoperative assessment of pectus excavatum. MRI is fast, free of ionizing radiation, and there is excellent inter-reader reliability for measurements of chest wall deformity, particularly for the HI.

CH-12

Comparison of radiation dose, image quality, and scan time in pediatric high-resolution chest CT using volumetric 320-detector row, helical 64-detector row, and non-contiguous axial acquisitions

Daniel Podberesky¹, Alan Brody¹, Terry Yoshizumi², Erin Angel³, Greta Toncheva³, John Egelhoff¹, Colin Anderson-Evans², Chris Alsip¹, David Dow⁴, Shelia Salisbury¹, Donald Frush²
¹Cincinnati Children's Hospital Medical Center, Cincinnati, ²Duke Medical Center, Durham, ³Toshiba America Medical Systems, ⁴University of Cincinnati College of Medicine (United States)

Purpose: To determine organ radiation dose estimates, scan time, and image noise for clinical high resolution computed tomography (HRCT) protocols on a 320-detector row scanner in volume and helical acquisition modes, and in non-contiguous axial mode on a 64-detector row scanner using a pediatric anthropomorphic phantom.

Materials and methods: Lung, heart, thymus, esophagus, breast, and spine organ doses were measured using twenty metal oxide semiconductor field effect transistor (MOSFET) dosimeters (Best Medical Canada Lmt.). Dose and scan time were determined for volumetrically and helically acquired HRCT protocols in a 5-year old



anthropomorphic phantom (CIRS Tissue Simulation Technology) on a 320-detector scanner (Aquilion One, Toshiba Medical Systems), and in the same phantom in non-contiguous axial mode on a 64-detector scanner (Aquilion 64, Toshiba Medical Systems), using similar clinical pediatric acquisition parameters. Multiple runs for each protocol were averaged to estimate maximum dose to each organ. Image noise was assessed as the standard deviation of Hounsfield units using multiple representative regions of interest in identical anatomical locations within the lungs, mediastinal soft tissue and spine on each protocol.

Results: There was a statistically significant decrease in the mean maximum organ dose between the volume and non-contiguous axial scans respectively for the following organs: lung with means of 0.18 vs. 0.41 cGy (p<.0001); thymus with means of 0.23 vs. 0.42 cGy (p=0.0109); breast with means of 0.18 vs. 0.36 cGy (p=0.0242); and esophagus with means of 0.20 vs. 0.34 cGy (p=0.0196). There was a statistically significant decrease in the mean maximum organ dose between the helical and non-contiguous axial scans respectively for the following organs: lung with means of 0.23 vs. 0.41 cGy (p < .0001); heart with means of 0.21 vs. 0.42 cGy (p=0.0396); and thymus with means of 0.24 vs. 0.42 cGy (p=0.0241). There was a statistically significant improvement in the median image noise between volume, helical, and non-contiguous axial scans respectively for lung (29.05 vs. 79.30 vs. 70.65, p=0.0005) and for soft tissue (38.80 vs. 111.25 vs. 89.9, p=0.0313). Scan times for the volume, helical, and noncontiguous axial acquisitions were 0.35, 3.9, and 9 s, respectively.

Conclusion: Volumetric HRCT on a 320-detector row CT scanner resulted in a decrease in chest organ doses of 2–30% in comparison to similar helically acquired scans, and a decrease in chest organ doses of 42–56% in comparison to non-contiguous axial scans using standard pediatric acquisition parameters. These organ dose savings were obtained while significantly decreasing image noise in lung and soft tissue with volumetric scanning. The reduced scan time with volumetric studies can also potentially reduce the need for sedation and decrease motion artifact. In addition, the volumetric acquisition allows for true isotropic multiplanar and 3-dimensional reformations.

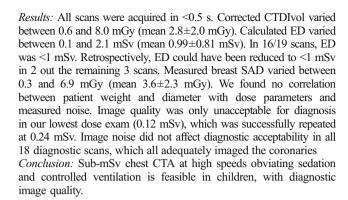
CH-13

Ultrafast sub-milliSievert Flash CTA of the chest

Sjirk Westra¹, Xinhua Li¹, Bob Liu¹, Mithya Barreto², Sarabjeet Singh¹, Mannudeep Kalra¹, Suhny Abbara¹, James Thrall¹ Massachusetts General Hospital, Boston, ²Siemens Healthcare Inc (United States)

Purpose: To demonstrate the feasibility of ultrafast high-pitch CTA of the chest with sub-milliSievert (mSv) dose, and to use estimates of effective dose and measurements of breast dose from these exams to optimize the balance between dose and image quality.

Materials and methods: On a dual source scanner (Siemens Definition Flash), we performed 19 CTAs of the chest in 17 children (1-18, median 10 year); 18/19 were done without sedation. Indications were coronary imaging in 8, congenital heart disease in 6, rule out pulmonary AVM in 2 and cardiac tumor in 1 patient. Scan parameters were kV=80 (<10 y) or 100 (>10 yr), pitch=3.0, 128×0.6 mm slice acquisition and 0.28 s gantry rotation time. Tube current was automatically modulated according to body habitus (CARE Dose4D). We recorded patient weight, diameter, effective mAs, CTDIvol, DLP and scan acquisition time. After correction of console CTDIvol and DLP (which are in reference to a 32 cm phantom) for pediatric body size (16 cm phantom), we calculated effective dose (ED) with ageappropriate conversion DLP-ED factors. In 9/19 scans we measured surface area dose (SAD) over the breasts with solid state dosimeters. We measured noise in HU in the descending aorta, normalized to 1.5 mm slice thickness. Two radiologists evaluated 4 aspects of image quality (including visualization of coronaries) on a 5 point scale



CH-14

Low-dose radiation CT angiograms are as accurate as standard chest CT in the diagnosis of congenital lung lesions *Monica Epelman*, Dustin Bermudez, Zhu Xiaowei, Kreiger Portia, Kenneth Liechty, Jeffrey Hellinger

Children's Hospital Of Philadelphia, Philadelphia (United States)

Purpose: Recent data have suggested that ionizing radiation from CT scans can increase the risk of malignancy. We hypothesize that low-dose CT angiography (CTA) is of equal or greater accuracy to standard CT and exposes the pediatric patient to significantly lower levels of radiation.

Materials and methods: This is a retrospective chart review of children who have undergone resection of a congenital lung lesion between July 2003 and December 2008 at our institution. Low-dose CTA has been employed since July 2006. Data for each patient were collected in accordance with our Institutional Review Board protocol. Results: A total of 119 children from the standard chest CT group and 114 from the low-dose CTA group were analyzed. Age and gender at the time of surgical resection were similar between the two groups and all differences revealed non-significant p-values. Similar frequencies were also noted for the various types of lesions (including cases of bronchial atresia, congenital pulmonary airway malformations, sequestrations, infantile lobar hyperinflation and hybrid lesions) between the two groups. The radiation dose was significantly lower for children who underwent low-dose CTA (7.9 mSv less per child, range of low dose CTA: 0.25–3.8 mSv, p < 0.01). The presence of an aortic feeder 'vessel, indicative of pulmonary sequestration, was not missed in the low-dose CTA group. Standard chest CT, however, was found to have missed 4 instances in which a feeder vessel from the thoracic or abdominal aorta was providing blood supply to the congenital lung lesion.

Conclusion: No significant demographic or clinical differences exist between our two study groups. Low-dose CTA can diagnose congenital lung lesions with significantly lower radiation exposure. The ability to detect systemic feeders with greater accuracy suggests that low-dose CTA should become the new standard of care in the evaluation of children with congenital lung lesions.

CH-R1

Mediastinal stacking and aorto-carinal syndrome in children with right lung volume loss—a cause of contralateral left main bronchus compression

Savvas Andronikou¹, Matthys J van Wyk¹, Pierre Goussard², Robert P Gie²

¹University of the Witwatersrand, Johannesburg ²University of Stellenbosch (South Africa)

Background: An abnormal relation between the superior mediastinal structures may cause compression of the left main bronchus from



mediastinal 'stacking'. A descending aorta in the midline may compress the carina and left main bronchus - aorta-carina compression syndrome. Patients with right-sided pneumonectomy and exaggerated compensatory response may lead to stretching and compression of other airways. TB causes compression predominantly of the bronchus intermedius with displacement of the mediastinum similar to right pneumonectomy. We propose that this is a cause of mediastinal stacking and compression of the left main bronchus which contributes to the severity of disease.

Purpose: To quantify the configuration of the mediastinal structures in children with right lung volume loss due to TB causing compression of the left main bronchus.

Materials and methods: Children with pulmonary TB and right lung volume loss on CT were included in this paper, as were 10 patients who had normal CT scans. CT scans were evaluated in the axial plane at the level of the: 1) Main pulmonary trunk and bifurcation to determine a) 'Anti-clockwise rotation of the aorta' b) 'Left Pulmonary artery rotation' c) 'Pulmonary outflow tract rotation' d) 'Right carinal angle' e) 'Left carina angle' f) 'Carinal angle' g) 'Carina Aorta distance' h) 'Aortic Lift' 2) Passage of the left main bronchus between the left main pulmonary artery and the aorta to measure: a) 'Aorta-right-pulmonary distance' b) 'Aorta-left-pulmonary distance' c) Left-interpulmonary distance'.

Results: Quantifications which reached statistical significant difference between the two groups included 'Left Pulmonary artery rotation' (p=0.05); 'Right carinal angle' (p=0.01); Aorta-left-pulmonary distance' (p=0.05); 'Aorta-right-pulmonary distance' (p=0.01).

Conclusion: A form of mediastinal stacking occurs in children with right lung volume loss due to TB that is successfully quantified with a variety of angles and measures. These can be used to predict impending worsening airway compromise in children already suffering from TB airway compression and advocate for surgical decompression.

CH-R2

Low dose dynamic pulmonary computed tomography in infants and small children

S Bruce Greenberg

Arkansas Children's Hospital, Little Rock (United States)

Purpose: Wide-detector computed tomography (CT) allows for simultaneous imaging of the entire airway and lungs in infants and small children. Multiple phases created by continuous scanning during respiration are viewed dynamically, allowing for more complete airway and pulmonary evaluation than static CT. My purpose was to evaluate if low dose techniques can be applied to dynamic airway and lung CT in infants and small children.

Materials and methods: The study included 15 infants and small children (mean age 8.1 months, SD 6.2 months) with persistent respiratory difficulty that underwent dynamic pulmonary CT (9 with intravenous contrast and 6 without contrast). Intubated patients had respirator rates set at 40 bpm. Continuous mode wide detector scans were performed at 350 msec gantry rotation for 1.4 s at 80 kVp. The formula: $mA = [(kg \ X \ 2.5) + 5] \div 0.35$ was used to determine mA for non-intravenous contrast patients. Some contrast enhanced studies for simultaneous vascular and airway evaluation used greater mA. Detectors used 0.5 mm collimation. The effective dose for each patient was calculated using the method of Thomas and Wang. T-tests were performed to compare patient ages and effective dose measurements.

Results: All studies were diagnostic, frequently providing critical information not available by other diagnostic tests. Dynamic evaluation of tracheo/bronchomalacia, bronchiectasis and air trapping were especially enhanced. No significant difference in

age between contrast (8.0 months, SD 7.5 months) and noncontrast (8.2 months, SD 5.6 months) groups was present (p= 0.95). The mean effective dose for a all patients was 1.8 mSV (SD 1.3 mSV). The contrast group mean effective dose was greater [2.2 mSV (SD 1.7 mSV)] than the non-contrast group 1.5 mSV (SD 0.9 mSV), but the difference was not significant (p=0.29). 11 of 15 examinations had effective doses less than 1.5 mSV (73%). *Conclusion:* Wide-detector dynamic CT is ideal for the evaluation of the airway and lungs in infants and small children with persistent respiratory distress. Effective doses are low, typically less than 2 mSV.

Disclosure: The author is on the Toshiba speaker bureau and is a Vital Images consultant

CH-R3

The pulmonary high-resolution CT findings of Langerhans cell histocytosis in infants

Xinyu Yuan, Surong Li, Li Che Capital Institute of Pediatrics, Beijing (China)

Purpose: To study the features of lung HRCT images of Langerhans cell histiocytosis (LCH) in infants, and the relationship of the CT manifestations with the age at onset and the course of the disease.

Materials and methods: HRCT data of 23 patients were reviewed retrospectively. All patients were divided into two groups (interstitial group, nodule-air cysts group) based on the findings of HRCT. The age at onset and course of disease were compared between the two groups.

Results: HRCT findings of 86.96% were found abnormalities. The HRCT patterns included interstitial lung disease, solitary or diffuse nodules and air cysts. The median course of the two groups (interstitial and nodular) was 3.0 (0.7–12.0) months and 6.0 (3.0–24.0) months, respectively. There was significant difference between two groups (P<0.05). Totally 15 patients were followed up with HRCT after chemotherapy, 12 patients returned to normal, 2 patients remained abnormalities, and one patient died. Conclusion: The HRCT findings of LCH in infants included interstitial changes, nodules, and (or) air cysts. Interstitial changes are the major abnormality in the early stage, and then evolve to nodular and (or) air cystic patterns with aggravation. The patients without diffused nodules and (or) air cysts in the lung would have good prognosis.

CV-1

Quantification of the distribution of the normal human fetal circulation using MRI

*Mike Seed*¹, Christopher Macgowan¹, Lars Grosse-Wortmann¹, Derek Wong², Grattan Michael³, Edgar Jaeggi¹, Susan Blaser¹, Shi-Joon Yoo¹

¹Hospital for Sick Children, Toronto, ²Children's Hospital of Eastern Ontario, ³Children's Hospital of Western Ontario, London (Canada)

Purpose: Metric optimised gating (MOG) is a new technique designed for fetal scanning where no ECG signal is available for conventional gating. It employs an image metric to find the average heart rate for each acquisition. The average heart rate is then used to retrospectively segment oversampled data to the correct cardiac phase. The objective of this study was to quantify the flow volume distribution of the normal human fetal circulation using phase contrast (PC) MRI with MOG after validating the technique using an in-vivo fetal vessel simulation.

Materials and methods: In a model devised to simulate fetal vessels, we compared neck vessel flow measurements by



conventional pulse gated PC MRI (gold standard) with MOG PC measurements. Volunteer heart rates were maintained at normal fetal heart rates using an MRI compatible bicycle. MOG PC flow measurements of the major vessels were then made in 20 human fetuses with normal hearts (gestational age range 33-38 weeks, mean 36 weeks).

Results: There was no significant difference between MOG and conventional gated flow volumes in the simulation. The following MRI PC mean flow volumes (ml/kg/min) and corresponding proportions of the combined ventricular output were obtained from the human fetal vessels (* indicates those values extrapolated from the other measurements); main pulmonary artery: 334 (62%), ascending aorta 190 (35%), ductus arteriosus 217 (41%), descending aorta 256 (48%), superior vena cava 134 (25%), umbilical vein 145 (27%), pulmonary blood flow* 112 (21%), foramen ovale* 93

Conclusion: MRI PC using MOG can be used to measure the distribution of the human fetal circulation near term. These values are similar to previous measurements made in fetal lambs and ultrasound estimates made in humans, although we have found more variation in the shunt volume across the patent foreman ovale (PFO), the pulmonary blood flow and ductus arteriosus flow, which might reflect individual variation in PFO anatomy and resultant changes in the PO2 of pulmonary arterial and ductus arteriosus blood.

CV-2

Preliminary experience with magnetic resonance imaging in evaluation of fetal congenital heart disease

Zhu Ming

Shanghai Children's Medical Center, Shanghai (China)

Purpose: The role of fetal magnetic resonance imaging (MRI) as an additional tool to ultrasound has grown exponentially; however, fetuses with congenital heart disease diagnosed by MRI have rarely been reported. We review 32 cases of fetal congenital heart diseases confirmed by postnatal operation and report our preliminary experience with fetal MRI in the evaluation of fetal congenital heart disease.

Materials and methods: Between 2005 and 2010, 32 fetuses with congenital heart disease were evaluated using ultrasound and MRI. All prenatal MRI was performed using a 1.5-T unit. Imaging sequences included a multiplanar fast imaging employing steadystate acquisition (FIESTA) sequence, non-gated cine FIESTA and a single-shot fast spin-echo (SS-FSE) sequence. Among these 32 cases, fetal cardiac MRI was performed at 17-34 weeks' gestation (mean 25 weeks). 90% MRI was performed between 20 and 30 weeks' gestation. The age of the pregnant women ranged from 22 to 38 years (mean 28 years).

Results: Fetal MR examination yielded the same diagnosis as postnatal surgery in 78% of patients (25 of 32). The diagnostic sensitivity of fetal echocardiographic examination by a fetal cardiac specialist was 84% (27/32). The 32 cases of congenital heart diseases included ventricular septal defect, atrioventricular canal defects, coarctation of the aorta, interruption of the aortic arch, tetralogy of Fallot, transposition of great arteries, double outlet right ventricle, hypoplastic left ventricle syndrome, tricuspid atresia and single ventricle. Most cases were complex congenital heart diseases. Conclusion: Unlike ultrasound imaging, MRI is unaffected by maternal and fetal conditions such as obesity, uterine myoma, twins and oligohydramnios, which particularly impair echocardiographic visualization of the fetal heart. MR imaging avoids exposure to ionizing radiation and has no adverse effects on the human fetus. We accordingly believe that fetal cardiac MRI can be an additional tool for fetal echocardiographic examination.

Anomalous aortic origin of coronary artery: pre- and post-operative cross-sectional imaging features in children

Andrada Popescu¹, Cynthia K. Rigsby², R. Andrew deFreitas³, Sunjay Kaushal³, Stanley T. Kim³

¹Northwestern Memorial Hospital, Chicago, ²Childrens Memorial Hospital, Chicago, ³Children's Memorial Hospital, Chicago (United States)

Purpose: To evaluate the pre- and post-operative imaging and clinical presentation of children with anomalous aortic origin of a coronary artery (AAOCA). AAOCA from the opposite sinus of Valsalva (SOV) is a rare congenital anomaly with the potential to cause myocardial ischemia and sudden death.

Materials and methods: Retrospective review of all coronary computed tomography angiography (CTA) and magnetic resonance angiography (MRA) studies performed from 2006 to 2010 identified 42 cases of AAOCA. For all identified cases, the imaging appearance of the coronary ostium was evaluated and categorized as round, oval or slit-like; proximal take off was characterized as normal or obliquely oriented; proximal intramural course length was measured; and narrowest and distal more normal caliber anomalous coronary diameter was measured. All evaluations were performed on a 3D workstation. Results: 32 patients had CTA, 10 had MRA and 3 had CTA and MRA, ages 0 to 19 years (mean age 10.4 years). 35 patients had a right AAOCA arising from the left SOV (RAAOCA) and 4 had a left AAOCA arising from the right SOV (LAAOCA). Single coronary artery was found in 3 patients, 2 arising from the right and 1 from the left SOV. Of the 35 patients with RAAOCA, 22 (62%) had symptoms of chest pain or syncope and 13 (38%) had no symptoms. 7 (100%) of patients with LAAOCA and single coronary arteries were symptomatic (chest pain). 29 (69%) had a slit-like ostium and oblique proximal course. Intramural coronary artery length ranged from 1.3 to 11 mm. 30% decrease in diameter of the proximal AAOCA in the intramural region was identified. 25 (59%) had surgical repair, 21 (84%) with RAAOCA and 4 (16%) with LAAOCA. Postoperative coronary CTA demonstrated no neo-ostial stenosis, normal origin obliquity and normal proximal caliber in all cases.

Conclusion: AAOCA can be identified in children. Imaging features that can be seen and described even in young children include slitlike orifice, oblique origin, and narrowed coronary diameter in the intramural region. Children with RAAOCA may be asymptomatic while those with LAAOCA are likely to be symptomatic.

CV-4

Assessment of pulmonary insufficiency in Fallot patients

by cine MRI—is cine imaging sufficient?

Erich Sorantin¹, Luis Riera², Robert Marterer², Franz Quehenberger³ ¹Division of Pediatric Radiology, Graz, ²Div. of Pediatric Radiology, Dep, of Radiology, Medical University Graz, ³Dep. of Medical Statistics, Information and Documentation, Medical University Graz (Austria)

Background: Pulmonary insufficiency (PI) is regarded one of the most important factors in the follow-up of Fallot patients. Cardiac MRI (cMRI) represents the method of choice for monitoring ventricular and valve function.

Purpose: Assessment of PI in Fallot patients using CINE and Velocity Encoding Imaging (VENC) based on cMRI.

Materials and methods: cMRI was performed as part of the routine follow-up in 79 Fallot patients (mean age 20±7.3 y, f:m=32:47). cMRI consisted of biventricular volumetry, CINE imaging of left



and right ventricular outflow tract and assessement of the pulmonary and aortic valve by VENC Imaging. For quantitative evaluation, Argus software installed by the manufacturers on the MRI machine was used. According to international guidelines, 4 grades of PI could be differentiated by visual inspection. Based on VENC imaging the regurgitation fraction (RF) of a valve could be calculated as the fraction of backward volume divided by forward volume. RF was correlated with the PI grades using the Spearman rank correlation coefficient and RF variation within the different visual PI grades was computed. For statistical evaluation, the open source softare R-Project (http://www.r-project.org/) was used.

Results: At visual inspection, PI was found in all but three patients with the following distribution: grade 1: 7(9%), grade 2: 15(19%), grade 3: 25(31%) and grade 4: 29(37%). Therefore 68% of patients suffered from high grade PI.On VENC imaging, pulmonary RF was found to be on average $36\pm17\%$, 50% of patients revealed a RF of more than 39.1%. A statistically significant correlation between visual PI grading and VENC based RF coud be found found (p<0.0001) but there was considerable RF variation and overlap between the visual PI groups: RF in grade 1: 9.6 ± 6.5 , grade 2: 30 ± 17 , grade 3: 40 ± 11 , grade 4: 46 ± 11 .

Conclusion: In our Fallot study group the majority of patients suffered from high grade PI. Due to the high variation of VENC-based RF within the visual PI grades, it seems advisable to use RF for monitoring pulmonary valve function. PI grading based on visual inspection of CINE images is therefore not favorable.

CV-5

Evaluation of the pulmonary valve function under physical stress using cMRI—could it be a prognostic value in the follow-up of TOF patients in the future?

Robert Marterer, Erich Sorantin, Bert Nagel Medical University Graz, (Austria)

Background: Cardiac magnetic resonance imaging (cMRI) is the gold standard in radiological imaging for follow-up examinations of Tetralogy of Fallot patients (TOF). The data acquisition is conducted during physical rest, so that the adaptability of the heart to everyday physical burdens is not recorded. At rest, a pulmonary insufficiency (PI) exists in the majority of TOF patients and PI should decrease normally during physical stress due to shortening of the diastolic phase.

Purpose: The aim of the pilot study was the assessment of pulmonary valve function during rest and physical activity.

Materials and methods: 9 TOF patients participated in this prospective pilot study. The MR stress test was an extension of the routine follow-up MRI examination and was confirmed by a local ethics committee. For the MR stress test with a rubber band, an own investigation protocol was created. Validation of the stress protocol was given by volunteers beforehand. cMRI protocol included at rest biventricular volumetry, CINE imaging of the left and right ventricular outflow tract and VENC imaging of the aortic and pulmonary valve. After stress, VENC imaging of the aortic and pulmonary valve was repeated. In addition all patients performed a spiroergometry on the same day and the lactate values at maximal physical stress served as reference values.

Results: cMRI at rest - pulmonary backward volume/BSA: 17.86 ± 13.79 ml/m2, pulmonary regurgitation fraction (RF): $34.47 \pm 23.60\%$; cMRI after exercise - heart rate increase: $22.74 \pm 20.05\%$ (p < 0.05), lactate load end: 48.9% of the maximum lactate load at spiroergometry, pulmonary backward volume/BSA: 12.92 ± 17.99 ml/m2, pulmonary RF: $21.04 \pm 23,02\%$; Spiroergometry: lactate load end: 8.24 ± 2.99 mmol/l.

Conclusion: Under physical stress there was a statistically significant decrease of the PI (p<0.05). As a trend it can be seen that the

improved PI under physical stress could be a prognostic value for the patients - meaning that an increase of PI during physical stress indicates a loss of normal adaptability and therefore worsening of pulmonary valve function.

CV-6

Systemic-pulmonic collateral flow differences observed in children with functional single ventricles from bidirectional Glenn to Fontan palliations

Adeka McIntosh, Marc Keller, Matthew Harris, Mark Fogel, Kevin Whitehead

Children's Hospital of Philadelphia, Philadelphia, (United States)

Purpose: To quantify and compare systemic-pulmonic collateral flow(SPCF) in children with single ventricle physiology following Bidirectional Glenn superior cavopulmonary connection (SCPC) and Fontan total cavopulmonary connection (TCPC)

Materials and methods: A retrospective review was conducted in 98 children with functional single ventricle palliated either by SCPC or TCPC who had cardiac MRI from 2008 to 2010. Flow in the pulmonary arteries, pulmonary veins, neoaorta, inferior venal cava (IVC), and superior venal cava (SVC) was measured by phase contrast MRI and also imaged by contrast-enhanced magnetic resonance angiography (CE-MRA).

Results: Sixty-two children had SCPC and 36 had TCPC. The average age in the SCPC group was 28 months(+/- 13) with an average body surface area (BSA) of 0.51 m2 (+/- 0.08). The average age in the TCPC group was 116 months (+/- 96) with an average BSA of 1.02 m2 (+/-0.48). The percentage of neoaortic output going to collaterals in the SCPC group was 34% (+/- 12%) vs 28% (+/-10%) in the TCPC group, p=0.015. The percentage contribution of SCPF to the overall pulmonary blood flow in the SCPC group was 50% (+/- 17%) vs 32% (+/- 13%) in the TCPC group, p<0.001. Indexed SPCF in the SCPC group was 1.6 L/min/m2 (+/- 0.83), while in the TCPC group it was 1.2 L/min/m2 (+/- 0.66), p=0.002.

Conclusion: Aside from the surgically created cavopulmonary connections, a substantial additional amount of SCPF occurs and can be both measured and imaged by MRI. Despite interval growth of children between operations, a decrease in indexed SCPF occurs between SCPC and TCPC which is not merely a lower percentage of SPCF owing to the new IVC flow contribution. BSA-indexed SPCF is significantly lower in children with single ventricle physiology following completion of Fontan palliation when compared to SPCF with Bidirectional Glenn physiology. The underlying reason(s) for this regression of SPCF following TCPC remains unknown.

CV-7

Evaluation of asplenia syndrome with bilateral tracheal bronchi using multidetector CT and MRI

Zhu Ming

Shanghai Children's Medical Center, Shanghai, China

Purpose: The purpose of this study was to report 10 cases of asplenia syndrome with bilateral tracheal bronchi and to evaluate the utility of mutidetector computed tomography (MDCT) and magnetic resonance imaging (MRI) for the determination of bilateral tracheal bronchi.

Materials and methods: From February 2005 to December 2010, 8566 consecutive children with congenital heart disease underwent MDCT or MRI examination in Shanghai Children's Medical Certer. Minimum intensity projection reconstruction was performed to evaluate tracheobronchial tree in every case using a GE AW4.2 workstation.



Results: Bilateral tracheal bronchi was found in 10 (0.1%) patients with congenital heart disease. The pathologic type of the congenital heart disease in this group was very distinct. All of the 10 patients had asplenia syndrome. All 10 cases of bilateral tracheal bronchi were confirmed by cardiac surgery or bronchoscopy. The diagnostic sensitivity of MDCT or MRI was 100% (10/10).

Conclusion: MDCT and MRI were reliable, non-invasive imaging techniques for the diagnosis of bilateral tracheal bronchi. The tracheal bronchus usually exits in the right lateral wall of the trachea. Patients with asplenia syndrome lack a spleen, and they typically have a bilateral right-sided tendency. Bronchi of both sides can be considered right-side bronchi in patients with asplenia syndrome. Thus, the bilateral tracheal bronchi can be considered bilateral right bronchi.

CV-8

Late gadolinium enhancement (LGE) MR in the assessment of restrictive right ventricular (RV) fibrosis after biventricular repair of pulmonary atresia and intact ventricular septum Wendy Lam, Xc Liang, Eddie Cheung, Sj Wong, Yf Cheung Oueen Mary Hospital (Hong Kong)

Purpose: Little is known of the prevalence of restrictive RV physiology, the extent of RV fibrosis, and the functional implications of RV diastolic dysfunction in long-term survivors of pulmonary atresia and intact ventricular septum (PAIVS) with a biventricular circulation. We tested if RV restrictive physiology is prevalent and related to RV fibrosis and exercise capacity, and if RV LGE score is a good clinical outcome indicator.

Materials and methods: Twenty-seven patients were recruited after biventricular repair of PAIVS. RV fibrosis was assessed by late gadolinium enhancement (LGE). Analysis of the RV and LV function, flow analysis of the pulmonary artery were obtained. LGE imaging was performed from 10 min after intravenous injection of gadolinium-DTPA 0.2 mmol/kg. To analyze the extent of RV LGE, a scoring system based on division of the right ventricle into 7 segments was adopted. For the left ventricle, a standard 17-segment model was used. Their RV function and score were compared with 27 healthy controls.

Results: Twenty-two (81%) patients demonstrated restrictive RV physiology. They had higher RV LGE scores, and greater percentage predicted maximum oxygen consumption. The RV LGE score correlated positively with exercise duration and percentage predicted maximum oxygen consumption. They had greater forward flow per cardiac cycle across the pulmonary trunk. The forward flow per cardiac cycle further correlated with percentage predicted VO2 max.

Conclusion: Restrictive RV physiology is prevalent in patients after biventricular repair of PAIVS, while the corresponding RV diastolic dysfunction is related to the magnitude of RV fibrosis and associated with better exercise capacity. RV LGE score was a good indicator of the patients' clinical outcome.

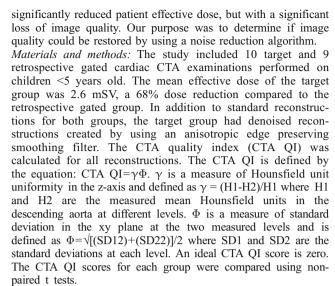
CV-9

Post-processing noise reduction restores image quality of low dose computed tomography angiography (CTA)

S Bruce Greenberg, Sadaf Bhutta

Arkansas Children's Hospital, Little Rock, (United States)

Purpose: The target CTA technique reduces effective dose in pediatric patients compared to retrospective gating by restricting imaging to a portion of the electrocardiogram (ECG) cycle. In a prior study, the target technique applied to children <5 years old



Results: The mean CTA QI scores for each group were: retrospective group 0.79 (SD 0.42), standard reconstruction target group 1.96 (SD 1.00) and denoised reconstruction target group 0.77 (SD 1.16). The standard reconstruction algorithm target group CTA QI was significantly worse than the retrograde study images (p=0.004) indicating image degradation. The denoised group CTA QI score was significantly better than the target group standard reconstruction (p=0.024) and not significantly different than the retrospective gated images (p=0.964).

Conclusion: The use of denoising software applied to target technique datasets allows for both significant radiation dose reduction compared to retrospective gating and restoration of image quality.

Disclosure: The author is at the Toshiba speaker bureau and is a Vital Images consultant.

CV-10

Quantitative assessment of blood flow with 4D phase-contrast MRI and autocalibrating parallel imaging compressed sensing Albert Hsiao¹, Michael Lustig², Marcus Alley¹, Mark Murphy², Shreyas Vasanawala³

¹Stanford University Stanford, ²University of California, Berkeley², ³Lucile Packard Childrens Hospital, Stanford (United States)

Purpose: Quantification of blood flow is an essential part of the congenital heart MRI exam, generally performed with 2D phase-contrast MRI (PC-MRI). 4D PC-MRI, because of its volumetric nature, may reduce operator-dependence, but is lengthy. Combined parallel imaging and compressed-sensing may reduce imaging time and improve image quality. However, it is unclear whether flow measurements remain accurate with a nonlinear compressed-sensing image reconstruction. Here we assess the accuracy of flow quantification using these techniques.

Materials and methods: Patients referred for cardiac MRI evaluation were recruited for a 4D PC-MRI with intravenous gadofoveset. 13 patients were included (4 months–10 years) with a body surface area (BSA) of 0.3–1.37 m². The 4D scan used poisson-disc k-space undersampling; images were reconstructed with both parallel imaging alone (ARC, GE) and with compressed-sensing (L1-SPIRiT) separately applied to each flow-encoding. Exams were performed with flip angle 12–15°, TR 3.74–5.35, TE 1.36–2.16, 2–4 views/segment, and ky and kz total acceleration factors of 1.6–5. Ventricular volumes and 2D PC-MRI flow calculations were performed on a GE Advan-



tage workstation. Custom software was developed for 4D PC-MRI flow and ventricular measurements.

Results: 4D PC flow rates at the aortic and pulmonary valves were tightly-correlated with and without compressed-sensing (Qs: r=0.97, Qp: r=1.00), spanning flow rates from 0.85 to 5.79 L/min. Using L1-SPIR-iT, 4D PC flow rates also correlated well with 2D PC (Qs: r=0.94, Qp: r=0.98), even with combined acceleration as high as 10x. Despite the presence of valvular regurgitation, these flow rates also correlated with cine SSFP ventricular volumes (Qs: r=0.87, Qp: r=0.87) and 4D PC-MRI ventricular segmentations, (Qs, r=0.86), with no mean difference on Bland-Altman analysis.

Conclusion: We demonstrate nearly identical quantitative blood flow measurements can be obtained from 4D PC-MRI with parallel imaging alone (ARC) or with a nonlinear compressed-sensing reconstruction (L1-SPIR-iT). Measured flow rates also correlate well with 2D PC, SSFP and 4D PC-MRI volumes.

CV-11

Pediatric cardiomyopathies: evaluation with advanced magnetic resonance imaging

Shobhit Madan, Michael Mishra, Gayathri Sreedhar, Sameh Tadros

Children's Hospital of Pittsburgh, Pittsburgh (United States)

Purpose: Advanced cardiac magnetic resonance imaging (CMRI) sequences are critical for timely assessment of pediatric cardiomyopathies (CMs). The purpose of this retrospective study was to evaluate the CMRI parameters pertinent to specific CMs.

Materials and methods: Approval from the institutional review board was obtained. 57 patients(pts) with an initial clinical suspicion for CM were examined on 1.5T MRI scanner.12 pts were evaluated for left ventricular noncompaction(LVNC), 42 for arrhythmogenic right ventricular dysplasia(ARVD), 1 pt with myocarditis and LV mass, 1 pt with CM and multiple coronary artery aneurysms secondary to Kawasaki disease(KD), 1 pt with family history of hypertrophic CM and septal hypertrophy. Noncompacted to compacted myocardium(NC/C) ratio of >2.3 at end-diastole below papillary muscle in 4-chamber SSFP sequence was used to diagnose LVNC. Dilated right ventricle(RV), dilated RV outflow tract (RVOT), abnormal wall motion, mural fat or myocardial delayed enhancement(MDE) were the criteria for ARVD. Bi-ventricular function, mass and MDE were used to evaluate myocarditis, hypertrophic and dilated CM.

Results: 10 pts were excluded because of lack of data due to arrhythmia. 47 pts (M=27,F=20;mean age = 14.11+4.2 yrs;BSA = 1.6+0.4 kg/m²) were included in the final assessment. 8 out of 12 pts(Mean age = 8+3.9) were positive for LVNC with a mean (NC/C) ratio of 3.1;LVEF (56+8%); LVEDV (123+33 ml); LVEDVI(80+14 ml/m2); FS(32+6.8%). 2 out of 9 pts had MDE of the NCM. 1 patient(Male, age=15) diagnosed with ARVD had marked RV dilatation(RVEDV = 292 ml; RVEDVI = ml/m2) with evidence of very low RVEF(17%), dilated RVOT, systolic bulge of the RVOT and hypertrabeculation of RV. The rest of the pts evaluated for ARVD had a mean RVEDV=118-+43 ml and RVEF = 45+6%. 2 out of 9 pts with LVNC had a history of Brugada syndrome; 5 out of 9 patients were evaluated for non-LVNC causes and were incidentally found to have LVNC on CMRI. A pt with myocarditis had a thrombus in the LV apex, which was differentiated from a neoplasm by the absence of MDE.

Conclusion: Advanced CMRI techniques are critical for diagnostic and follow-up assessment for appropriate clinical management of varied pediatric CMs.

CV-R1

CT determination of intramural course of malignant aberrant coronary artery

Frandics Chan, Deirdre Sheahan, Shreyas Vasanawala, Richard Mainwaring, Mohan Reddy, Frank Hanley, Beverly Newman Lucile Packard Children's Hospital, Stanford (United States)

Purpose: Interarterial aberrant coronary artery (IACA) is associated with sudden death. The presence of intramural course of the IACA permits surgical unroofing to relieve the obstruction, while its absence requires coronary translocation or bypass. We test if CT and MRI coronary angiography can reliably determine intramural coronary artery.

Materials and methods: From 2004 to present, patients who had IACA imaged by cardiac CT or MRI and had surgical correction were identified with retrospective IRB approval. Surgical findings served as the standard of reference. Each study was anonymized and presented independently to three cardiac radiologists. They interpreted the type of IACA and its anatomic characteristics, such as location of the coronary origin. The certainty of intramural course was scored on a five-point scale. Interobserver variability was evaluated with the kappa coefficient. The accuracy of intramural interpretation was assessed by the area under the receiver operating characteristic curve(ROC) area. Statistical significance of anatomic characteristics was tested with the Fisher's exact test.

Results: 16 cases (15 CT and 1 MRI) were identified. Age ranged from 1 month to 46 years, average 13 years. There were 10 cases of RCA from the left coronary cusp, 3 cases of RCA from the LMCA, 1 case of LMCA from the right coronary cusp, and 2 cases of coronary origin above the sinotubular junction. 13 cases were found to have intramural coronary in surgery. The ROC areas for detecting intramural coronary were 0.81, 0.67, and 0.38 for the three readers. Interobserver variability was great (k=0.03). The best sensitivity and specificity were 0.77 and 1.00. In one reader, there was a significant correlation between intramural course and tapered coronary narrowing (p=0.0018). There was no correlation with the origin of the IACA, angle of take off, and closeness to the aortic root relative to the pulmonary trunk.

Conclusion: No anatomic detail firmly predicts intramural course, with the possible exception of coronary narrowing. The large interobserver variability points to the need for standardization of imaging findings and interpretation.

EM-1

Liver elastometry in healthy children and patients with cystic fibrosis (CF)

Clemens Wirth, Verena Wiegering, Kerstin Klotz, Negar Mahlmeister, Meinrad Beer

Institute of Radiology, Unniversity of Wuerzburg, (Germany)

Purpose: To evaluate the feasibility of sonographic hepatic elastometry using Acoustic Radiation Force Impulse (ARFI) in children. To compare healthy children and pediatric patients with CF *Materials and methods:* 34 healthy controls (0−15 y/o) and 25 patients with CF (3−25 y/o) were included in the study. In addition to an abdominal routine scan three-fold elasticity measurements using ARFI (Acuson S2000; Siemens Medical Solutions, Erlangen, Germany) were conducted in 5 standardized planes: segment II, III, V/VI, VII/ VIII in a transversal and segment VII/VIII in a transcostal approach. *Results:* Elasticity measurements were possible in all patients. The transcostal approach showed the lowest variability in the control group(Mean +/− SD: 1.24 +/− 0.21 m/s; Mean of SD: 0.18). Mean of the CF group was significantly higher in the CF group(1.61 +/− 0.81 m/s; p<0.05).



Conclusion: Liver elasticity imaging in children using ARFI is fast and reproducible. The transcostal approach shows the lowest variability. Elasticity imaging shows higher liver stiffness in patients with CF and might reflect hepatic involvement due to CF-associated liver disease.

EM-2

Value of quantitative viscoelasticity mapping of paediatric liver using supersonic shear imaging in the assessment of hepatic fibrosis: a preliminary clinical study

Stephanie Franchi-Abella, Lucie Corno, Monique Fabre, Emmanuel Gonzales, Danièle Pariente Hôpital Bicêtre, Paris (France)

Purpose: Non invasive assessment of hepatic fibrosis is a major challenge to avoid liver biopsies in children. Supersonic Shear Imaging (SSI) is a real-time ultrasound imaging concept that quantitatively measures local tissue stiffness in kPa and provides a color-coded map of tissue stiffness. There is actually no study published concerning paediatric applications. The aim of this study is to evaluate the correlation between the elasticity of the liver measured with SSI and liver fibrosis assessed by liver biopsy in children.

Materials and methods: We prospectively studied 36 children with chronic liver disease that underwent SSI using a linear or a curved ultrasonic probe to measure liver stiffness in kPa (10 measures/patient) and liver biopsy with METAVIR Score for reference. Results are expressed by mean +/- standard deviation (Sd). Statistical analysis is limited by the small sample.

Results: Seventeen of the 36 children had a liver transplant, 8 had biliary atresia, 5 had other cholestasis and 6 had miscellaneous hepatopathy. According to the METAVIR score, 4 of the 36 children were F0, 17 were F1, 5 were F2, 4 F3 and 6 F4. Young's modulus for each METAVIR score were in kPa: F0 (6,84+/ -2,28)), F1 (9.77 +/- 3,12), F2 (15,45 +/- 4,30), F3 (25,82 +/-23,05); F4 (45,70+/- 23,82). Sd was high in F3 and F4 groups. SSI and METAVIR score seemed to be well correlated in 25 patients (70%). In 11 patients (30%), the SSI values seemed not to be well correlated with fibrosis: 4 of them had cholestasis, 3 had venous stasis, one had a sepsis and one subcapsular necrosis after liver transplantation, 2 did not have particular pattern on biopsies. Conclusion: SSI seems to be a promising non-invasive and rapid ultrasonic method for assessing liver fibrosis in children. Further evaluation is necessary to confirm its accuracy and to establish the cut-off values for each fibrosis stage and better identify factors that could lead to over- or underestimation of liver fibrosis in order to establish the indications and limits of this technique. This study is on-going.

EM-3

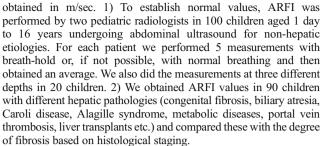
Acoustic radiation force impulse (ARFI): a preliminary study of liver elastography in children

Mehrak Anooshiravani, Michela Tempia, Anne-Laure Rougemont, Sylviane Hanquinet

Geneva University Children's Hospital, Geneva (Switzerland)

Purpose: To define the normal wave velocity values in healthy livers in children using a new ultrasound technique that combines impulse elastography (ARFI) with imaging. We also report preliminary measurements in the evaluation of fibrosis in different hepatic pathologies.

Materials and methods: Acoustic radiation force impulse imaging (Acuson S2000 ultrasound system, Siemens Healthcare) was performed with two different probes; linear 9 MHz or convex 4 MHz depending on the size of the child. The measurements were



Results: Normal values in children were between 1.11 and 1.21 m/s (average of 1.15 m/s). These measurements seemed independant of the type of breathing, the depth of the tissue sampling and the age of the child. The interobserver agreement seemed very good. We present our preliminary results in the evaluation of liver fibrosis in different pathologies with histological correlation.

Conclusion: The gold standard for the evaluation of liver fibrosis in children is biopsy, an invasive technique. ARFI is a simple, reproducible and non-invasive technique already used in adults which has the advantage of real-time imaging during measurements. Our preliminary results in pediatric diffuse hepatic pathologies show a good evaluation of fibrosis which may result in less biopsies in the future.

EM-4

Cine MRI technique in pediatric radiology

Tamara Feygin, Larissa T. Bilaniuk, Avrum N. Pollock, Arastoo Vossough, Leslie Sutton, Robert A. Zimmerman The Children's Hospital of Philadelphia, Philadelphia (United States)

Purpose: To demonstrate the utility of real-time cine-MRI in the evaluation of various pathologic entities of the central nervous (CNS) and upper gastrointestinal (GI) systems in fetuses and pediatric patients.

Materials and methods: We retrospectively reviewed MRI examinations performed between 2005 and 2009 comprising, in addition to conventional sequences, real time cine techniques. We divided these studies into the following groups: 1) 380 fetal MRIs with True fast imaging with steady-state precession (FISP) cine imaging for evaluation of different organ systems functions in real time; 2) 65 brain MRIs in children with obstructive hydrocephalus with Integrated Parallel Aquisition Techniques (IPAT) cine and/or Phase Contrast (PC) cerebro spinal fluid (CSF) flow imaging, including 24 examinations following endoscopic third ventriculostomy and 6 examinations performed after endoscopic fenestration of arachnoid cysts; 3) 11 MR Cine "fluoroscopy" examinations in healthy volunteers and a patient with 22Q deletion for swallowing and phonation evaluation and for detection of the position of ligament of Treitz.

Results: Real-time cine MRI techniques successfully depicted normal and abnormal organs/systems function related to motion/ flow of fluid. Fetal cine MR sequences were useful for evaluation of impairment/preservation of swallowing in fetuses with cervical masses causing pharyngeal/tracheal obstruction. Normal anatomy and abnormality of fetal great vessels and heart, such as coarctation of aorta and cardiac aneurysm were demonstrated in real time. Both IPAT and PC Cine MR Techniques were shown to be equally valuable in evaluation of site of obstruction in postnatal hydrocephalus and in evaluation of the functioning of ventriculostomy and cyst fenestration sites. Detailed depiction of soft palate motion, esophageal peristalsis and gastroesophageal fuction were demonstrated in volunteers.

Conclusion: Cine-MRI is an easy performed, fast technique for assessment of intracranial CSF flow dynamics and evaluation of



effectiveness of endoscopic neurosurgical procedures performed to divert CSF flow. It appears to be a useful tool for evaluation of functioning various organs/systems both in fetuses and children.

EM-5

Pineapple juice for neonatal gut MRI

Owen Arthurs, Martin Graves, Andrea Edwards, Ilse Joubert, Pat Set, David Lomas

University of Cambridge, Cambridge (United Kingdom)

Purpose: Vomiting in very young infants will be frequently investigated by the X-ray fluoroscopy upper GI contrast study (UGI) for abnormalities such as malrotation. We are developing an MR equivalent of this test, but the optimal contrast medium for MR imaging of the neonatal gut is unclear. Ideally it should be easily visualized (either T1w or T2w), well tolerated, but readily distinguishable from pre-existing bodily fluid. Several commercial fruit juices (e.g. pineapple) may be suitable as they have a short T1 (high in manganese). Here, we evaluate an interactive MR sequence incorporating an Inversion Recovery (IR-prep) pulse, to image pineapple juice (PJ) within the neonatal gut.

Materials and methods: Interactive MR was performed using an in-house developed pulse sequence that allows real-time variation of Inversion Recovery pulse timing (TI) during interactive T2-weighted (SSFSE) pulse sequences. The T1 of different contrast media was measured and compared: water, Iopamidol (Gastromiro, Bracco), Neocate (amino-acid based milk fomula) and three dilute pineapple juices (PJ A-C). We then tested the optimal solution during an upper GI contrast study using interactive MR, as part of an ethically approved study.

Results: The T1 relaxation times of pineapple juice was short (PJ-A 290 ms, PJ-B 285 ms, and PJ-C 240 ms) compared to other contrast media (Gastromiro 810 ms, Neocate milk 900 ms). In vitro, a TI of 500–600 ms effectively suppressed background fluid whilst PJ-C gave the highest signal. However, in-vivo, an interactively adjusted TI of 1000 ms provided optimal suppression of bowel fluid and high signal for PJ in a neonatal male.

Conclusion: In vivo, pre-existing bowel contents can be effectively nulled using an inversion recovery pulse during interactive MRI. The ability to optimise the TI allows relatively long T1 bowel contents to be suppressed, whilst short T1 PJ acts as a positive contrast medium to allow accurate delineation of the gut. This strategy may allow the examination to be tailored to the individual in real-time, making interactive MR a suitable alternative to the UGI series.

EM-6

Utilizing surgical specimen sonography to improve US detection of appendicitis and the normal appendix in patients with abdominal pain

Terri Love, MD, John Wendel, Sandra Allbery, Lisa Wheelock Omaha Childrens' Hospital and Medical Center, Omaha (United States)

Background: Obstacles to improving the sensitivity of ultrasound (US) in the identification of the appendix include a lack of expertise, a lack of perseverance, and a financial disincentive. Given recently renewed attention to the risk of ionizing radiation in pediatric patients, it is time to evaluate whether innovative training techniques may be used to increase the rate of appendix detection by sonography. This study assesses the effect of a single one-hour lecture on the sonographic appearance of the appendix followed by US of 25 surgical appendix specimens, on the rate of appendix visualization.

Materials and methods: Quantification of baseline identification of the appendix was performed by retrospective review of US exams performed July 2008-June 2009. The test period for improved performance was evaluated by a retrospective review of exams performed February 2010-January 2011. An Acuson Seguoia 512 model with 15L8 transducers and the "superficial" exam preset were used for both sonography of patients and specimens, with occasional use of 9L4 and 6C2 probes. The rate of in vivo visualization before and after the training program will be assessed utilizing the paired sample T-test in February 2011. Results: From July 2008 to June 2009, the baseline rate of appendix visualization was 34/60 (57%). After our training program, the initial seven months' data show an increase in sensitivity to 72/101 (71%). Preliminary evaluation of data suggests a statistically greater rate of identification of the appendix after implementing our training program. An additional five months' data will be presented at the completion of the study. Conclusion: A one hour lecture supplemented by sonography of 25 surgical appendix specimens has been shown to significantly improve rates of appendix visualization within 1 year to rates approaching those reported by Wiersma et al. (5) and Peletti et al. (4). Our study suggests that a single lecture followed by evaluation of a relatively small number of surgical specimens can lead to significantly improved rates of appendix identification in pediatric patients with RLQ pain.

EM-7

How much better is small intestine contrast sonography (SICUS) than sonography in diagnosing inflammatory bowel disease in children?

Ildikó Várkonyi, Anna Nyitrai M.D., Gábor Veres M.D., Éva Kis M.D. Semmelweis University Budapest (Hungary)

Purpose: Diagnosis of inflammatory bowel disease (IBD) is based on clinical data and imaging findings. Noninvasive modalities without radiation play an increasing role. Sonography (US) is the first choice modality if IBD is suspected in children, although it is limited by intestinal gas. This limiting factor can be avoided by filling the bowel with fluids (polyethylene glycol or mannitol) on SICUS (Small Intestine Contrast Ultrasonography).

Materials and methods: Thirty-six children (16 M, 20 F, aged 4-18.5 years, mean 13.6 years) with suspected or proven IBD between February 2009 and May 2010, 31 with Crohn disease and 5 with ulcerative colitis were retrospectively evaluated. All patients (pts) underwent abdominal US followed by SICUS. Filling fluid for SICUS was mannitol in 14 pts and PEG in 22. For evaluation purposes, the GI-tract was divided into 8 sections: 1. esophagus, 2. stomach, 3. duodenum, 4. terminal ileum, 5. cecum and ascending colon, 6. transverse colon, 7. descending colon and sigma, 8. rectum. Results: Findings on US and SICUS were retrospectively compared. The same bowel sections were found to be pathological in 25 (69%) pts. More sections could be found by SICUS in 5 (14%) pts. In 1 patient (3%) the number was the same, but was detected in other localisations by the two methods. In 4 (11%) pts fewer pathological sections could be shown by SICUS than by US. Bowel depiction of SICUS versus US was subjectively compared as well: in 7 (19%) pts both were of the same value. Lumen narrowing could be better visualized in 8 (22%) pts, alterated peristalsis of the pathological segments in 9 (25%), wall stiffness in 6 (17%). Normal peristalsis of a thickened segment could be demonstrated on SICUS in 2 pts, loss of haustration in 2 pts, and wall thickening could be better depicted in 3 pts. Prestenotic dilatation and fistulas were proven only by SICUS in 1 pt.

Conclusion: SICUS was able to show more details of bowel pathology compared with US in pediatric patients with IBD.



EM-8

Diffusion-weighted imaging as a marker of activity in paediatric Crohn disease

Jorge Davila, Nagwa Wilson, David Grynspan, David Mack, Barry Smith, Elka Miller

Children's Hospital of Eastern Ontario, Ottawa (Canada)

Purpose: magnetic resonance enterography (MRE) is being used broadly in the assessment of Crohn's Disease (CD). There are a few reports describing diffusion-weighted imaging (DWI) as a sequence that can be used to better assess CD. The purpose of this study is to correlate Apparent Diffusion Coefficient (ADC) values to the activity of paediatric CD in different segments of affected bowel

Materials and methods: 27 patients with proven CD underwent MRE including DWI with b value 1000. Diffusion was considered restricted when the bowel wall showed high signal on b 1000 and low signal on ADC map. ADC values were measured separated and blinded (from the MRE results) in the jejunum, ileum, terminal ileum, ascending, transverse, and descending colon. Findings were correlated with the pathology results of the biopsies taken by upper and lower endoscopy performed within the three-month time frame of MRE. In cases where the biopsies were taken outside this time frame, the Paediatric Crohn's Disease Activity Index (PCDAI) was used in conjunction to MRE findings (bowel wall thickening, hyperaemia and abnormal peristalsis in cine MRE) to determine the segments of bowel that show activity of CD. Mean differences of the ADC values were calculated for active and non active CD. Area under the receiver operating characteristic (ROC) curve was also calculated.

Results: 22 of 27 patients had active CD according to biopsy and PCDAI. All of them showed at least one segment of bowel with restriction diffusion and 1 of the 5 patients with non active disease showed restriction diffusion in at least one segment of bowel. 54 of the 162 evaluated segments of bowel were positive, 100 were negative and 8 were not assessed due to previous surgical resection. The mean ADC value of the segments of bowel with active CD was 0.001432 (+/- 0.0003) and non active CD was 0.002887 (0.0006) (p<0.0001). The area under the ROC curve was 0.975 (0.948–1.00; p<0.0001). Taking the ADC value of 0.00198, sensitivity was 0.963 and specificity was 0.97.

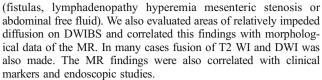
Conclusion: DWI is an excellent MR sequence to assess for activity of CD. It can be used solely or as a complementary tool in the assessment of CD. Poor distension of the bowel may cause false positives.

EM-9

Intestinal MRI in inflammatory bowel disease in paediatric patients: the added value of diffusion-weighted imaging (DWI). *Ignasi Barber*, Lina Cadavid, Amparo Castellote, Marina Alvarez, Goya Enriquez

Hospital Materno-Infantil Vall d'Hebron, Barcelona (Spain)

Purpose: To assess the value of DWI for the evaluation of bowel inflammatory changes in paediatric patients with Crohn's disease. Materials and methods: MR imaging was performed after the administration of 500–1000 mL of oral hyperosmolar solution (Plantago ovata or polyethylene glycol) one hour before the scan. The images were obtained using 1.5-T using T2 WI, T1 WI before and after Gad administration, and DWI with body signal supression (DWIBS) under free-breathing. We evaluated the intestinal wall thickening (3–6 mm considered as moderate and >6 mm severe), mucosal uptake (moderate if it was less than the uptake of renal cortical, and severe if higher) and extraintestinal complications



Results: We evaluated 26 MRI studies in 23 patients (age range 5-17 years) with inflammatory ileocolonic CD. MRI findings were confirmed on the endoscopic studies in all cases. MRI underestimated colonic involvement in 1 patient and was not assessable in 3 patients. Correlation between areas of intestinal involvement, evaluated with morphological criteria and Gadolinium enhancement, and areas of relative diffusion restriction on DWI was very good in almost all the studies (18 studies), in 2 cases areas of apparent restricted diffusion were not represented by anatomical anomalies. In the other 6 cases the complete imaging protocol (including DWI and Gad administration) could not be completed. Conclusion: DWI with body suppression is useful to detect intestinal inflammatory changes on Crohn's disease. DWI has a high lesion-to-background contrast, which may increase lesion detection rate while decreasing image interpretation time. A larger number of patients need to be evaluated for statistical analysis.

EM-10

NdH/dT: a new quantitative measure of tumor response using diffusion-weighted imaging

Stephan Voss, Moti Freiman, Robert Mulkern, Simon Warfield Children's Hospital Boston, Boston (United States)

Purpose: Diffusion Weighted Imaging (DWI) has been proposed as an imaging bio-marker for quantitative evaluation of tumor response to therapy. Changes in Apparent Diffusion Coefficient (ADC) values are inversely correlated with tumor cellularity and serve as a surrogate for treatment response. Changes in ADC are complex, due to pre- and post-treatment heterogeneity observed within human tumors. The purpose of this work was to develop a new approach that encapsulates overall tumor diffusivity change over time to provide a quantitative assessment of global tumor response.

Materials and methods: Data from 7 pts (3 NB, 2 Wilms, 1 Adrenal CA, 1 VM) were evaluated. Each dataset consisted of structural and DW images, pre- and post-Rx. DWI was typically performed with b-values of 0, 500, 800 sec/mm2. ADC maps were calculated using custom software. Regions of interest (ROIs) were segmented manually and ADC cumulative sum histograms were computed and differentiated over time. Areas under the curve were calculated to provide a single number that encapsulates global change in ADC. Positive values indicate increased diffusivity; negative values represent reduction in ADC. This measure was computed for both tumor (dH/dTt) and for healthy organs (dH/dTh). Next, the overall tumor response was normalized relative to normal tissues (NdH/dT = (dH/dTt)/ (dH/dTh)) to account for global changes in body diffusivity due to Rx. Thus, positive values >1 provide a true measure of increased diffusivity in tumor.

Results: The proposed measurement was calculated for each pt, and compared to tumor response as defined qualitatively and by RECIST. Comparison of quantitative ADC cumulative sum histograms pre- and post-Rx confirmed treatment response, or lack thereof. Representative NdH/dT values for 3 cases were: 0.37, 2.97, and 6.02 and correlated with qualitative assessment of diffusivity change.

Conclusion: These data present a method of assessing global tumor response to therapy based on diffusion imaging. The NdH/dT are simple and intuitive to interpret, encompass the entire tumor



response, account for tumor heterogeneity, and are comparable or superior to qualitative evaluation and size-based response criteria.

EM-11

Dedicated pediatric high-density torso phased-array coil for submillimeter isotropic abdominal MRI

Shreyas Vasanawala¹, Thomas Grafendorfer², Paul Calderon², Greig Scott¹, Marcus Alley¹, Michael Lustig², Anja Brau², Arvind Sonik¹, Peng Lai², Vijay Alagappan², Brian Hargreaves¹ ¹Stanford University, Stanford ²GE Healthcare (United States)

Background: We design and construct a pediatric high-density phased-array torso coil for highly accelerated MRI, testing whether it enables sub-millimeter isotropic resolution.

Materials and methods: A 32-channel torso phased array was designed/constructed to fit an average 7 year old child. Preamplifier oscillation was mitigated via feedback compensation. Phantom tests assessed signal-to-noise ratio (SNR) and coil decoupling. 8 consecutive children referred for abdominal 3T MRI who had millimeter resolution volumetric T1 and T2 scans were identified. Ages were 2-5 years. Coronal 3D T2 FSE had acceleration factor of 8, 320×320 matrix, FOV 22-30 cm, and 0.8 mm slices in 6/ 8 cases, 0.6 mm for 1/8, and 1 mm for 1/8. Coronal enhanced fatsat 3D SPGR with poisson-disc k-space sampling had acceleration 7.2-8 (mean 7.8), matrix 288×288, FOV 24-30 cm, and 0.8 mm slices (5 cases) or 1 mm (3 cases). Routine clinical axial 2D FSE T2 and axial 3D navigated enhanced dual-echo SPGR were also obtained. 2 radiologists graded on a 5 point scale the following: 3D scan SNR at source slice thickness (0.6-1 mm), 3D scan SNR at 3 mm slices, aliasing artifacts of 3D scans, 3D T2 axial reformat sharpness versus conventional 2D axial T2, spatial resolution adequacy of 3D T1 axial reformats, and 3D T1 axial reformat sharpness relative to navigated axial T1.

Results: Phantoms, SNR, coil decoupling, and g-factor were better than that of an adult coil. 3D T2: 8/8 cases had diagnostic SNR on thin source images and 3 mm slices, 7/8 had only mild aliasing artifacts and 1/8 had none. Reformat sharpness was slightly inferior to 2D T2 in 2/8, equivalent in 3/8, and superior in 3/8. 3D T1: Thin source image SNR was slightly limited in 2 cases, but of diagnostic quality on 3 mm slices for all cases. No coherent aliasing artifacts were noted. Axial reformats were diagnostic in 8/ 8 cases; 3/8 had mildly inferior reformat sharpness compared with direct axial images.

Conclusion: A high-density pediatric torso coil may enable true isotropic millimeter resolution volumetric abdominal T1 and T2 MRI with diagnostic quality SNR and reformats.

EM-12

Virtual neonatal autopsy — developing a clinically useful CT protocol.

Nathan Dobbs, Kamran Ali, Charles McGuire, Debbie Desilet-Dobbs, Curt Dorn, William Palko

Kansas University Wichita, (United States)

Purpose: Determining the cause of death of a neonate can be medically challenging as well as taxing to the infant's family. CT is proposed as useful in determining a cause of death. Due to physiologic differences of neonates compared to other pediatric and adult cases, a specific protocol was developed.

Materials and methods: From 4/1/10-10/31/10, 17 CTs were completed. Helical CT was performed on a 64 slice GE unit: slice thickness-5 mm; pitch-0.5. Scans were obtained at 120 kV and mA from 80 to 600. Gestational age ranged from 23 wks to term. Correlation with standard autopsy was made in 4 cases.

Results: Post-mortem CT scanning was initially protocoled using standard pediatric settings. This low mA returned images of low diagnostic value. As dose reduction is no longer an issue, mA was increased to 600 and auto-mA was disabled. Time after death is important in post mortem CT. As the time interval increases, so does the density of static blood, leading to potential confusion of intravascular blood for pathology. This was most noticeable in the dural sinuses and the cardiac atria. Thus, scans are most useful when obtained soon after death. Other findings were initially concerning for hemorrhage, then were determined as normal for neonates. These included increased attenuation of the germinal matrix and dense meconium within the bowel. CT demonstrated renal calculi in patients requiring frequent Lasix, and in other cases showed increased liver density, correlating with multiple transfusions. CT was also effective in the evaluation of support line placement. Limitations of CT included lack of microscopic evaluation of solid organs and fluid collections. Illustrating the need for a non-invasive post-mortem evaluation, consent was given for only 4 autopsies in the 17 cases. CT correlated with many of the findings made on autopsy and provided detail of intracranial contents that would not have otherwise been available. Conclusion: Post-mortem CT virtual autopsy is a non-invasive method to aid in determination of the cause of death in neonates.

EM-13

Dynamic 3D pulmonary perfusion in cystic fibrosis

Janaka Wansapura, Tam Le, Ian Chaves, Rhonda VanDyke, Gary McPhail, Raouf Amin, Robert Fleck Cincinnati Children's Hospital (United States)

Purpose: Chronic pulmonary infection and the progressive destruction of lung parenchyma are major causes of morbidity in Cystic fibrosis (CF). There is evidence in CF that abnormally low pulmonary perfusion carries a high risk of death independent of the presence of pulmonary hypertension. Here we evaluate the feasibility of quantifying pulmonary perfusion in CF patients using dynamic 3D gadolinium enhanced MRI.

Materials and methods: Fourteen patients with CF and six control patients were studied. 3D gradient echo images with fat saturation in the thoracic cavity were obtained every 1.0 to 1.5 s after power injection of Gd-DTPA. Perfusion data were analyzed using custom built software. An arterial input function was defined in the main pulmonary artery using a region growing technique. The pulmonary blood flow (PBF) was calculated according to the modified indicator dilution theory using a singular value decomposition method to deconvolve the time concentration curve. From the maps of PBF, pulmonary blood volume (PBV) and mean transit time (MTT), maps were generated and the mean values were assessed in the inferior and superior lobes of the lungs.

Results: CF patients (mean age = 16.8 years, mean FEV1=79%) were stratified depending on their forced expiratory volume in 1 s as: FEV1≥100%, 80%-99%, 60%-79%, and <60%. PBF and PBV were increased and MTT decreased in CF patients with a baseline FEV1≥100% of predicted compared to controls. Subjects with a FEV1%≥100% had higher blood flow by approximately 30% than healthy controls. While blood flow to the upper lobes decreased in a dose dependent manner across the 4 groups with CF, flow to the lower lobes in patients with FEV1%<60% exceeded the flow in patients with FEV1 between 60%-99%. PBF and PBV were decreased and MTT increased in CF patients with a baseline FEV1<99% of predicted when compared to controls in a dose dependent

Conclusion: Our results show that pulmonary perfusion abnormalities begin with a state of hyper-perfusion when CF patients



have normal lung function. A large loss of lung perfusion is observed when lung functions are only mildly decreased. The data strongly suggest that pulmonary vascular remodeling begins at very mild lung disease and therefore might precedes destruction of the lung parenchyma and loss of lung function.

EM-14

Oxygen-enhanced functional low-field MRI of the lung in very low birth weight infants with and without bronchopulmonary dysplasia (BPD)

Clemens Wirth, Sandra Weiß, Daniel Stäb, Helge Hebestreit, Herbert Köstler, Meinrad Beer

Institute of Radiology, University of Wuerzburg, (Germany)

Purpose: To assess functional lung abnormalities in formerly very low birth weight infants (VLBW) with and without BPD in compared with children born at term without lung pathology in an oxygen-enhanced open low-field MRI.

Materials and methods: 40 children aged 7–12 years were included in this study. 10 children had BPD, 15 were VLBW without BPD (non-BPD) and 15 formerly term infants served as controls. Sagital T1-weighted single inversion Multi-Gradient-echo sequences were acquired for both lungs at an open low-field MRI (Magnetom Open 0.2 Tesla, Siemens Medical Solutions, Erlangen, Germany). Acquisition was performed in 2 cycles: whilst breathing ambient air, then 100% oxygen via a breathing mask. The mean relative change of the T1 relaxation time (Δ T1) between the two cycles was calculated after pixelwise subtraction of the parameter maps. Δ T1 of the different groups was compared statistically.

Results: $\Delta T1$ of the different groups was calculated as follows: CON 10.7 +/- 2.3%; Non-BPD 10.8 +/- 3.0%; BPD 9.2 +/- 3.1%. $\Delta T1$ was significantly lower in the BPD group compared to both other groups (Mann–Whitney-U; p<0.05). There was no significant change of $\Delta T1$ between the Non-BPD and the control group (p=0.93).

Conclusion: Functional oxygen-enhanced MRI shows significant differences of $\Delta T1$ in patients with BPD compared to children without BPD, reflecting probable long term functional sequelae of disturbed pulmonary vascular and alveolar development of the disease.

EM-R1

Comprehensive cardiac flow and function assessment with 3D-time-resolved volumetric phase-contrast MRI

Albert Hsiao, Marcus Alley, Frandics Chan, Robert Herfkens, Shreyas Vasanawala

Stanford University, Stanford (United States)

Purpose: Comprehensive MRI assessment of cardiac flow and function is a lengthy, operator-dependent exam with multiple 2D phase-contrast (2D PC) and cine 2D steady state free precession (SSFP) scans. Techniques to quantify flow from 3D time-resolved phase contrast (4D PC) MRI have been previously reported and validated. Ideally, 4D PC MRI should provide ventricular volume and function as well. To achieve this aim, we (1) describe acceleration to obtain finer resolution, (2) develop methods to extract ventricular volumes from 4D PC data, and (3) assess the accuracy of volume and ejection fraction measurements relative to short axis stack cine SSFP. Materials and methods: With IRB approval, we investigated 26 patients with congenital heart disease. The first 13 patients previously had 4D PC acquisitions with parallel imaging acceleration in the phase direction. The last 13 patients had 4D PC scans with 2Dacceleration (phase and slice) to obtain higher spatial resolution.

Ventricular volumes from short-axis stack cine SSFP and aortic and pulmonic flow from 2D PC-MRI were obtained on a GE Advantage workstation. 4D PC flow was obtained with custom software, which was extended to also obtain ventricular volumes.

Results: Stroke volumes obtained by cine SSFP and 4D PC-MRI were tightly correlated in both populations, slightly improved in the latter group $(r=0.88,\ 0.96)$, spanning a range from 9 to 107 mL. Excluding ventricles with inlet or outlet valvular insufficiency, cardiac outputs were closely matched between 4D PC flow and ventricular measurements $(r=0.97,\ 0.93)$, while 2D PC flow and SSFP ventricular measurements were also well-correlated $(r=0.93,\ 0.83)$. Ejection fractions measured by SSFP and 4D approaches were comparable, but better correlated in the later, higher-resolution patient population $(r=0.39,\ 0.75)$.

Conclusion: We demonstrate a method to assess ventricular volumes and ejection fraction from 4D PC magnitude data, and show tight correlation with flow and volume measurements by conventional methods. With high spatial resolution from 2D acceleration and the new software, 4D PC now provides flow, ventricular volumes, and function in a single acquisition.

EM-R2

Dynamic imaging of conjoined twins

Kieran McHugh, Agostino Pierro, Edward Kiely Great Ormond Street Hospital for Children, London (United Kingdom)

Purpose: to show video files of CT and MRI studies of conjoined twins with thoracic, abdominal or pelvic conjunction.

Materials and methods: Our centre, almost certainly, has had the greatest experience with conjoined twins in the world. This would be both from a pre-surgical radiological assessment (we receive referred cases for pre-operative evaluation from all over the world) and later surgical separation.

Results: In oral presentation format, six recent cases of thoraco-abdominal fusion will be played in scroll through viewing to give radiologists a better insight into, and feel for, the complexities regarding the imaging of conjoined twins. Four pairs of twins were female. The mean age at first cross-sectional imaging was 2 months (range 1–8 months). Three twins were omphalopagus in type, two ischiopagus and one parapagus. One pair, who required emergency surgical separation, died. Ten pre-operative CT studies and five pre-operative MRI examinations were performed.

Conclusion: Our experience has already been written up in journals. The printed page, however, does not allow a scroll-through or cine type assessment of the imaging sequences, specifically the MRI or CT examinations. Lessons learnt to improve CT and MR imaging will be presented. These lessons include better communication with the ward staff (by personally going to the ward to see the twins and family), intubation for breath-holding sequences, and methods to ensure the optimal timing of contrast-enhancement.

EM-R3

The value of hybrid bone SPECT/CT in children

Helen Nadel

British Columbia Children's Hospital, Vancouver (Canada)

Purpose: 1. To review a consecutive series of bone SPECT/CT studies to determine the utility of hybrid imaging technique in a pediatric population. 2. To retrospectively identify specific pediatric indications or populations for this technique.

Materials and methods: 118 bone SPECT/CT studies were performed consecutively from 2007 to 2010. Bone SPECT was acquired first as



part of a bone scintigraphic examination. A non-attenuation corrected helical CT scan (6 slice) was acquired in the same position on the hybrid SPECT/CT scanner to co-register to the SPECT area of interest. CT images were reconstructed for bone and soft tissue windows; co-registered to the SPECT study; and displayed as multiplanar projections.

Results: On retrospective review, there were 80 positive studies; 38 negative studies. Positive diagnoses included: fracture (27), developmental/variant (14), osteoid osteoma (9), spondylolysis (7), infection (6), tumor-or tumor-like condition (4), arthropathy (4), avascular necrosis (AVN) (3), osteochondral defect (OCD) (3), reflex sympathetic dystrophy (RSD) (1), prosthesis loosening (1), heterotopic ossification (1). In all positive cases, a specific diagnosis was suggested by the hybrid study. A specific diagnosis was made by bone SPECT/CT on 8/11 studies of neurodevelopmentally delayed non-verbal children presenting with a change in behaviour and suspected pain: fracture (4), heterotopic ossification (1), spondylolysis (1), OCD (1), developmental variant (1). True negative results were confirmed In 5/5 patients with known prior diagnosis of neoplasm. Conclusion: Hybrid bone SPECT/CT improves the specificity of already sensitive but non-specific bone scintigraphy. It is particularly helpful in the neurodevelopmentally delayed nonverbal child to determine a specific cause for a change in behaviour or suspected pain.

Disclosure: The author has received an honorarium from Siemens Nuclear Medicine Canada as a speaker at an Imaging Symposium.

FN-1

Results of the Society of Pediatric Radiology (SPR) Fetal Imaging Task Force survey

Lucia Carpineta¹, Judy Estroff², Christopher Cassady³

¹McGill University Health Center/Montreal Children's Hospital, Montreal (Canada), ²Children's Hospital, Boston, ³Texas Children's Hospital (United States)

Purpose: To assess practices in fetal MR, with attention to the type of center performing such studies, indications, case load and type, techniques used, physicians performing fetal MR, work habits and training of fetal imagers, added value of fetal MR, organizational practices and educational needs of fetal imagers. *Materials and methods:* The Fetal Imaging Task Force sent out an online 38-question survey to all the members of the SPR. The survey was open 01/06/2009 to 31/10/2010.

Results: 89 responses were received from 76 sites on 4 continents. Most fetal MR appears to be performed in large centers in university hospitals (~1/2 in children's hospitals). Most centers have been providing fetal MR for 10 years or less. The annual case loads vary widely, with just under 1/2 of sites reporting 50 cases or less and only ~18% reporting >200 cases/year, with these higher volumes at sites also offering fetal interventions. Most centers have 2-3 fetal imagers, and the majority have had no formal training in fetal MR. Most fetal imagers read fetal MR is in addition to other clinical work. Referrals came mostly from obstetricians or their imaging facilities, with 1/2 of respondents receiving referrals also from fetal care centers. Only 35% of respondents conduct systematic US before the fetal MR; the rest accept the report of an outside US as sufficient prior to fetal MR. Although various indications are accepted, neuro evaluations predominate. $\sim 2/3$ of sites perform a full fetal survey, while <2/3 also routinely evaluate maternal structures. Trends were noted in imaging protocols. 84% of respondents reported unsuspected findings on MRI "sometimes" or more. Only 15% of respondents reported MR "rarely" added to the US diagnosis. >1/2 of sites have a fetal care center, most of which are run by obstetricians/MFMs. Most respondents were in favor of formal fetal MR education and creation of an SPR Fetal Imaging Consultation Service.

Conclusion: Survey results are helpful in understanding the current models of practice for radiologists working in centers offering fetal MR in order to provide appropriate resources for education and consultation to pediatric radiologists.

FN-2

Diffusion-weighted imaging (DWI) of the fetal brain in utero: reproducibility study and normal values

Marianne Alison, Agnès Sartor, Nadia Belarbi, Bogdana Tilea, Emilie Josserand, Corinne Alberti, Jean Francois Oury, Monique Elmaleh-Berges, Guy Sebag

Hôpital Robert Debré, Paris (France)

Purpose: To study the intra and inter-observer reproducibility of measurements of Apparent Diffusion Coefficient (ADC) of the fetal brain. To determine regional normal values during the 3rd trimester of pregnancy.

Materials and methods: Retrospective study of 101 fetal brain MRI with DWI, performed at a mean age of 33 weeks of gestation (range: 30 to 381/2) from November 2005 to May 2009 on a 1.5T scan (Philips Medical system). Patients were referred for extracerebral malformation, suspicion of brain anomaly on ultrasound, family history or maternal indication. Patients referred for ventriculomegaly, infection or abnormal dopplers were excluded. Inclusion criteria were singleton, normal fetal brain morphology, signal and biometry, with a normal follow-up at birth. EPI sequence with b-factor 0 and 700 s/mm2 was performed. ROI-based measurements for ADC values were performed in the centrum semi ovale, frontal and occipital white matter, basal ganglia, cerebellum hemispheres and pons. Intra and inter-observer reproducibility study (between 4 operators) was performed on 27 cases.

Results: Depending on the anatomic location, the measurement precision varied from 0.3 to 0.43 mm2/sec for intraobserver and from 0.25 to 0.52 mm2/sec for interobserver. Regional ADC was not significantly different between right and left hemispheres. ADC decreased with gestational age in all brain areas. Mean values of ADC were 1.84–1.91, 1.26 and 1.48.mm2/sec respectively for white matter, basal ganglia and cerebellum. A normal fronto-occipital gradient was observed: the mean ADC was higher in frontal than in occipital white matter, but this gradient was inverted in some individuals. ADC was always higher in the white matter than in the cerebellum and the white matter/cerebellum ADC ratio increased with gestational age.

Conclusion: Intra and interobserver reproducibility of measurement of fetal brain ADC are moderate and should be taken into account for individual diagnosis. Normal regional gradient and gestational variation of ADC are demonstrated.

FN-4

Dynamic evaluation of the secondary palate during fetal swallowing: a novel application for cine-FIESTA MRI

Neil Lester, Susan Connolly, Carol Barnewolt, Robert Mulkern, Judy Estroff

Children's Hospital Boston, (United States)

Purpose: While T2-weighted single shot fast spin echo (SSFSE) imaging is the workhorse sequence of fetal MRI for evaluating fetal palatine anatomy, its ability to evaluate the fetal secondary palate can present a dilemma due to inadequate contrast related to direct apposition of the fetal tongue, secondary palate, and nasopharyngeal soft tissues. This study aims to use CINE FIESTA MRI to better evaluate the secondary palate during fetal swallowing.

Materials and methods: Fetal imaging was performed with a 1.5T scanner using an 8 channel body coil array. In addition to standard



T2-weighted SSFSE imaging, the exam included a fully balanced steady state free precession sequence (FIESTA) to scan between two and four 3 to 8 mm thick slices at and around the fetal midsagittal plane in CINE mode (for a total of over 200 images at ~0.65 s intervals) using a 340×192 matrix, TR/TE/fractional anistropy (FA) = 3.5/1.5/45 and ~50×30 cm² FOV's. All cases referred to our institution for fetal cleft lip and/or palate over the past 14 months were retrospectively reviewed to evaluate for the utility of CINE imaging as an adjunctive technique.

Results: 39 cases were reviewed. In 25 of these cases, CINE imaging was performed in addition to standard T2-weighted SSFSE imaging. With CINE imaging capturing dynamic fetal swallowing events, excellent contrast between the bony hard palate, muscular soft palate, tongue, and swallowed fluid distending the mouth and nasopharynx, allowed accurate depiction of the region of the entire fetal palate in general, and the secondary palate in particular. CINE imaging successfully confirmed a diagnosis of either intact or cleft secondary palate suspected by standard T2-weighted FSE imaging in 16 of 25 cases, and CINE imaging was the only sequence on which a diagnosis could be made in 2 of 25 cases.

Conclusion: Dynamic imaging during fetal swallowing with CINE FIESTA MRI consistently and reliably demonstrates the integrity, or lack thereof, of the fetal secondary palate, and as such, is a useful adjunctive technique to standard T2-weighted SSFSE imaging.

FN-5

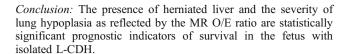
Predictive factors in fetal survival with isolated left congenital diaphragmatic hernia

Teresa Victoria, Michael Bebbington, Enrico Danzer, Alan W Flake, Mark P Johnson, Scott N Adzick, Holly Hedrick Children's Hospital of Philadelphia, Philadelphia (United States)

Purpose: Prior studies have evaluated the correlation of MRI measured fetal lung volumes (FLV) with survival and postnatal ECMO use in fetuses with isolated left congenital diaphragmatic hernias (L-CDH). The goal of this study is to determine the prognostic value of MRI-FLV in L-CDH fetuses when both prenatal and postnatal care are provided by the same institutional team. We also evaluate the prognostic value of stomach position and volume of herniated liver.

Materials and methods: With IRB approval, all fetal MR studies of isolated L-CDH from 1/1997 to 7/2010 were reviewed. Study inclusion criteria: all pre- and postnatal care performed at our hospital, MR images available for review, gestational age >21 weeks, and no additional chromosomal/congenital anomalies. Total lung volume (TLV), MR observed/expected lung volume (O/E LV), and percentage of herniated liver were calculated. The position of stomach relative to the heart was noted. A neonatal chart review was performed for treatment and outcome data. Statistical tests included t-test for continuous variables, chi-square for dichotomous variables, ANOVA and multivariate logistic regression. p<0.05 was considered significant.

Results: 70 patients met criteria and were included in the study. The overall survival was 64%. In patients with liver up, survival was 43% while in the liver down group survival was 96%. Using O/E LV as a proxy measure for pulmonary hypoplasia, survival was 15% if O/E < 25, 71% if the O/E was 25–35, and 78% if O/E>35 (p<0.05). The percent of herniated liver was less in survivors than in non-survivors: $16.8\%\pm9.0$ (mean \pm SD) vs 25.5 ± 15.2 (p=0.03). All 9 fetuses with the stomach below the diaphragm survived, while survival with an intrathoracic stomach was 60% (p=0.02). On multivariate analysis only liver herniation and MR O/E LV <25 were statistically significant predictors of survival (p<0.05).



FN-6

Prenatal US imaging of congenital lung lesions (CLL): proper reporting of salient findings alleviates postnatal confusion

Laurent Garel, Françoise Rypens, Andrée Grignon, Josée Dubois, Chantale Lapierre, Denis Filiatrault, Marie-Claude Miron, Julie Dery, Jean Claude Decarie, Gilles Perreault

University Hospital of Sainte-Justine, Montreal (Canada)

Purpose: Prenatal recognition of CLL has markedly increased, thanks to routine obstetrical US. Postnatal confusion (imaging and management) is, in part, linked to improper wording of the fetal findings.

Materials and methods: Retrospective review of 100 CLL seen in the last 10 years in a single institution with pre-postnatal correlations. Critical analysis of the prenatal descriptors and conclusions as in the reports. Suggested standardized descriptive terms for improving postnatal management: timing of conspicuity (WGA); location of lesion (upper lobe (UL), lower lobe (LL), suprarenal); shape, geometry and echostructure of lesion (cysts, diffuse hyperechogenicity, bronchocele); systemic vascular feeder or not.

Results: 1. Overall appropriate reporting (80% of cases): mid 2nd trimester cystic lesions referred as congenital pulmonary airway malformation (CPAM) or hybrid when evidence of systemic vascular supply; triangular posterobasal echogenic lesions with systemic feeder properly referred as pulmonary sequestration (PS); mid 2nd trimester suprarenal lesions adequately reported as PS or hybrid. 2. Inappropriate reporting (20% of cases): diffusely echogenic CLL without systemic vascularization systematically called microcystic CPAM, because of the rare recognition of bronchocele, suggesting a bronchial atresia component in echogenic CLL and because trapping (idiopathic or secondary) was not suggested as a potential cause, especially in UL location.

Conclusion: 1. Description of CLL was inappropriate in the diffusely echogenic lesions without systemic vessel. 2. Although prenatal imaging features are not inclusive of all findings at pathology, some patterns allow for a "leading" diagnosis. 3. Bronchocele conspicuity in fetal CLL is worth being searched for. 4. There were no tumors in the early cystic CLL, nor any malignancy on follow-up of CLL.

FN-7

Antenatal and postnatal diagnosis and follow-up of renal vein thrombosis

Fred Avni, Michel Wlasdorff Erasme Hospital, Brussels, Belgium

Purpose: 1) to compare the pre- and postnatal imaging data of renal vein thrombosis in the fetus and neonate (RVT) 2) to compare the prognosis and follow-up of pre- and postnatally occurring RVT

Materials and methods: we have collected through a multicentric survey (Group for research in pediatric and perinatal imaging -GRRIF-), cases with fetal or acute neonatal diagnosis of RVT. We have reviewed the imaging features techniques (including fetal MRI) at diagnosis and during follow-up. We have reviewed the clinical circumstances and morbi-mortality of the patients.

Results: 12 cases of fetal RVT and 5 cases of acute neonatal RVT were collected. Among the 12 fetal RVT, 6 displayed the classical acute phase pattern - enlarged kidney without cortico-medullary differentiation (CMD) and/or hyperechoic thick stripes-; 6 had the



sequelar pattern - normal size kidney with CMD and thin hyperechoic stripes. 6 cases were bilateral; there were 4 associated adrenal hemorrhage. A thrombus was found in 4 cases witnin the IVC or/and Renal vein. In two of these fetuses, the affected kideny shrunk. There was no sign of renal failure or other clinical symptom. Among the 5 cases with neonatal onset, only one was bilateral; they all displayed the typical acute appearance. The patient with bilateral RVT evolved towards renal failure and died rapidly. The affected kidney in one other case stopped growing and appeared "dysplastic" but without renal failure.

Conclusion: In our series, fetal RVT occured more frequently than post natally onset acute RVT. The imaging features of pre- and postnatally diagnosed RVT are similar. Prognosis is appearantly better in prenatal than post natal RVT.

FN-8

Ultrasonographic study of postnatal renal growth in premature infants

Yun-Jung Lim, Woo Sun Kim, Su-Mi Shin, Jung-Eun Cheon, In-One Kim, Yoo Jin Kim, Ji Young Kim, Kyung Mo Yeon Seoul National University (South Korea)

Purpose: To determine the normal range of renal size and postnatal renal growth in premature infants by ultrasound and to look for the parameter that has an effect on postnatal renal growth in premature infants.

Materials and methods: Informed consent was obtained from parents. Ultrasound (US) was prospectively performed in 125 premature infants, defined as gestational age (GA) below 37 weeks (GA 23–36 weeks M:F=65:60). Large for gestational age, offspring of diabetic mother, and infant with hydronephrosis or congenital renal anomaly were excluded. Initial US was performed within the first 72 h of life and again at every 2 weeks until postmenstrual age (PMA) 40 weeks. After the expected date of delivery, US was repeated at 1 and 6 months of corrected age. US was performed by one pediatric radiologist. Renal sizes of premature infants were compared with those of fetus from published data (J Urol. 2007; 178:2150–4.) Correlation between renal size and GA, gender, birth weight, height, and body surface area were investigated retrospectively. Wilcoxon's signed rank and 1 sample t-test was used for statistical analysis.

Results: Renal size in premature infant gradually increased with GA. The left renal length was significantly larger than the right one (p-value <0.0001). Renal size was correlated with GA, birth weight, height, and body surface area. There was the best correlation between renal size and birth weight (p<.0001). At 28 to 33 weeks of GA, renal length was significantly smaller than that of fetus (p<.01), while there was no significant difference between above two data beyond 34 weeks of GA.

Conclusion: By the use of US, normal range of renal length and postnatal renal growth was determined in premature infants. Birth weight showed the best correlation with renal size in premature infant.

FN-9

Hypoxic ischemic injury: intestinal appearances and perfusion measurements using ultrasound and dynamic color Doppler sonography in neonates submitted to therapeutic hypothermia. *Guilherme Cassia*, Ricardo Faingold, Linda Morneault, Guilherme Sant'Anna, Anna Ben Ely

Montreal Children's Hospital, Montreal (Canada)

Purpose: The aim of this retrospective study was to evaluate intestinal gray-scale ultrasound (US) appearances and intestinal perfusion intensity (IPI) in neonates with Hypoxic Ischemic Injury (HII), submitted to hypothermia treatment.

Materials and methods: Gray-scale abdominal US images of the bowel and DICOM color Doppler videos of the mural blood flow were acquired with an 11LW4 MHz linear transducer to assess the IPI. The videos were analyzed by 2 radiologists using the Pixelflux Chameleon software, which allows automatic quantification of color Doppler data from a region of interest (ROI), by dynamically assessing color pixels and flow velocity during the heart cycle. The IPI, bowel wall thickness and echotexture were evaluated in all neonates. Evidence of sloughed mucosa was defined as the presence of a halo of echogenic material with echotexture similar to the mucosa, within the intestinal lumen.

Results: A total of 28 neonates were included: 16 male, 12 female, mean gestational age 39±2 weeks, birth weight 3469±607 g, US performed at 17.1±10.5 h of life. Seven neonates died, and 6 of them had sloughed mucosa on US. The presence of sloughed mucosa was highly predictable of mortality with a sensitivity = 86, specificity = 100, PPV=100 and NPV=95. Bowel wall was relatively thicker in the neonates that died (1.600±0.39 mm vs. 1.439±0.31 mm p<0.01). There was a trend to decreased mural perfusion (0.040±0.015 cm/s vs. 0.052±0.029 cm/s) in neonates that died.

Conclusion: Intestinal US and Color Doppler perfusion measurements performed in neonates with HII, during hypothermia, provided important information. Neonates that died had significantly increased bowel wall thickness and a trend towards decreased mural perfusion. The presence of sloughed intestinal mucosa was highly associated with mortality. The software Pixelflux Chameleon was acquired with a grant from Canadian Heads of Academic Radiology (CHAR-GE Development Award).

FN-10

Thrombosis associated with umbilical artery catheterization Natalia Simanovsky¹ Zivanit Franz Shaltiel¹ Katya Rozovsky¹

*Natalia Simanovsky*¹, Zivanit Ergaz Shaltiel¹, Katya Rozovsky², Nurith Hiller¹, Benjamin Bar Oz¹

¹Hebrew University Hadassah Medical Center, P.O. Box 24035, Mount Scopus, Jerusalem (Israel), ²Children's Hospital of Eastern Ontario, Ottawa (Canada)

Purpose: Umbilical artery catheter (UAC) is used for management of critically ill infants. The insertion of UAC may be associated with thrombus formation. Complications include renal failure, hypertension, septicemia and death. It is unclear how common subclinical thrombi are and what their implication is. Thrombolytic and antithrombotic treatments were proved effective, but some series detected spontaneous resolution in half the infants, and spontaneous regression in all neonates. Our aim was to reveal the incidence of UAC related thrombosis, to define the risk factors associated with thrombi formation, and to establish indices of arterial resistance.

Materials and methods: 60 infants who had UAC were included. The catheter was situated in the descending thoracic aorta. The UAC position was confirmed by an X-ray. Abdominal US and Doppler examinations of the renal arteries were carried out during the first week after the UAC withdrawal. Infants who had aortic thrombosis were followed until thrombus resolution.

Results: We found a frequency of 31.6% (19/60) of UAC related arterial thrombosis. Two of the male infants who had aortic thrombosis also had umbilical vein thrombosis. We had M/F ratio of 14/5, significantly higher than among infants with UAC who did not develop thrombi. In all infants, spontaneous resolution of the thrombus was observed in less than 1 year of follow-up. There was no difference in the time of resorption between sexes. Only one newborn with UAC related thrombosis had transient hypertension. Two infants suffered from transient oliguria with increased creatinine levels that resolved sponta-



neously. None of the babies had limb color changes or reduced pulses. No statistical significance was found in resistive indices of renal arteries between the infants with and without thrombus. The only statistically significant risk factor for thrombi formation was catheter time in situ.

Conclusion: The UAC related thrombosis in our cohort was a self resolving disease, with few transient complications that did not necessitate medical treatment.

FN-11

Cerebellar injury in very low birth-weight infants—preliminary results at a tertiary institution

Michalle Soudack, Lisa Raviv-Zilka, Aviva Ben-Shlush, Jeffrey Jacobson

Edmond and Lily Safra Children's Hospital, Tel Hashomer (Israel)

Background: Cerebellar hemorrhages are not uncommon in premature infants and despite the associated morbidity may be clinically silent. They can exist with or without supratentorial injuries and often go unnoticed on ultrasound examinations performed via the standard anterior fontanel approach.

Purpose: The purpose of this study was to determine the prevalence of cerebellar lesions in very low birth weight infants on routine head ultrasound examinations with mastoid fontanel views.

Materials and methods: Between January 2008 and June 2009, 512 premature newborns (defined as less than 37 weeks gestational age) were hospitalized in the premature or neonatal intensive care departments at our institution. All infants had at least one head ultrasound examinations including both anterior and mastoid fontanel scans. The 125 very low birth weight (equal or less than 1500 g at birth) newborns constituted the study group. The hospital's Institutional Review Board approved this retrospective study and informed consent was waived.

Results: There were 70 female and 55 male patients weighing 465 to 1500 g (average 1120 g) born at 23–36 weeks (mean 30 weeks) gestational age. Eighteen infants (14%) had sonographic evidence of central nervous system hemorrhage including 4 posterior fossa lesions, interpreted as bleeds. Three were associated with supratentorial hemorrhages and one was isolated. All cerebellar lesions were clearly demonstrated via the mastoid fontanel and none were initially seen by the standard anterior fontanel views. We are presently following up these infants in the hospital's outpatient clinic. Conclusion: Cerebellar injury is not an uncommon finding in very low birth weight neonates and is best diagnosed with the mastoid fontanel approach. Mastoid views should be included in routine head ultrasound examinations.

FN-12

The spectrum of associated brain lesions in cerebral sinovenous thrombosis: relation to gestational age and outcome

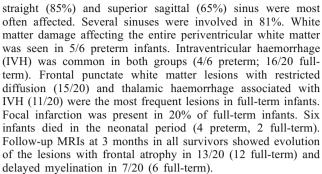
Rutger A.J. Nievelstein¹, K. Kersbergen¹, F. Groenendaal¹, M. Benders¹, H. Van Straaten², R. Nievelstein¹, L. De Vries ¹

¹UMC Utrecht, Utrecht, ²Isala Clinics, Zwolle (the Netherlands)

Purpose: To describe different patterns of associated brain lesions in preterm and full-term infants with cerebral sinovenous thrombosis (CSVT) and to assess whether these different patterns are related to gestational age at onset.

Materials and methods: MR scans of all neonates (6 preterm, 24 full-term) with suspected CSVT, collected over a 7 year period in 2 neonatal intensive care units, were evaluated to assess patterns of associated brain lesions. Comparisons between the two gestational age groups were made.

Results: CSVT was confirmed on MR-venography in 26 out of 30 neonates (6 preterm, 20 36 weeks gestational age). The



Conclusion: Preterm and full-term neonates show different patterns of associated brain lesions. Extensive white matter damage is the predominant pattern of injury in the preterm infant, while an IVH associated with a thalamic haemorrhage and punctate white matter lesions are more common in the full-term infant.

FN-13

Brain MRI based choice of best time for transition of the great arteries surgery: inside brain protection

Yevgeniya Yershova, Tetyana Yalynska, Andrey Maximenko, Illya Yemets

Ukranian Children's Cardiac Centre Kyiv (Ukraine)

Background: We consider immediate postnatal arterial switch operation (ASO) as the best way of brain injury protection due to elimination of postnatal hypoxemia and post- BAS thromboembolic risk.

Purpose: The goal of our research is to compare diffusion-weighted imaging (DWI) brain morphology of newborns with TGA during first hours after birth and before ASO, define the number of pre- and post-surgical brain complications in both groups. To draw a parallel between reviled pre-surgical brain injury and the level and duration of postnatal hypoxemia and BAS.

Materials and methods: 69 newborns with TGA underwent brain MRI with ADC measurement in basal ganglia, thalamus, optic radiation, corticospinal tracts, frontal and parietal white matter. Group A: 56 newborns with TGA had MRI before ASO, mean age 6.1±3.9 days, SaO2 70.2±13.4%.Group B: 13 newborns with TGA, mean age at MRI 3±3.9 h, including 10 with additional MRI after ASO, mean age for ASO 3h36min, age for postoperative MRI 10.8±3.2 days, pO2 31.9±5.6, SaO2 67.2±18.8%.

Results: Group A: 29(53%) newborns with brain injury before ASO with white matter injury (WMI) prevail 21(72%), 4 patients had additional injury of basal ganglia. Mean age of patients with WMI 7.25±4.2 days, average SaO₂ 60.2±13.7% vs 4.6±3.1 days and SaO2 77.5±8.4% without WMI. 8 patients had focal stroke, 2 of them with WMI, all these underwent BAS at the age 5 days +. Group B: none of the patients had preoperative brain injury, 4 (40%) patients had postsurgical WMI, 3 of them had small subdural hemorrhage, no one had stroke or basal ganglia injury. ADC decrease in most areas of measurements though stayed closer to normal limits compared to group A.

Conclusion: Newborns with TGA more suffer from preoperative brain injury, mostly WMI, influenced by the level and duration of postnatal hypoxemia. Strokes are rare and mostly connected to thrombembolia after late BAS. Upon early TGA surgery intracerebral injuries are limited to WMI occurring rarely comparing to preoperative injury (53% vs 40%). Our research shows that the best TGA surgery time is first hours after birth but no later than 5 postnatal days.



FN-14

A potential new marker for fetal karyotype abnormality: dense, premature ossification of the calcaneum on post mortem fetal radiograph

Susan Morris, Denise Robinson, Edgar Lazda, Gordon Vujanic University Hospital of Wales, Cardiff (United Kingdom)

Purpose: The significance of very dense and prematurely ossified calcanea on post mortem fetal radiographs was investigated and found to be strongly associated with fetal karyotype abnormalities. This is a previously unreported association which can also be seen on ultrasound from 12 weeks gestation and is therefore a potential new marker for fetal chromosomal abnormality.

Materials and methods: A review of 580 fetal post mortem radiographs performed between January 2005 and December 2010 identified 22 cases with abnormally dense, prematurely ossified calcanea. A further 3 cases with skeletal dysplasia were excluded. Correlation with autopsy findings, chromosomal analysis and where possible, ultrasound findings was undertaken.

Results: There were 22 cases of very dense calcanea with gestational ages from 12 to 18 weeks. 15 cases had confirmed abnormal karyotype: 7 Triploidy, 4 Trisomy 21, 3 trisomy 18 and one MonosomyX. Three cases had multiple features consistent with Triploidy at autopsy but no karyotype available. Two cases with normal karyotype had multiple structural abnormalities. Two cases of early spontaneous miscarriage had no karyotype data and had extensive maceration. In 4 cases of Triploidy, where ultrasound images were available, the prematurely ossified calcaneum was easily seen retrospectively from 12 weeks gestation. Relevant ultrasound images were not available for the other cases

Conclusion: The normal fetal calcaneum begins to calcify from 18 to 20 weeks gestation and is visible on X-ray from approximately 20 weeks. The presence of very densely ossified calcanea on post portem fetal radiograph prior to this gestation is strongly associated with karyotype abnormalities. This may be of diagnostic value in cases of unexplained miscarriage. On ultrasound the ossification centre of the calcaneum is usually visible from 20 to 24 weeks gestation. The ultrasound finding of a bright, prematurely ossified calcaneum is a potential new marker for fetal karyotype and structural abnormality. The significance of this finding for prenatal diagnosis warrants further large scale investigation.

FN-R1

National survey of obstetric and pediatric specialists' attitudes regarding pregnancy management

Stephen Brown⁷, Jeffrey Ecker², Johanna Mailhot³, Elkan Halpern⁴, Sadath Sayeed⁵, Terry Buchmiller⁶, Christine Mitchell¹, Karen Donelan⁷

¹Children's Hospital Boston and Harvard Medical School, Boston ²Vincent Memorial Obstetric Service, Massachusetts General Hospital, Boston ³Department of Health Policy and Management, Harvard School of Public Health Boston ⁴Institute for Technology Assessment, Massachusetts General Hospital, Boston ⁵Division of Newborn Medicine, Children's Hospital Boston; Division of Medical Ethics, Harvard Medical School, Boston ⁶Department of Surgery, Children's Hospital Boston, Boston, MA; Advanced Fetal Care Center, Boston, ⁷Mongan Institute of Health Policy (United States)

Background: Pregnancy management for congenital fetal conditions increasingly involves both fetal care pediatrics specialists (FCPs) and obstetric-based maternal-fetal medicine specialists (MFMs). This trend raises issues of whether pregnant patients

will receive different information or clinical options depending on where and from whom they receive care.

Purpose: To profile the practices, counseling, and recommendations of FCPs and MFMs for pregnancies with diagnosed fetal conditions.

Materials and methods: Self-administered survey of 434 MFMs and FCPs in 21 states, with \$70 prepaid incentive. Response rate was 60.9% for MFMs and 54.2% for FCPs. Main outcome measures: Specialists' attitudes regarding patients' decisions to terminate a pregnancy, importance of providing selected information, and appropriate timing of pediatric specialist consultation, and their reported proportions of patients who terminate the pregnancy. Bivariate and multivariate analyses assessed differences between groups and whether differences persisted for key dependent variables.

Results: For three fetal conditions, Down syndrome, Congenital Diaphragmatic Hernia (CDH), Spina Bifida: MFMs were more likely than FCPs to support a decision to terminate the pregnancy (Down syndrome 52% vs. 35%, p<0.001; CDH 49% vs. 36%, p<0.001; Spina Bifida 54% vs. 35%, p<0.001); MFMs were more likely to think that offering options for pregnancy termination is of high importance (Down syndrome 90% vs. 70%, *p*<0.001; CDH 88% vs. 69%, p<0.001; Spina Bifida 88% vs. 70%, p<0.001). FCPs were more likely to say it is important to offer personal contact with individuals or families with the condition (MFM vs. FCP responses, respectively, Down syndrome 50% vs. 60%, p= 0.008; CDH 46% vs. 54%, p=0.035; Spina Bifida 53% vs. 61%, p< 0.024); MFMs reported higher rates of pregnancy termination among their patients (Down syndrome 29.6% vs. 9.2%, p<0.001; CDH 12.9% vs. 7.8%, p < 0.027; Spina Bifida 18.8% vs. 11.5%, p <0.018). 75% FCPs and 54% MFMs thought that pediatric-specialist consultation with the pregnant woman should take place prior to the decision to continue or terminate for Down syndrome (p < 0.001). Conclusion: Our study suggests that prenatal counseling about congenital fetal conditions varies considerably between MFMs and FCPs, and may affect options offered to patients and outcomes for these pregnancies.

FN-R2

Correlations between pre- and postnatal cerebral MRI

Amira Dhouib, Amira Dhouib, Eléonore Blondiaux, Marie-Laure Moutard, Thierry Billette de Villemeur, François Chalard, Jean-Marie Jouannic, Hubert Ducou le Pointe, Catherine Garel Hôpital d'Enfants Armand-Trousseau, Paris (France)

Purpose: To evaluate the diagnostic accuracy of fetal cerebral Magnetic Resonance Imaging (MRI) on a large cohort and to compare pre-and postnatal MRI data.

Materials and methods: This was a prospective study (2006–2009). The inclusion criteria were: absence of termination of pregnancy, fetal death or stillbirth and at least one postnatal MR examination. The pre- and postnatal diagnoses established by MRI were compared and divided into five subgroups: same diagnosis (group 1), same diagnosis but different appearance related to the natural course of the disease (group 2), different diagnosis (group 3), same diagnosis with additional findings discovered on the postnatal MRI examination (group 4), or same data as for group 2, associated with additional findings (group 5). The prognostic impact of a possible disagreement between pre-and post-natal findings was evaluated.

Results: 100 fetuses were included. Fetal MRI was performed at a mean gestational age of 33 weeks (24–39 weeks) and postnatal MRI, at a mean age of 3.5 months. Group 1 (n=52), group 2 (n=32), group 3 (n=4), group 4 (n=11) and group 5 (n=1). In 16 cases, the postnatal diagnosis was different from the prenatal one



(mostly corpus callosum anatomy, cortical and migration disorders) with a prognostic impact in 10/16 cases. In 8 cases, 2 postnatal MRI were performed. In 1 case, postnatal MRI showed subependymal heterotopias which were not detectable on the first examination.

Conclusion: Pre and postnatal MRI data showed good agreement in 84%. Disagreement had a prognostic impact in 10% of the cases.

FU-1

Effectiveness of pre-medication and pre-warming for suppression of fluorodeoxyglucose (FDG) uptake in brown adipose tissue

Michael Gelfand¹, Jessica Huang², Susan Sharp¹

¹Cincinnati Children's Hospital, Cincinnati ²University of Cincinnati College of Medicine, Cincinatti (United States)

Purpose: Both pre-medication and pre-warming have been shown to decrease the frequency of brown adipose tissue visualization in young patients undergoing F-18-FDG PET imaging. In children and adolescents with lymphoma, both brown adipose tissue and abnormal lymph nodes may be found in the same anatomic regions. The purpose of this study is to determine the effectiveness of a combined program of pre-warming and pre-medication for suppression of brown adipose tissue uptake in children and adolescents with lymphoma.

Materials and methods: 84 F-18-FDG PET/CT scans of 35 pediatric and adolescent lymphoma patients were reviewed. All patients were warmed for 30–60 min prior to radiopharmaceutical injection. 63 patients also received pre-medication with fentanyl IV 10 min prior to radiopharmaceutical injection; fentanyl was not administered if patients were already receiving opiate pain medications or had previous adverse reactions to fentanyl. FDG uptake in brown adipose tissue was graded for severity: grade I uptake was minimal in amount and did not affect scan interpretation and grade II uptake was moderate or large in amount and required careful correlation of foci of FDG uptake with co-registered CT to facilitate differentiation of brown adipose tissue activity from lymph node uptake.

Results: Of the 84 scans, there was grade I brown adipose tissue uptake in 3 (3.6%) and grade II uptake in 2 (2.4%). No patient had brown adipose tissue uptake on more than one study.

Conclusion: Brown adipose tissue uptake of FDG that interferes with PET/CT interpretation can be reduced in pediatric and adolescent patients from published rates of 26–31% to less than 3%. This removes a potential source of error in image interpretation, and permits more rapid interpretation of PET/CT studies.

FU-2

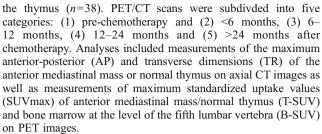
Differentiation of the normal thymus from mediastinal lymphoma on pediatric PET/CTs $\,$

Heike Daldrup-Link¹, Rakhee Gawande¹, Aman Khurana¹, Randy Hawkins²

¹Stanford University, ²Department of Radiology, University of California, San Francisco (United States)

Purpose: To evaluate the role of PET/CT for the differentiation of the normal and rebound thymus from mediastinal lymphoma and lymphoma recurrence in pediatric patients.

Materials and methods: 75 pediatric oncology patients, who received 351 18F-FDG PET/CT scans, were divided into four groups: (A) patients with anterior mediastinal lymphoma (n=16), (B) patients with recurrent anterior mediastinal lymphoma (n=5), (C) patients with lymphoma outside of the mediastinum (n=16), and (D) control patients with other malignant tumors outside of



Results: The AP and TR values were significantly different between Groups A and B compared to groups C and D. The average T-SUV values of prechemotherapy scans of group A was 4.5, group B was 6.9, group C was 1.8 and group D was 1.9. The average T-SUV value of group B (recurrent mediastinal lymphoma) on post chemotherapy scans was 9.2. Thymic rebound was seen in 27 patients in the 6 to 24 months post-chemotherapy scans (Group A n=4, Group C n=6 and Group D=17). The average T-SUV value of thymic rebound was 2.7.

Conclusion: Thymus infiltration by lymphoma results in more pronounced thymic enlargement compared to thymic rebound. T-SUV is a sensitive biomarker for differentiating mediastinal lymphoma from normal thymus and thymic rebound. A T-SUV of 4.5 or more is a strong predictor of mediastinal lymphoma.

FU-3

PET with selective CT at follow-up in pediatric and adolescent patients with lymphoma

Michael Gelfand¹, Jessica Huang², Susan Sharp¹
¹Cincinnati Children's Hospital, Cincinnati, ²University of Cincinnati College of Medicine, Cincinnati (United States)

Purpose: FDG PET scans in most patients with lymphoma normalize after one or two cycles of chemotherapy, at the first follow-up PET examination. PET/CT may be performed with diagnostic CT, reduced dose localization (loc) CT or microdose CT for attenuation correction (AC) only. In lymphoma patients with normal follow-up PET scans, loc CT may have little or no diagnostic value. The purpose of this study is to determine the fraction of patients in whom one might consider omitting loc CT or limiting loc CT to a few bed positions.

Materials and methods: 84 FDG PET/CT scans of 35 pediatric and adolescent lymphoma patients were reviewed retrospectively. Available follow-up PET scans (from scan 2 through scan 4) were included. Each PET scan alone was reviewed to determine if it could confidently be interpreted as normal without a loc CT. If the PET scan had abnormal or questionable findings, the number of CT bed positions that require rescanning with loc CT to assure the usual level of diagnostic certainty was determined.

Results: When all 84 scans (scans 2, 3 and 4) were considered, 41 PET studies (49%) could be interpreted without a loc CT scan, 6 (7%) needed loc CT of one bed position, 27 (32%) needed a 2 bed position loc CT, 6 (7%) needed a 3 bed position loc CT and 4 (5%) needed a 4 or more bed position loc CT. When only 52 later follow-up scans (scans 3 and 4) were included, 31 (60%) could be interpreted without loc CT, 17 (33%) needed a 1 bed position loc CT, and 3 (8%) needed a 2 or 3 bed position loc CT. The average effective dose (ED) from CT when the selective CT approach is used is 0.59 mSv (including microdose CT for AC), about 11% of the typical 5 mSv ED from loc CT.

Conclusion: Selective use of loc CT in follow-up PET/CT, where the *a priori* probability of an abnormal study is low, can significantly decrease total ED from CT. This approach requires that the initial PET scan be reviewed to determine how many bed



positions need to be repeated with loc CT, an approach that is feasible in well-staffed departments.

FU-4

MRI vs. PET/CT for detection of focal splenic lesions in paediatric and adolescent lymphoma at initial staging

Shonit Punwani, King Kenneth Cheung, Nicholas Skipper, Alan Bainbridge, Stuart Taylor, Ashley Groves, Sharon Hain, Simona Ben-Haim, Ananth Shankar, Paul Humphries

University College London, London (United Kingdom)

Purpose: Compare performance of MRI (Short TI Inversion Recovery - Half Fourier Single Shot Turbo Spin Echo [STIR-HASTE] ± Dynamic Contrast Enhanced [DCE] Imaging) and PET/CT for detection of focal spleen involvement at initial staging of lymphoma.

Materials and methods: 44 patients (80% of all patients) imaged between August 2007 and January 2010 met study eligibility criteria (<=18 yrs, histological ∆ lymphoma, pre-treatment MRI and PET/CT staging, post-treatment imaging follow up). Respiratory and electrocardiogram gated axial and coronal STIR-HASTE images of the neck, chest, abdomen and pelvis were acquired with the patient supine using the manufacturer's body and spine array coils and a Siemens 1.5T MR system. Twenty-three of the 44 patients underwent additional DCE-MR imaging of the spleen using axial 3D Fast Low Angle Shot technique (FLASH). Fluorodeoxyglucose (FDG) PET/CT data were acquired by using a dedicated combined in-line GE system. Anonymous STIR-HASTE images of the spleen were first evaluated independently, then in consensus by two radiologists (n=21). For patients with DCE-MR (n=23), radiologists independently assessed STIR-HASTE, then DCE-MR images, followed by a final consensus of combined MR datasets. PET/CT images of the spleen were independently and then in consensus assessed by two nuclear medicine physicians (n=44). At each assessment readers recorded presence or absence of focal splenic disease. An independent expert multi-disciplinary panel derived reference based on all concurrent imaging, clinical details and follow-up formed the reference standard for MRI and PET/CT

Results: Sensitivity and specificity for detecting focal splenic disease was 100% for STIR-HASTE and STIR-HASTE+DCE-MR, and 83.3% and 87.5% for PET/CT at consensus. Reader concordance was 88.6% for STIR-HASTE MRI (κ =0.73), 95.7% for STIR-HASTE +DCE (κ =0.90) and 84.1% for PET/CT (κ =0.63).

Conclusion: STIR-HASTE MR imaging accurately detects focal splenic involvement by lymphoma and compares favorably with PET/CT. Addition of DCE-MR to STIR-HASTE improves overall reader concordance.

FU-5

PET/CT and MRI capability of detection of early soft tissue inflammatory changes in knees of a blood-induced arthropathy rabbit model

Afsaneh Model
Afsaneh Amirabadi¹, Amer Shammas¹, Elka Miller², Anguo Zhong¹, Ruth Weiss¹, Tammy Rayner², Rahim Moineddin³, Harpal Gahunia¹, Marianne Rogers⁴, Roland Jong⁴, *Andrea Doria*¹The Hospital for Sick ChildrenToronto ²Children's Hospital of Eastern Ontario, ³University of Toronto, ⁴Mount Sinai Hospital

(Canada)

Purpose: Early identification of inflammatory soft tissue changes in hemophilic joints allows for early intervention thus avoiding further joint degeneration. Our purpose was to compare MRI and 18F-FDG PET/CT with regard to their capability of demonstrating interval soft tissue inflammatory effects in knees of a bloodinduced arthropathy rabbit model according to prior limited versus extensive intraarticular blood injections.

Materials and methods: 10 juvenile white New Zealand rabbits were evaluated. Arthritis was induced in one of the rabbits' knees by intra-articular autologous blood injection (1.5 cc/kg). Animals were divided into 2 groups (G1,n=5; G2,n=5). G1-rabbits received 8 blood injections into the same knee over 17 weeks and G2-rabbits, 2 injections. PET/CT (60 min after 18F-FDG administration [0.25 µCi/kg]) and unenhanced T1 map sequence at 1.5T MRI were performed at baseline, weeks 5 and 17 of the experiment. FDG uptakes were measured in regions-of-interest (ROIs) within perisynovial soft tissues of arthritic and contralateral knees by maximal standardized uptake (SUVmax) and standardized uptake ratio (SUR) on PET/CT images. Signal to noise ratios (SNRs) of ROIs anatomically-matched to SUVmax ROIs were measured on MR images.

Results: PET: At week 17 all G1 rabbits demonstrated asymmetric increased uptake in their affected knees with higher SUVmax (P= 0.018). None of the G2 rabbits showed an asymmetric increased uptake. Mean SUR values of G1 at baseline, and weeks 5 and 17 were 1.00, 1.05, and 1.56, respectively. SUR of G1 was higher at week 17 compared to SUR measured at baseline (P=0.001) and week 5 (P=0.002). SUR at week 17 was different for G1 and G2 rabbits (P=0.006). MRI: No SNR changes were identified in affected knees compared to contralateral knees in any of the rabbits at baseline (G1, P=0.93; G2, P=0.97), weeks 5 (G1, P=0.97), weeks 5 (G1, P=0.97). 0.90; G2, P=0.96) or 17 (G1, P=0.95; G2, P=0.86).

Conclusion: FDG PET/CT was superior to MRI to detect inflammatory soft tissue changes associated with blood-induced arthropathy, which seem to relate to number of prior intraarticular blood injections rather than to time interval in this experimental model.

FU-6

Clinical experience with lower dose fluorodeoxyglucose (FDG) pediatric brain PET/CT

Jeffrey Miller, Gerald Mandell, Richard Towbin, John Curran Phoenix Children's Hospital, Phoenix (United States)

Purpose: PET protocols have been revised to establish weightbased recommendations for FDG dose. Current recommendation for brain FDG PET dose is 0.1 mCi/kg. In this retrospective review, we report experience of clinical brain PET performed with FDG doses of 0.075 mCi/kg or less.

Materials and methods: PETs performed with doses of 0.075 mCi/kg or less were identified. Each patient also had prior MRI done for tumor or epilepsy. These MRIs were reviewed prior to PET evaluation. Based on the MRI, PETs were classified by the suspected findings. These categories were 1) high-grade tumor (hypermetabolism), 2) structural epileptogenic lesion (hypometabolism), 3) low-grade tumor (isometabolism) and 4) possible tumor recurrence (hypermetabolism). For tumor surveillance patients, in order to confirm the etiology of lesions that were not biopsied/resected, exams were excluded if a follow-up MRI of greater than 6 months was not available. Exams that met criteria were reviewed to determine if the lesion on MRI was visible on PET and if so, what was its metabolism. Results: 23 PETs met criteria. 6 were excluded due to lack of structural abnormality or follow-up MRI. Either hyper or hypometabolic lesions were identified in 14/23. All 9 done for epilepsy showed hypometabolism within MRI lesions. 5 showed hypermetabolic lesions. 3 of these correlated with high-grade primary tumor and 2 with suspected recurrent tumor. The other 6 suspected tumor recurrences did not show metabolic abnormality and



remained stable on follow-up MRI consistent with post surgical changes. Of the 3 exams in which a low-grade tumor was suspected, all 3 showed no significant metabolic alteration. Each of these underwent resection (2) or tissue biopsy (1).

Conclusion: In this small series, PET performed with lower than recommended FDG dose maintained a high specificity and sensitivity for the delineation and characterization of lesions seen on MRI. Further clinical experience would be helpful to support the use of reduced FDG dose lower than currently recommended.

FU-R1

PET/CT in pediatric rhabdomyosarcoma

Beth McCarville, Matt Krasin, Sheri Spunt, Catherine Billups, Jianrong Wu, Barry Shulkin

St. Jude Children's Research Hospital, Memphis (United States)

Purpose: To assess the value of PET/CT in staging pediatric rhabdomyosarcoma (RMS).

Materials and methods: 30 patients, median age 7.3 years, with newly diagnosed RMS, underwent PET/CT before or on the day of initiating chemotherapy. PET/CTs were retrospectively, independently reviewed by two pediatric radiologists and two nuclear medicine physicians who determined the presence of pulmonary, nodal, bone or bone marrow disease. PET findings were considered positive if FDG avidity was greater than normal tissue without physiologic explanation. PET/CT findings were compared to conventional imaging (CI) (chest CT, MRI or CT of primary site and local-regional nodal basin, Tc99m MDP bone scan) reviewed by one pediatric radiologist, bone marrow biopsy and clinical follow-up. Standardized uptake values (SUV)of nodes and pulmonary nodules were correlated with lesion histology using the Spearman's correlation coefficient and the Wilcoxon rank sum test.

man's correlation coefficient and the Wilcoxon rank sum test. *Results:* Seventeen patients had 37 lymphnodes >1 cm on CI. Nineteen of the 37 were indeterminate for malignancy by CT and 1 was indeterminate by PET/CT. Using clinical assessment as the gold standard, PET/CT had a sensitivity and specificity of 94% and 100% for nodal disease. The median SUV of malignant lymphnodes was 7.9 and of benign 1.5 (p<0.001). Six patients had 7 pulmonary nodules; 3 nodules could not be identified by PET/CT and 2 were indeterminate by both PET/CT and CI. Only 1 nodule was malignant and this nodule had the highest SUV (3.4). Two patients had bone disease, 1 was identified by bone scan and both by PET/CT. There were 2 false-positives for bone disease by PET/CT. Four patients had bone marrow disease, 2 were positive on PET/CT while all were negative on bone scan. There was one false positive for marrow disease by PET/CT.

Conclusion: PET/CT appears to be superior to CI in identifying nodal and bone marrow disease in children with RMS and may be superior for the detection of bone metastases. While PET/CT has limited value in the detection of pulmonary nodules the SUV may help distinguish the benign or malignant nature of those that can be detected with this modality. Validation of these findings requires further investigation and larger sample sizes.

GI-1

Should the abdominal radiograph be the initial imaging examination in the pediatric patient with abdominal pain?

Gloria del Pozo Garcia, Veronica MuÑoz Carpio, Amaya Hilario, Daniel Hernandez Aceituno, Gabino gonzalez de Orbe, Carmelo Serrano

Hospital Universitario 12 de Octubre, Madrid (Spain)

Purpose: To determine the value of abdominal radiography in the diagnosis of acute abdominal pain in children beyond the neonatal

period by comparing the findings of abdominal plain films with those of abdominal ultrasound (US). Final diagnosis was based on surgical findings, enema and/or clinical follow-up.

Materials and methods: During a 3-year period, 1204 abdominal radiographs of children between the ages of 2 months to 14 years were prospectively analyzed. In 550 of these patients abdominal US was also available. All children with suspected appendicitis or intussusception underwent ultrasound evaluation to confirm diagnosis and evaluate perforation prior to surgery. Radiological findings were classified as normal, non-specific and abnormal. Abnormal findings included pneumoperitoneum, bowel obstruction, ileus, fecaliths, target sign, mass effect, urolithiasis and gallstones.

Results: Radiographs of the abdomen were negative in 709 patients, non-specific in 409 and abnormal in 86 children. 224/550 abdominal US showed pathological findings. In those cases, plain radiography was interpreted as negative in 49.5% and abnormal in 32.5%. Pneumoperitoneum was never identified. 98/550 children underwent surgery, of which 44.8% showed negative radiography. Apendicitis (87) and ileocolic intussusceptions (54) were the most frequent findings. In the appendicitis group 14.9% had fecaliths. Only 66% of ileocecal intussusceptions had abnormal plain films.

Conclusion: Appendicitis and intussusception were the most frequently diagnosed pathologies in the child with acute abdomen. Only 14.9% of appendicitis showed underlying specific plain film abnormalities. No signs of free air were detected in plain radiograph. Most intestinal obstructions were caused by appendicitis and intussusceptions. At our institution, plain radiography has been substituted by US as the initial imaging modality for accurate diagnosis of acute non-traumatic pain in children

GI-2

The role of delayed repeat ultrasound in children with right lower quadrant pain

Hamzaini Abdul Hamid, Alan Daneman, Georges Azzie, Trent Mizzi

Hospital for Sick Children, Toronto (Canada)

Purpose: Accurate diagnosis of acute appendicitis (AA) at ultrasound (US) obviates the use of CT. The purpose was to determine role of delayed repeat US in improving diagnostic accuracy, sensitivity and specificity in AA and to determine its impact on use of CT, false positive diagnosis of AA and perforation rate.

Materials and methods: Retrospective analysis of clinical, imaging, surgical and histological findings in all patients who presented to Emergency Department with right lower quadrant pain between July 2008 and July 2009. Exclusion criteria: previous appendectomy or for follow up.

Results: 601 patients were included in the study. US was performed in 574(96%). Delayed repeat US was performed in 59(10%) due to equivocal initial US findings. Final diagnosis was AA in 237. The diagnostic accuracy, sensitivity and specificity of first US for AA was 84%, 98% and 73% respectively when equivocals considered as false positive and 84%, 76% and 95% respectively when equivocals considered false negative. After delayed repeat US these improved to 92%, 98% and 86% respectively (equivocal considered false positive) and 92%, 89% and 95% respectively (equivocals considered false negative). CT was only performed in 74/601(12%). Perforations were seen in 94(40%): 82/206(40%) of those with AA who had only 1 US and 12/31(39%) who had delayed repeat US and/or subsequent CT scan. False positive preoperative diagnosis of AA occurred in 10(4%), 2 of whom had a complicated Meckel diverticulum requiring surgery.

Conclusion: The accuracy, sensitivity and specificity of US for diagnosis of AA improved with the implementation of delayed



repeat US, almost similar to CT. This strategy limited the use of CT in patients with right lower quadrant pain, was not associated with an increased perforation rate and did not contribute to an unacceptable rate of false positive diagnosis of AA.

GI-3

Difference in size of abdominal nodes and bowel wall thickness in children with recurrent abdominal pain in comparison with age-matched controls

Winnie CW Chu, Vivian YF Leung, Darshana Dattatray Rasalkar The Chinese University of Hong Kong, Hong Kong (China)

Purpose: Recurrent abdominal pain (RAP) is one of the most common gastrointestinal disorders in children after exclusion of organic causes. Prevalence across nations ranges 10 to 15%. However, there is a lack of definitive valid tools for diagnosis of RAP. The objective of this study is to study the size of abdominal lymph node and thickness of bowel wall in pediatric patients who presented with RAP but without organic cause found on ultrasound screening. Comparison was made with age-matched controls without gastrointestinal complaints.

Materials and methods: From 2005 to 2010, prospective ultrasound studies were carried out in 572 RAP patients (292 girls and 280 boys, age range 3.5 to 16.7, median 9.2 years). 494 age matched controls with no history of gastrointestinal tract (GI) disorders were also recruited for comparison (207 girls and 287 boys, age range 3.0 to 16.9, median 10.1 years). Subjects with any morphological abnormality detected on ultrasound were excluded from analysis. Size and number of the abdominal lymph nodes in the following three sites were measured: hepatoduodenal ligament (HDL), caval-duodenal chain (CDC) and mesenteric regions. Bowel wall thickness was measured at the stomach, jejunum, ascending and descending colon.

Results: Statistically significant difference was found between RAP and controls in the following aspects: (i) mean size of the lymph nodes at HDL, CDC and mesenteric regions were larger in RAP (p<0.05, Mann–Whitney U test); (ii) RAP children had significantly more lymph nodes (P<0.005, Chi-square test) on the left side of the abdomen and (iii) bowel wall thickness was increased in all sites in RAP (p<0.005, linear regression and Mann–Whitney U test).

Conclusion: The above sonographic findings could be considered as ancillary features for diagnosis of RAP after exclusion of organic causes. These features can reassure both clinicians and parents about the diagnosis of RAP, hence avoiding further unnecessary investigation while early medication for symptomatic relief can be commenced.

GI-4

Prospective comparison of CT enterography and MR enterography for the evaluation of pediatric Crohn's disease *Michael Gee*, Keith Quencer, Mari Mino-Kenudson, Esther Israel,

Michael Gee, Keith Quencer, Mari Mino-Kenudson, Esther Israel, Jeffrey Biller, Aubrey Katz, Mukesh Harisinghani, Katherine Nimkin Massachusetts General Hospital/Harvard Medical School Boston (United States)

Purpose: Determine the accuracy of MR enterography (MR-E) for evaluation of pediatric Crohn's disease imaging features compared with CT enterography (CT-E) imaging standard. Additionally, MR-E and CT-E were compared for detection of active bowel inflammation and chronic fibrosis using a histologic reference standard.

Materials and methods: 21 pediatric patients with histologyproven Crohn's disease were enrolled in a prospective protocol approved by the IRB. All patients underwent CT-E and MR-E examinations on the same day using a combined oral contrast regimen. CT and MRI exams were evaluated in a blinded fashion by experienced pediatric radiologists for the presence of specific Crohn's disease imaging features. In addition, CT and MRI studies were independently reviewed for the presence of active bowel inflammation and chronic fibrosis, and imaging assessment was correlated with histologic reference obtained from endoscopic biopsy or surgical bowel resection.

Results: Compared with CT-E, MR-E demonstrated high accuracy (>80%) for detection of Crohn's imaging features including bowel wall thickening, lymphadenopathy, focal fluid collections, mesenteric inflammatory changes, and fistula formation. When compared with histologic reference, MR-E and CT-E demonstrated similar accuracy (82% vs 78%, respectively), sensitivity (85% vs 94%), and specificity (79% vs 59%) for the detection of active bowel inflammation. In contrast, MR-E demonstrated superior accuracy (78% vs 57%), sensitivity (74% vs 44%), and specificity (82% vs 69%) compared with CT-E for detection of mural fibrosis.

Conclusion: MR-E provides similar accuracy to CT-E for detection of Crohn's disease imaging features and active bowel inflammation in pediatric patients, without the ionizing radiation risk associated with CT. MR-E is superior to CT-E for detection of chronic mural fibrosis, likely due to the superior soft tissue contrast and enhancement kinetics provided by MRI. Non-invasive detection of mural fibrosis would be useful for predicting potential response to biological therapies and identifying possible need for surgical resection, suggesting a unique for MR-E in assessing disease activity.

GI-5

Comparison of high resolution bowel ultrasound (US) with MR enterography (MRE) in children with inflammatory bowel disease (IBD).

Sudha Anupindi¹, Emily Janitz¹, David Biko², Melkamu Adeb¹, Kassa Darge¹

¹The Children's Hosptial of Philadelphia, Philadelphia ²National Naval Medical Center, Bethesda, (United States)

Purpose: Show bowel US is sensitive for detecting IBD. Evaluate intra- and extramural bowel pathology on US and correlate with MRE.

Materials and methods: 19 patients with known or suspected IBD (7 F, 12 M, age 14.7+/- 3.3 yrs) had bowel ultrasound and MRE within a 2 month period and histological confirmation of IBD. On US and MRE, 10 bowel segments were evaluated. Number of bowel segments visualized, bowel wall thickening (BWT), bowel wall hyperemia/enhancement (BWH/BWE), abnormal peristalsis on cine, stricture, fistula, abscess, and mesenteric inflammation (hyperechogenicity/high signal) were reviewed by 2 radiologists, blinded to biopsy results. BWH/BWE & mesenteric changes were scored on a 4 point scale (0 = normal,1 = mild,2 = moderate,3 = severe).

Results: In 18/19 patients (95%) 8 or more of 10 bowel segments were demonstrated on US. In 1/19 (5%) all segments were seen. On MRE, in 18/19 subjects (95%) 10 bowel segments were seen; in one, 8/10 segments seen due to prior ileocecotomy. Incidence of diseased bowel on US/MRE: terminal ileum (TI) 68.4%/63.2%, cecum 36.8%/31.5%, ascending colon (asc) 26.3%/26.3%, transverse colon(tran) 26.3%/10.5%, descending 21.0%/21.0%, jejunum 15.8%/21.0% No duodenal disease seen on US or MRE. In diseased segments mean BWT on US/MRE: TI 5.7 mm/8.4 mm, cecum 5.6 mm/8.4 mm, asc 4.9 mm/9.2 mm, trans 4.7 mm/6.7 mm. Higher BWT on MRE may reflect surrounding extramural inflammation. The score of BWH/BWE for these segments was 2.4–3.0. Mean score for mesenteric changes was 2 for US and MRE. In 1 patient US identified a TI stricture not seen on MRE. Phlegmon on US was seen in 3, 2 of these



had bowel perforation and 1 had an abscess, all confirmed on MRE. Using MRE as reference, sensitivity/specificity for detection of disease on US in the small bowel was 100%/67% and colon 100%/90% respectively. Negative predictive value (NPV) for bowel was high, 88–100%.

Conclusion: Compared to MRE, bowel US is sensitive in detecting intra- and extramural bowel pathology. High NPV suggests US should be used as a screening prior to MRE.

GI-6

Comparison of gray scale and colour Doppler sonographic findings with plain radiography findings in neonates with necrotizing enterocolitis (NEC)

Akshay Saxena, Gaurav Arora, Kushaljit Sodhi, Praveen Kumar, Niranjan Khandelwal

Post Graduate Institute of Medical Education and Research, Chandigarh, (India)

Purpose: To compare abdominal sonographic findings with abdominal radiography in neonates clinically suspected to have NEC and to correlate sonographic findings with clinical outcome. Materials and methods: 33 neonates with clinical suspicion of NEC were included in the study group (Group I). 20 neonates with feed intolerance but not suspected to have NEC served as the control group (group-II). Abdominal radiography was performed in group I at the time of enrollment, and during follow up radiographs ascertained whether there was clinical deterioration. Radiographic examinations were followed by sonographic evaluation within 6 h. Sonographic evaluation included thickness, echogenecity and perfusion of bowel wall, pneumatosis, pneumoperitoneum, portal venous gas and peritoneal fluid. Neonates in group II were evaluated by sonography alone. The radiographic findings were compared with sonographic findings. Sonographic findings were also co-related with adverse clinical outcome (defined as patients who required surgical management and/or died because of NEC). Results: 1. The two groups were similar to each other in terms of gestational age, body weight and sex (p=0.21,0.20 and 0.13)respectively). 2. Sonography in group II provided normative data for bowel wall thickness, echogenicity and perfusion. 3. Sonography was superior to radiography in detection of pneumoperitoneum, portal venous gas and peritoneal fluid. 4. Radiography and sonography were complimentary to each other for detection of pneumatosis. 5. Spectrum of sonographic findings for bowel wall in NEC included mural thickening, increased mural echogenecity, increased mural perfusion and reduced mural perfusion. 6. During follow up in six patients, sonography detected deterioration in five patients compared to three with radiography. 7. Sonographic detection of free and echogenic peritoneal fluid, portal venous gas, pneumatosis, pneumoperitoneuam and increased bowel perfusion had statistically significant (p<0.05) correlation with adverse clinical outcome.

Conclusion: Abdominal sonography has the potential to make a significant contribution to the clinical management of patients with NEC.

GI-7

Sonographic hepatic and portal blood flows in patients with adolescent idiopathic scoliosis: the effect of prone positioning *Pierre Schmit*¹, John Trask¹, P. Christopher Cook², Ron El-Hawary¹ IWK Health Centre, Halifax (Canada) ²Orthopedic Department Dartmouth-Hitchcock Medical Center, Labanon (United States)

Purpose: Numerous publications have shown that prone positioning can adversely affect IVC and intra-abdominal pressures. Given that there have been 3 case reports of

ischemic hepatic events during prone scoliosis surgery, we decided to sonographically evaluate hepatic artery (HA) and portal vein (PV) blood flows in different surgical positions in patients with adolescent idiopathic scoliosis.

Materials and methods: The project was ERB approved. Sixteen females with adolescent idiopathic scoliosis (right main thoracic, >45°) were sonographically evaluated: first, in supine control position, second, in a mock surgical prone position with the abdomen hanging free with a one-piece chest pad (P1) and with a two-piece chest pad (P2) used for spinal surgery. Resistive index, diastolic and systolic velocities were measured for the main, left and right HA. Flow velocity and pressure gradients were measured for the main, left and right PV. Paired sample t-tests were used to compare control vs P1, control vs P2, and P1 vs P2.

Results: The age of the patients was 14.8 years (± 1.94) and the average scoliosis Cobb angle was 64.2° ($\pm 9.55^{\circ}$). As compared to the control position, systolic flow velocity decreased for both prone positions in the main and right PV (p<0.05). Prone positioning also decreased pressure gradients in the main and right PV (p<0.05). There was a significant increase in right HA resistive index for the P1 position (p<0.05) with a significant decrease in flow velocity in the left HA (p<0.05).

Conclusion: The decreased portal flow velocity and portal gradients observed in the prone position may be implicated in hepatic ischemia as PV delivers 75% of the liver blood supply. Right and left HA measurements show changes that are supportive, to a lesser extent of decreased arterial perfusion. Hence, prone positioning for spinal surgery, regardless of the number of chest pads utilised, impairs PV and HA blood flows.

GI-8

Evaluation by color-Doppler ultrasonography (CDU) in children benefiting from the Meso-Rex bypass (MRB) for extra-hepatic portal vein thrombosis

Cristina Lo Zupone¹, Lidia Monti¹, Arianna Bertocchini¹, Giuseppe D'Ambrosio¹, Alessandro Latini², Roberta Silvestri², Chiara Grimaldi¹, Fabrizio Gennari¹, Paolo Toma¹, Jean De Ville de Goyet¹ Ospedale Pediatrico Bambino Gesù, Rome²Policlinico Agostino Gemelli, Rome, ²Policlinico Agostino Gemelli, Rome (Italy)

Purpose: Extra-hepatic portal vein thrombosis (EPVT) is a condition in which the obstruction of the portal vein trunk results in non-cirrhotic portal hypertension (pre-hepatic type) with complications ranging from variceal hemorrhage, hypersplenism, biliopathy to growth/development deficiency or subclinical encephalopathy. MRB (a direct bypass from mesenteric to left portal vein (LPV) has been shown to restore the physiologic portal flow to the liver. This study intend to evaluate the role of CDU for assessing of patency of the shunt and intra-hepatic portal flow at the long-term.

Materials and methods: Between 2007 and 2010, 30 children affected by EPTV with recurrent bleeding from esophageal varices and/or severe hypersplenism (age range: 9 months –18 years), underwent MRB. Intra- and extra-hepatic vascular anatomy was assessed preoperatively using CDU, CT, MRI and retrograde portography. Only CDU was used for intra-operative checks, during the early (1 week) (EPO) and late post-operative period (LPO). Current follow-up ranges from 1 to 36 months.

Results: Peri-operative flow problems diagnosed at CDU led to successful immediate revision of the shunt in two cases and conversion into a meso-caval shunt in another one. We evaluated maximum flow velocity in the MRB and within the liver either at EPO and at LPO. At long-term patency of the MRB was 100% with 27/29 MRB patients showed resolution of CDU signs of portal hypertension.



Conclusion: This study confirms that: 1- MRB restores normal portal flow through the liver and cures portal hypertension; 2-CDU alone is adequate to efficiently check bypass patency and portal flow at long-term; 3- Intra- and immediate post-operative CDU monitoring is essential for achieving best clinical results.

GI-9

Impact of specialised ultrasound examination on the investigation of infants with neonatal cholestasis

Terry Humphrey, Narasimharaju Dantuluri, Sanjay Rajwal, Helen Woodley, Naved Alizai, Patricia McClean Leeds General Infirmary, Leeds (United Kingdom)

Purpose: No single investigation can confirm the diagnosis of biliary atresia (BA) with certainty. Between 2002 and 2005 we investigated the use of specialised abdominal ultrasound scans (USS), looking for specific ultrasound features to differentiate infants with BA from those with other causes of cholestasis. Combining these features gave an overall accuracy in diagnosis of 98% and this method has been adopted in our unit. The aim of this study was to assess if the incorporation of this technique has reduced the need for invasive investigations.

Materials and methods: Medical notes were reviewed retrospectively from 2 groups of 50 consecutive infants referred for investigation of neonatal cholestasis before (Gp 1) and after (Gp 2) the USS study. Patient demographics, stool colour, laboratory tests, radiological and histological reports and final diagnoses were recorded. The number and types of investigations needed to exclude a diagnosis of BA were noted.

Results: Notes were available for 48 infants in Gp 1 (24 male, median age 5 weeks [range 1–19 weeks]) presenting between Apr. 2000 and Feb. 2002, and 49 infants in Gp 2 (29 male, median age 6 weeks [range 1–20 weeks]) presenting between Nov. 2005 and Jul. 2007. 10 infants in Gp 1 and 7 infants in Gp 2 had a final diagnosis of BA. All infants had the standard first line laboratory investigations for neonatal cholestasis and an USS; standard USS in Gp 1, specialised USS in Gp 2. The number of other investigations such as scintigraphy or operative cholangiogram required to confirm or refute a diagnosis of BA did not differ significantly between the two groups. However there was a significant reduction in the number of biopsies, from 22 in Gp1 to 4 in Gp2 (p<0.05).

Conclusion: The introduction of specialised USS into our routine investigation of infants referred with neonatal cholestasis has been associated with a significant decrease in the number of liver biopsies performed to diagnose BA.

GI-10

Abdominal sonography in the preoperative diagnosis of extrahepatic biliary atresia (EHBA) in children

Akshay Saxena, Vinayak Mittal, Kushaljit Sodhi, Baburam Thapa, Katragadda Rao, Ashim Das, Niranjan Khandelwal Post Graduate Institute of Medical Education and Research, Chandigarh (India)

Purpose: To assess the role of abdominal sonography in the pre operative diagnosis of extrahepatic biliary atresia (EHBA) in children <90 days of age.

Materials and methods: This was a prospective study with clearance from ethical committee of our institute. Informed written consent was obtained in all cases. Abdominal sonography was performed in 99 children of age <90 days with biochemically proven conjugated hyperbilirubinemia. All children were examined after 4 h of fasting. The children were evaluated for triangular cord (TC) sign, presence and morphology of gall bladder (GB),

GB contraction after oral feed, common bile duct (CBD), liver size and echotexture, spleen size, caliber of right branch of hepatic artery, caliber of right branch of portal vein and ratio of caliber of right branch of hepatic artery and right branch of portal vein. Final diagnosis of EHBA was made on preoperative cholangiogram. The diagnostic performance of various parameters in isolation and in combination was evaluated.

Results: There were 68 males and 31 females. Final diagnosis of EHBA was made in 30 cases. TC sign had sensitivity, specificity, PPV, NPV and accuracy of 23.3%, 97.1%, 77.8%, 74.4% and 74.7% respectively. GB was not visualized in 7 cases all of which had EHBA. Sensitivity, specificity, positive predictive value (PPV), Negative predictive value (NPV) and accuracy of abnormal GB for diagnosis of EHBA were 83.3% %, 82.6%, 67.6%, 91.9% and 82.8% respectively while for non contraction of GB after oral feed were 87%, 72.5%, 51.3%, 94.3% and 76.1% respectively. Non-visualized CBD had sensitivity, specificity, PPV, NPV and accuracy of 93.3%, 47.8%, 43.8%, 94.3% and 61.6% respectively. The enlarged right hepatic artery had sensitivity, specificity, PPV, NPV and accuracy of 80%, 49.3%, 40.7%, 85% and 58.6% respectively while increased ratio of right hepatic artery diameter to right branch of portal vein diameter had sensitivity, specificity, PPV, NPV and accuracy of 76.7%, 46.4%, 38.3%, 82.1% and 55.6% respectively. Negative TC sign with normal GB morphology had 83.3% sensitivity and 82.6% specificity for ruling out EHBA with NPV of 91.9%.

Conclusion: Comprehensive sonographic evaluation can help in segregating babies (age <90 days) who are at high risk of having EHBA from those who are at low risk.

GI-11

Delineation and characterization of pediatric focal liver lesions using contrast-enhanced ultrasound (CEUS): preliminary results

Joseph Jacob, Preena Patel, Annamaria Deganello, Dino Hadzic, Maria Sellars, Paul Sidhu

Kings College Hospital, London (United Kingdom)

Purpose: To determine the accuracy of CEUS in characterizing pediatric focal liver lesions (FLL) in comparison to computerized tomography (CT), magnetic resonance (MR) and positron emission tomography (PET) imaging or histology as the reference standard.

Materials and methods: Children referred for assessment of FLL over a 3 year period underwent a CEUS examination following fully informed parental consent. CEUS was performed by experienced examiners using a Siemens (Mountain View CA) S2000, a 4 C1 transducer, and 1.2–2.4 mls of SonoVue (Bracco SpA Milan). A standard multiphase CEUS was performed and recorded with all children undergoing further imaging or follow-up with ultrasound. A comparison of the CEUS results, arrived by consensus, was compared to the reference standard to ascertain the accuracy of CEUS in characterizing FLL.

Results: A total of 20 children, (Female = 11, Male = 9, mean age 13.5, range 15 mths- 17 yrs) were examined with no contrast reactions recorded. 15 children were referred for assessment of a FLL in chronic liver disease, 2 for suspected metastases (treated primary malignancy) and 3 with FLL and no relevant clinical history. Following CEUS, the following were identified: regenerative nodules (n=7), focal fatty sparing (n=5), hepatic adenoma (n=2), hemangioma (n=3), metastases (n=1), focal fatty infiltration (n=1) and focal nodular hyperplasia (FNH) (n=1). On comparison with CT, MR, PET imaging or biopsy, 16/20 (80%) demonstrated full concordance with CEUS. In 2 discordant cases, neither CT nor



MR imaging could characterize the nature of the FLL and in the other 2 cases other modalities diagnosed a different benign lesion to CEUS.

Conclusion: These findings demonstrate the usefulness of CEUS in characterizing FLL compared to traditional methods. CEUS represents a viable, safe, radiation free, cost-effective method for the assessment of FLL in this group and most importantly has the potential of reducing the radiation burden in a young population.

GI-12

Rapid MRI techniques for quantification of hepatic fat content in pediatric patients with non-alcoholic fatty liver disease

Jie Deng, Mark Fishbein, Cynthia Rigsby, James Donaldson Children's Memorial Hospital, Chicago (United States)

Purpose: Nonalcoholic fatty liver disease (NAFLD) is the most common liver disease among obese children and adolescents in North America. Liver fat quantification using MRI has evolved greatly in the past few years. The purpose of this study was to compare the conventional 2-point Dixon imaging (in and opposed phase) and LIPO-Quant (Liver Imaging of Phase-related signal Oscillation and Quantification) methods for liver fat fraction measurement.

Materials and methods: A phantom model with known fat fraction of 2.5-50% was used to test the measurement accuracy. Studies were performed on 4 healthy volunteers and 8 patients (13±2 yrs) referred by pediatric NASH clinic. Imaging was acquired on a Siemens 1.5 T AVANTO scanner. Two-point Dixon methods included 2D FLASH and 3D VIBE with small flip angle (10° and 15°) to reduce T1 effect. Multi-echo GRE images were acquired in 2 breath-hold: TR=122 ms, TE=2.3-13.8 ms, Δ TE=2.3 ms, flip angle=10°. In the Dixon method, water and fat signals were derived by the sum and difference of in and opposed phase images. LIPO-QUANT separated water and fat signals using non-linear fitting of the signal oscillation. It constructed the fat spectrum with single and multiple peaks (centered at 2.1, 1.3 and 0.9 ppm). It also corrected for T2* effect, in the situation of co-occurrence of hepatic steatosis and siderosis. Fat fraction (FF) was calculated as Sfat/ (Swater+Sfat).

Results: In the phantom model, LIPO-QUANT modeling with single or three fat peaks and two T2* (T2*water and T2*fat) provided the most accurate measurements for FF≥5%. For FF≤ 2.5%, the most robust method is the triple-echo and 3-peak, 1-T2* model. 2D FLASH underestimated all FF. In healthy volunteers, FF=1.9±0.6%. FF in 8 patients was $9.4\pm6.6\%$ (FLASH), $14.9\pm8.4\%$ (VIBE) and $14.1\pm5.9\%$ (LIPO-QUANT). There were significant differences for FLASH vs.VIBE and FLASH vs. LIPO-QUANT. However, VIBE and LIPO-QUANT were not significantly different (p=0.38).

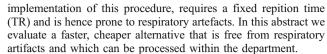
Conclusion: LIPO-QUANT provided a promising method for rapid and accurate fat fraction measurement in NAFLD patients. Future studies will investigate the reproducibility and its correlation with gold-standard biopsy results.

GI-13

Measuring liver iron concentration with breath-hold gradient recalled echo (GRE) imaging

Richard Jones, Laura Hayes, Damien Grattan-Smith ¹CHOA/Emory, Atlanta (United States)

Introduction: Measurement of liver R2 is an accepted, non-invasive, MRI-based method of determining liver iron concentration (LIC) that uses previously established calibration data to calculate the LIC from the measured R2 value (St Pierre et al. Blood. 105:855; 2005). Ferriscan, the commercial, web-based



Materials and methods: We developed modified GRE sequences which acquire trains of 12, 6 or 4 echoes after each RF pulse and which, for the shorter echo trains, acquire interleaved echo times. Each acquisition is acquired in a single breath-hold in order to minimize respiratory artefacts. The analysis of the GRE data is carried out using in-house software written in interactive data language (IDL) in which a user manually defines the liver, a pixel by pixel R2* fit is then performed for all pixels within the liver. A histogram of the R2* values is calculated and fitted to a normal distribution. The extrapolation of the LIC from the derived R2* was based on the calibration data published by Wood et al. (Wood et al. Blood 106:1460; 2005). Ferriscan data were also obtained from the same subjects.

Results: For the initial 25 subjects the LIC derived with the modified gradient echo sequence were well correlated (r2=0.94) with the Ferriscan results. A Bland-Altman analysis of the LICs from the Ferriscan and the modified GRE method showed that the mean differences were not significantly different from zero (-0.17 ± 1.03), implying that the modified GRE method can accurately measure LIC. Conclusion: The modified GRE sequence provides a rapid, artifact free means of determining the LIC and the results obtained are in good agreement with those obtained using Ferriscan. The data analysis can be performed rapidly by a technologist within the department resulting in a more rapid report turn-around and a considerable cost saving.

GI-14

Limitations of using linear fitting after logarithmic transformation to estimate relaxation rates in iron-loaded liver

Seth Friedman¹, Randolph Otto¹, Ferguson Mark¹, Kenneth Marro², Dennis Shaw², Ed Weinberger²

¹Seattle Childrens, Seattle, ²University of Washington, Washington (United States)

Purpose: MRI is used as a front-line tool to measure changes in relaxation that occur in the liver with iron loading. Typically, a number of echoes (10–12) are acquired and curve-fitting performed. Most commercial scanners, and some software, use a linear fit after logarithmic-transformation (LFLT) to generate a relaxation estimate (T2*). Because most centers do not collect their own paired MRI-biopsy data, literature equations are employed to convert T2* into an iron concentration. Unfortunately, these equations are derived from non-linear fit methods. While there is high correspondence between LFLT and non-linear T2* estimates when iron levels are low, substantial divergence in results occur as iron-levels increase. Using human and simulation data, this report quantifies the degree of error that can occur, and suggests guidelines for future use.

Materials and methods: After IRB approval, LFLT and non-linear methods were compared in a cohort of twenty pediatric patients (7 F/13 M, 14.5±7.5 years) that were evaluated for hepatic iron overload. Simulation analyses in MATLAB (Mathworks, Natick MA) were performed to characterize the two main factors impacting derived results.

Results: In human subjects, the T2* curve calculated using LFLT demonstrates significant deviation from non-linear methodology at T2* of 5 ms. This error results in consistent under-estimation of liver iron of a magnitude or more as iron levels increase. Simulation analyses demonstrated the primary factors for these differences: a) noise truncating the mono-exponential function, and b) multiple signal components present in iron-loaded tissue impacting fit concordance.



Conclusion: LFLT results in erroneous estimation of tissue relaxation at moderate to high levels of iron overload. As LFLT methods are often implemented to generate automated maps, these errors have the potential to go unappreciated. Therefore, while LFLT fitting will provide reasonable results in patients with none to minimal iron loading, we suggest that it should not be used for routine patient care.

GI-15

Does visceral fat volume predict duodenal compression in superior mesenteric artery (SMA) syndrome?

Urmil Mehta, *Owen Arthurs*, Pat Set University of Cambridge, Cambridge (United Kingdom)

Purpose: SMA syndrome is a rare condition in which the duodenum becomes compressed by an abnormally acute angle between the superior mesenteric artery and aorta, causing abdominal pain and vomiting. In this study, we measured the duodenal distance between SMA and aorta, and abdominal fat distribution in asymptomatic children undergoing abdominal CT in order to define the normal range.

Methods: We retrospectively identified all childhood abdominal CT examinations in our department over a 4 year period (2005–2008). We measured SMA to aorta distance at the midpoint of the third part of the duodenum ("duodenal distance") on 3D reconstructed sagittal/oblique slices. Total and visceral intraabdominal fat at the level of the umbilicus were measured at the level of the umbilicus using automated software.

Results: The mean duodenal distance in 205 consecutive paediatric abdominal CT examinations was 11.3 ± 4.8 mm (range 3.6-35.3 mm). There was no significant gender difference (males, 11.5 ± 4.5 mm, females 11.1 ± 5.3 mm; p=0.56), nor significant correlation between duodenal distance and age (p=0.66). Duodenal distance was accurate to within 1.3 mm (inter-observer variability). There was a weak but significant correlation between duodenal distance and total fat volume (Y=1.24 X+11.7; R=0.23; p<0.005) as well as visceral fat volume (Y=0.39 X+1.88; R=0.32; p<0.001).

Conclusion: There is a wide range of normal duodenal distances in children, which correlate weakly with visceral fat and total body fat volume. Using a duodenal distance definition of <8 mm (Unal et al., 2005) would diagnose 42 of our 205 asymptomatic children (20%) with SMA compression. Our findings suggest that apparent duodenal compression by a narrow SMA angle is not the sole contributor to this rare syndrome.

GI-16

Differentiation between Hirschsprung alied disease and Hirschsprung disease in childhood with barium enema Shuochun Wu, Xinyu Yuan

Capital Institute of Pediatrics, Beijing (China)

Purpose: To compare the barium enema features between Hirschsprung alied disease (HAD) and Hirschsprung's disease

Materials and methods: Nineteen cases of HAD aged from 30 days to 10 years (median age 14 months) and nineteen cases of HD aged from 42 days to 8 years (median age 8 months) were randomly enrolled in this study. All cases underwent a barium enema examination prior to operation. The X-ray data were reviewed to calculate the appearance rate of the narrow zone, 'truncation sign', spasm notch, and R/C ratio (the longest diometer of rectum/that of colon) respectively by two experienced pediatric radiologists independently. Otherwise, the position of barium retained was observed. Statistically, the parameters of both groups

were compared by SPSS11.5, and P<0.05 was considered to be significant.

Results: Appearance rate of the narrow zone: group HAD is 9/19, group HD is 18/19, c2=10.364, P=0.001<0.05, statistical significance is found between the two groups. Appearance rate of the 'truncation sign': group HAD is 4/19, group HD is 1/19, P=0.34>0.05,no statistical significance is found between the two groups. Appearance rate of the spasm notch: group HAD is 3/19, group HD is 1/19, P=0.604>0.05,no statistical significance is found between the two groups. R/C ratio: group HAD is 0.42±0.15, group HD is 0.29±0.12, t=2.892, P=0.006<0.05, statistical significance is found between the two groups. Position of barium retained in HAD: distal descending colon 37% (7/19), distal sigmoid colon 5% (1/19), distal transverse colon 5% (1/19), total colon 32% (6/19). In HD: distal descending colon 16% (3/19), distal sigmoid colon 68% (13/19), distal rectum 16% (3/19).

Conclusion: There are differences between HAD and HD on barium enema though they have similar clinic experience. HAD appears less narrow zone and less R/C ratio than HD; HAD and HD have similar appearance rate of the 'truncation sign' and the spasm notch. Most position of barium retained of HAD is distal descending colon, while that of HD is distal sigmoid colon. Therefore, position of barium retained should be a helpful parameter for differentiation.

GI-17

MRI predictors of treatment response for fistulizing Crohn's disease in pediatric patients.

Anuradha Shenoy-Bhangle¹, Katherine Nimkin, Dana Goldner, Esther Israel, Michael Gee

Masachusetts General Hospital, Boston (United States)

Purpose: To evaluate MRI predictors of clinical response in pediatric Crohn's patients with perianal disease.

Materials and methods: We performed a retrospective analysis of pediatric patients with Crohn's disease who underwent MRI for assessment of perianal fistulae between September 2003 to February 2010. The parameters studied included number and type of fistula according to Park's classification; length of each fistula and presence of associated abscess. In patients who had follow up MRI, response to treatment or disease worsening was analyzed. Clinical response was determined based on presence or absence of perianal pain and discharge on subsequent follow up visits.

Results: 26 patients(15 male and 11 female; mean age range 17 years) were included. Of these, 22 had a follow up MRI while 4 exhibited clinical remission and did not require repeat imaging. All fistulae were well visualized on the T2 fat sat and T1 fat sat post gadolinium sequence. According to Park's classification, out of the 40 fistulae in 26 patients, 4 were noted to be suprasphincteric, 31 transsphincteric and 5 were intersphincteric. 14 patients had multiple fistulae with individual length in the range of 0.5 to 4.5 cm. 18 patients had an associated perianal abscess. Of the 26 patients, 18 had clinical response, 1 was lost to follow up. MR imaging features associated with better prognosis include presence of a single fistula, cumulative length of fistula less than 2.5 cm and absence of an associated abscess. In addition, there is a significant positive correlation between lack of disease progression on subsequent MRI and clinical response.

Conclusion: MRI plays a critical role in the clinical management of pediatric fistulizing Crohn's disease. In addition to anatomic delineation, MR assessment of fistula number and length as well as presence of an associated abscess predicts treatment response. Stability of fistula on follow up MRI correlates significantly with subsequent clinical response. These results suggest a role for serial



MRI exams for determining therapeutic susceptibility and early assessment of response.

GI-18

Imaging features of irreducible or atypical intussusception

Sophie Swinson, Annmarie Jeanes

Leeds General Infirmary, (United Kingdom)

Purpose: Diagnosis of intussusception with ultrasound has a sensitivity of up to 100%. Fluoroscopic air reduction is widely used as first line treatment and published reduction rates vary (65-90%). Cases of failed air reduction or those unsuitable for the procedure undergo surgical reduction or resection. The incidence of paediatric intussusception appears to be declining with fewer idiopathic, reducible cases resulting in an increasing proportion of atypical cases. Previously described ultrasound features of decreased reducibility include reduced Doppler flow, trapped fluid and atypical location. The aim of this study was to review practice at a large tertiary referral centre highlighting the ultrasound characteristics of atypical or irreducible cases. Materials and methods: A retrospective review of all cases of intussusception over a 3 year period was carried out. Ultrasound findings, reduction rate, complications, surgical notes and histopathology were reviewed.

Results: Thirty nine cases were included. Eight cases (21%) had a pathological lead point (2 lymphoma, 4 Meckel's diverticulum, 1 hamartomatous polyp and 1 Henoch Schönlein purpura), which is higher than previously quoted in the literature (10%). Twenty one of 31 attempted air reductions were successful (68%). There were no perforations. Five of ten failed reductions and all 8 cases going straight to theatre required subsequent resection due to infarcted bowel or lead points. The presence of reduced Doppler flow was significantly associated with failed reduction (p=0.01). Trapped fluid and an atypical position in the abdomen were also associated with non-reduction but this did not reach statistical significance (p=0.11 and p=0.22 respectively).

Conclusion: The number of intussusception cases over the 3-year study period is smaller than might be expected and our reduction rate is at the lower end of that quoted in the literature. The latter may be due to an increase in the proportion of atypical cases, with a higher than expected number of lead points. Reduced Doppler flow was significantly associated with failed air reduction.

GI-19

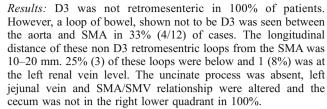
Is a retromesenteric location of the third portion of duodenum an indicator of malrotation?

Darshit Thakrar, Cynthia Rigsby, Katherine Barsness, Emma Boylan, James Donaldson

Children's Memorial Hospital, Chicago (United States)

Purpose: Ultrasound (US) of the retromesenteric position of the third portion of the duodenum (D3) has been suggested as an indicator for diagnosing or excluding malrotation in newborns. The purpose of this study is to validate this by CT in a broader population of children with surgically proven malrotation.

Materials and methods: Retrospective review of 111 patients between 2001 and 2010 with surgically proven malrotation. 12 patients also had abdominal CT (ages 9 days to 16 years). CT studies were reviewed by 3 pediatric radiologists for the suggested findings of malrotation including D3 position, its relationship to the aorta and superior mesenteric artery (SMA), uncinate process, left jejunal and renal veins. SMA/superior mesenteric vein (SMV) relationship and cecal position were also evaluated. Any bowel loop seen between the aorta and SMA was assessed for its specific location.



Conclusion: Absence of a retromesenteric D3 appears to be a reliable indicator for diagnosing malrotation. A loop of small bowel known not to be D3 by CT was identified between the aorta and SMA (33%) and at the level of the left renal vein (8%) with known malrotation. Caution should be exercised when excluding malrotation to assure that all suggested US criteria are met including D3 location between SMA and aorta associated with a normal uncinate process, left renal vein and left jejunal vein. If these criteria are met, excluding malrotation appears to be reliable.

GU-1

Uterus didelphys with unilateral vaginal atresia: is multicystic dysplastic kidney the precursor of "renal agenesis" and the key to early diagnosis of this genital anomaly?

Ingmar Gaßner, Ursula Kiechl-Kohlendorfer, Theresa Geley, Kathrin Maurer

Medical University Innsbruck, Innsbruck (Austria)

Purpose: Uterus didelphys with obstructed hemivagina (UDWOH) and ipsilateral renal agenesis is a distinct but rare entity. The purpose of this article is to show both the association between UDWOH and multicystic dysplastic kidney disease (MCDK) detected in neonates and the usefulness of sonography with fluid instillation into the vagina in diagnosing this genital anomaly early and reliably in females with MCDK.

Materials and methods: Our patients were five female neonates with MCDK that had been detected in utero. We performed sonography of the inner genitalia in each girl before and after filling the vagina with saline solution.

Results: In all five patients, sonographic examination revealed uterus didelphys with obstruction of one of the vaginas ipsilateral to the MCDK. In three patients a dilated ureter originating from the MCDK and extending to the level of the vagina could be clearly demonstrated, in one of them even the ureteric insertion into the atretic vagina.

Conclusion: MCDK is a key to early diagnosis of UDWOH that hastens the provision of appropriate treatment. The neonatal period provides a unique opportunity for detecting uterine anomalies by sonography. MCDK usually involutes and eventually mimics renal agenesis later in life.

GU-2

Prognostic implications of MR urography in the evaluation of ureteropelvic junction obstruction

Damien Grattan-Smith¹, Richard Jones², Wolfgang Cerwinka², Stephen Little², Hal Scherz², Andrew Kirsch²

¹Children's Healthcare of Atlanta at Scottish Rite, 1001 Johnson Ferry Rd, Atlanta, United States, ²Children's Healthcare of Atlanta

Purpose: To determine the prognostic value of MR urography in assessing UPJ obstruction before and after pyeloplasty

Materials and methods: 45 children with unilateral hydronephrosis were evaluated with MR urography both before and after technically successful pyeloplasty. Their ages ranged from 3 months to 14 years. A successful pyeloplasty was defined by rapid calyceal excretion of contrast, improved hydronephrosis



and drainage from the renal pelvis. The pre-operative scans were classified as decompensated if there was evidence of physiologically significant obstruction (PSO) manifested by delayed calyceal excretion of contrast and asymmetric renal function. If there was no evidence of PSO they were classified as compensated systems. Both volumetric (vDRF) and Patlak differential function (pDRF) were assessed pre and post-operatively and the asymmetry index calculated.

Results: 19 children were classified as having decompensated hydronephrosis and 26 were considered to have compensated hydronephrosis. The mean asymmetry index for the decompensated group was 0.17 and for the compensated group 0.03. There was significant improvement in the pDRF in the decompensated group following pyeloplasty with little change in function in the compensated group. The asymmetry index was an important indicator of the degree of functional derangement and for potential improvement. Underlying uropathy was a confounding issue that was particularly significant in the group with congenital hydronephrosis.

Conclusion: MR urography has the ability to predict the outcome following successful pyeloplasty: children with decompensated hydronephrosis show significant improvement. Children with compensated hydronephrosis show little functional improvement following pyeloplasty and these children should be followed rather than undergo operative treatment.

GU-3

A novel method of identifying ureteropelvic junction obstruction: a comparative study of imaging modalities in assessing renal function and degree of obstruction in a swine model

Jeanne Chow, Courtney Rowe, Brian Minnillo, Alan Retik, Hiep Nguyen

Children's Hospital Boston, Boston (United States)

Purpose: There is currently no gold standard test for diagnosing clinically significant ureteropelvic junction obstruction (UPJO). We introduce the novel use of a fluorescent contrast agent for the urinary tract and compare it to commonly used imaging techniques in swines with UPJO.

Materials and methods: Twenty swine underwent partial or complete unilateral ureteral obstruction: 5 complete obstruction, 5 partial, 5 complete obstruction for 2 days followed by release of obstruction, and 5 sham. Groups were survived for 3–7 days(short term), 10–14 days(long term), and 28–30 days (chronic dilation without obstruction). All subjects underwent imaging ultrasound (US), magnetic resonance urography (MRU), intravenous pyelography (IVP), and MAG-3 lasix renogram, as well as the fluorescence after ligation (days above) and pyeloplasty repair (small subset). Fluorescent images and calculated parameters were compared to the other imaging modalities. Histology was obtained in all cases.

Results: Our models of UPJO could be distinguished by US, MRU, IVP, MAG-3 and fluorescence. Subjective assessment of the images obtained from fluorescent imaging provided excellent anatomic details similar to MRU and US. Detailed visualization of urinary flow could be performed continuously without concern of radiation exposure. Measurement of fluorescent parameters (perfusion time, peak time, relative renal fluorescence (RRf), fluorescent intensity, ureteral transit time) provided objective assessment of renal function and the degree of obstruction similar to renography and MRU. Perfusion time and peak time increased significantly with the degree of obstruction. The degree of obstruction correlated with decreasing absolute amount of renal fluorescence from the obstructed kidney and decreasing RRf of the obstructed kidney, similar to diuretic renography.

Conclusion: Using a large animal model, we demonstrate that dynamic fluorescent imaging can determine the degree of ureteral obstruction based upon subjective and objective measurements.

GU-4

Defining urinary collecting system distension in ultrasound reports: a survey of referring physicians

Seth Crapp, J. Herman Kan, Marta Hernanz-Schulman, Kathy Jabs, John Brock, John Thomas

Monroe Carell Jr. Children's Hospital at Vanderbilt University, Nashville (United States)

Purpose: The terms employed by radiologists to describe various degrees of urinary collecting system distension identified on renal sonography can be variable and the meaning intended by the radiologist may not coincide with the understanding of referring physicians from various clinical backgrounds. The purpose of this study is to determine how referring physicians interpret various commonly used terms by radiologists to describe distension of the ureter and the renal collecting system.

Materials and methods: After IRB approval, an on online survey was distributed to 393 pediatric practitioners. The survey asked the practitioners' interpretation of the terms: hydronephrosis, hydroureter, megaureter, and pelvocaliectasis.

Results: There were 89 respondents. Pediatricians comprised 95% of respondents, 58% attending-level. Hydronephrosis was interpreted as obstruction only by 19%, as reflux by 2.3%, and as reflux or obstruction by 42%; 24% thought it could also refer to an extrarenal pelvis or other pathology. Hydroureter was defined as non-specific dilatation of the ureter by 65%, with obstruction or reflux <4% each; megaureter was described as "the same as hydroureter" by 59%, but 4% thought this term synonymous with a normal ureter. Pelvocaliectasis had the widest spread in clinician interpretation, with 33% considering it synonymous with minimal hydronephrosis, 21% thought it was "other pathology", 27% thought it could refer to reflux, obstruction, extrarenal pelvis, minimal hydronephrosis or other pathology, and 4% thought this term synonymous with normal anatomy.

Conclusion: Imaging descriptors of dilatation of the urinary tracts may lead to diverse and sometimes unintended diagnostic implications. Our findings support continued efforts to structure and standardize the radiology lexicon and radiology report.

GU-6

Predictors of vesicoureteric reflux in infants with urinary tract infection using National Institute for Clinical Excellence (NICE) criteria

Neil Gupta, Osama Abulaban, Tom Goodfellow, Emma Helm University Hospitals Coventry and Warwickshire NHS Trust, Coventry, (United Kingdom)

Purpose: To examine the relative value of the UK NICE criteria for UTI for prediction of vesicoureteric reflux in infants.

Materials and methods: A retrospective review was performed of all micturating cystourethrogram (MCUG) examinations performed for UTI in our large secondary care setting between January 2006 and September 2010. Inclusion criteria included confirmed UTI and age less than 6 months at the time of infection. Indication for MCUG was analysed according to the NICE criteria for recurrent or atypical UTI. Atypical UTI was defined as septicaemia, atypical organism (non-E.Coli), abnormal ultrasound, raised creatinine, poor urine flow or seriously ill. Seriously ill was defined by the NICE Feverish Illness in Children guideline, which uses a traffic light system for signs and symptoms to classify the severity of illness in children.



Data were obtained from the radiology request card, microbiology results and the electronic patient record. Chi-squared test was used to compare the incidence of abnormal MCUG according to each of the NICE indications.

Results: A total of 126 MCUG examinations were performed in infants with prior UTI. Indications for the test were as follows: seriously ill (59); recurrent UTI (7); abnormal ultrasound (14); atypical organism (25) septicaemia (14), raised creatinine (1) and poor urine flow (1). Overall, vesicoureteral reflux (VUR) was seen in 40/126 (31%) of examinations with grades including 16 (40%) grade II, 15 (37.5%) grade III, 6 (15%) grade IV and 3 (7.5%) grade V. Non-E. Coli UTI was associated with a significant increased incidence of VUR (33% vs 14%, p=0.02, RR 2.3) and age less than 1 month was also significant (77% vs 28%, p=0.002, RR 2.8).

Conclusion: In our population of 126 infants, the strongest predictors of VUR were aged less than 1 month at time of infection and non-E Coli UTI. None of the other criteria was independently associated with increased risk of VUR.

GU-7

The role of second-generation echo-enhanced voiding urosonography in the first year of life

Damjana Kljucevsek¹, Mojca Tomazic², Nina Battelino³, Rajko B Kenda³, Tanja Kersnik Levart³

¹Universty Medical Centre Ljubljana, Children's hospital, Ljubljana ²Medical Centre Ljubljana, ³University Clinical Centre, Ljubljana, (Slovenia)

Purpose: The sensitivity of echo-enhanced voiding ultrasonography (VUS) in detecting vesicoureteric reflux (VUR) has greatly improved by the development of contrast-specific ultrasound (US) techniques and the introduction of second-generation US contrast agent. The purpose of our prospective study was to evaluate, whether echo-enhanced VUS using improved US techniques and the second-generation US contrast agent can safely replace voiding cystourethrography (VCUG) in detecting VUR in the first year of life. The predictive value of US urinary tract findings in selecting the most appropriate cystography was also evaluated.

Materials and methods: 66 children, 35 boys and 31 girls, aged 5 days to 1 year (mean 5 months) were enrolled in the study. In each child the urinary tract US and echo-enhanced VUS were performed, followed immediately by VCUG using the same urinary catheter. US findings were assessed as normal or mildly, moderately or severely abnormal.

Results: During the study 66 children were evaluated, contributing 132 potentially refluxing renal units. According to VCUG, VUR was present in only 16/132 renal units, and according to echoenhanced VUS in 42/132 renal units. Considering VCUG as the reference method to detect VUR, the sensitivity of echo-enhanced VUS, regardless of the grade of VUR was 100% and the specificity 77, 5%. According to US findings, 85/132 renal units were found to be normal and 47/132 abnormal, of which 23 were severely, 8 moderately and 16 mildly abnormal. Abnormal urinary tract US findings were not associated with a higher incidence of VUR, but the severity of US changes were associated with higher grade of VUR. The echo-enhanced VUS was shown superior to VCUG in detecting VUR no matter of the severity of US findings of the upper urinary tract.

Conclusion: The second generation echo-enhanced VUS could safely replace VCUG in children less than one, including the boys after first urinary tract infection with normal voiding pattern no matter what the degree of US abnormality of the upper urinary tract.



GU-8

Voiding urosonography with a second-generation contrast agent as a first step study for the diagnosis and grading of vesicoureteric reflux in children

Frederica Papadopoulou¹, Katerina Ntoulia¹, Fotis Papachristou², Ekaterini Siomou¹, Kostantinia Sarantidou³, Kassa Darge⁴

¹Ioanninina University Hospital, Thessaloniki, ²Aristotle University Thessaloniki (Greece), ³IKA Organization Thessaloniki, ⁴Children's Hospital of Philadelphia, Philadelphia (United States)

Purpose: To assess the efficacy of Voiding Urosonography (VUS) with a second-generation contrast agent (CA) as a first step study for the diagnosis and grading of vesicoureteric reflux (VUR) in children

Materials and methods: Two hundred and ten consecutive children (86 boys, 124 girls, mean age 33.4 m) with 421 kidney-ureter-units (KUU) were evaluated with VUS to rule out (n=180) or follow-up VUR (n=30). In all children VUS was performed with a contrast-specific-harmonic-imaging-mode and 1 ml of a second generation CA (Sonovue, Bracco, Milan), according to ESPR working group recommendations. The VUS was recorded on digital clips and read twice by two blinded radiologists. The diagnosis in discordant cases was reached by consensus. The intraobserver and interobserver reproducibility was calculated by kappa coefficient.

Results: VUR was diagnosed in 178 KUU (42%) from 87 (41%) patients (34/84 boys and 53/126 girls). The rate of reflux was not significantly correlated with the sex, age, clinical indications and the presence or side of dilated pelvis. VUR was significantly more common in duplex than in single kidneys (p<0.001). The intraobserver and interobserver reproducibility was excellent for the detection of VUR (k>0.85) and moderate to excellent for the grading of VUR (k=0.75–0.84).

Conclusion: VUS with a second generation CA is an efficient first step study for the diagnosis and grading of VUR in children and it can reliably be used as an alternative radiation-free imaging method for this purpose.

GU-9

Voiding urosonography: normal and abnormal appearance of the urethra

Carmina Duran Feliubadaló, Luis Riera Soler, Cesar Martin Martinez, Francesc Novell Teixido UDIAT-CD, Sabadell (Spain)

Purpose: Voiding urosonography (VUS) enables high quality morphologic studies of both the upper urinary tract and male urethra. The main purpose of this work is to demonstrate the diagnostic capacity of VUS for congenital anomalies of the urethra or related conditions.

Materials and methods: Between October 2005 and May 2009, we performed VUS in 261 boys (age range 2 days–16 years). We used a 6–4 MHz convex transducer to study the entire urinary tract including the urethra through a transperineal and/or transpelvic approach. To perform VUS, we used a specific harmonic imaging mode based on pulse inversion with a predetermined low (0.16–0.22) mechanical index and administered a galactose-based contrast agent. During voiding, we focused on whether there was adequate distention and homogeneous caliber of the whole urethra, as well as continuous progression of the contrast material. If any deviation from the normal appearance of the urethra was observed at VUS, voiding cystourethrography (VCUG) was performed to confirm the findings.

Results: Pathological urethral findings in newborns: 5 patients studied for oligohydramnios and prenatal hydronephrosis were diagnosed with posterior urethral valves; 2 patients with scrotal hypospadias were diagnosed with diverticulum of the prostatic utricle (one in the context of WARG syndrome). Pathological urethral findings in boys: two 7 and 16-year-old boys with difficulty in urinating and recurrent infections were respectively diagnosed with anterior urethral valves and congenital stricture of the bulbar urethra. In all these cases, the findings at VUS and VCUG showed good correlation. Variants of normality were also identified with VUS: a small prostatic utricle and one Cobb's Collar. Moreover, 3 ureteroceles were identified with VUS, making it possible to rule out ureterocele prolapse which could cause bladder outlet obstruction.

Conclusion: VUS not only enables the correct morphological study of the male urethra, but it also enables the specific diagnosis of congenital urethral anomalies. In conclusion, VUS is as accurate as VCUG and spares the patient's pelvis and gonads from radiation.

GU-10

The Mickey Mouse sign: a useful sonographic finding in the diagnosis of torsion of the testicular appendages (TTA). *Anna Ben Ely*, Ricardo Faingold, Guilherme Cassia Montreal Children's Hospital McGill, Montreal (Canada)

Purpose: The purpose of the study was to evaluate the significance of the sonographic Mickey Mouse (MM) sign in the diagnosis of torsion of the testicular appendages (TTA).

Materials and methods: 28 cases with a diagnosis of TTA from 2008 to 2010 were retrospectively reviewed. Age range was 36 days to 14 years, mean 9.04 years. All sonographic exams were performed with a standard technique, including a coronal oblique view. This view depicted the upper pole of the testis, the epididymal head and the torsed testicular appendage on the same plane thus resembling the appearance of Mickey Mouse.

Results: The MM sign was demonstrated in 27 of the 28 cases (96.4%) with the use of the coronal oblique view: 17 cases (60.7%) left-sided and 11 cases (39.3%) right-sided. All showed an avascular extratesticular nodule (3–11 mm, mean 6.3 mm). Secondary inflammatory changes included: thickened epididymis in 26 cases (92.9%), increased blood flow to epididymis/testis in 25 (89.3%), scrotal wall edema in 25 (89.3%) and hydrocele in 24 cases (85.7%). Conclusion: Our study shows that the MM sign is very useful in the diagnosis of TTA and was demonstrated in 96.4% of the cases. Adding the coronal oblique view to routine examinations increases the reproducibility of the MM sign and awareness of this important diagnosis. In our practice, it had a positive clinical and educational impact, because most exams are performed by residents and technologists.

GU-11

Pediatric testicular microlithiasis: experience at a single institution *Matthew Cooper*, Boaz Karmazyn

Indiana University School of Medicine, Indianapolis (United States)

Purpose: To determine the incidence of testicular microlithiasis in the pediatric population and any associated testicular pathologies. Materials and methods: From the radiology information system of a tertiary children's hospital, we retrieved all testicular ultrasound (US) scans and selected all pediatric US studies with a diagnosis of testicular microlithiasis (TM) from 2003 to 2010. The patients with TM were categorized by classic TM (greater than 5 microliths on a single ultrasound image) and limited TM (fewer than 5 microliths on a single ultrasound image). Any associated testicular and scrotal pathologies were noted. Medical charts were reviewed for underlying pathologies.

Results: Testicular US studies were performed on 2,577 patients with 58 (2.2%) of them having TM. The most common indication for the US scans was scrotal pain (n=26, 45%). Patient ages ranged from 2 to 18 years with an average of 12.5 years. Forty-two (72%) of the patients were older than 10 years of age. Forty-three (74%) patients had classic TM and 15 (26%) patients had limited TM. Bilateral TM was seen in 41 (71%) patients. Associated pathologies were observed in 13 (22%) patients, including one or more of the following: cryptochidism (n=5), testicular tumor (n=3), leukemia (n=1), contralateral testicular agenesis or atrophy (n=2), Klinefelter's syndrome (n=1), mixed gonadal dysgenesis (n=1), and/or McCune-Albright syndrome (n=1). Follow-up (range 1–5 years, average 3 years) US studies were performed in 13 patients; 12 had stable TM and 1 with bilateral TM had resolution of the TM after 2 years. Conclusion: The incidence of TM in children is low (2.2%). Most of the TMs were diagnosed after the age of 10 years and none before the age of 2 years. Most TMs are bilateral. The prevalence of associated testicular malignancy was 5% (3/58).

GU-R1

Uterine artery pulsatility index (PI) in the diagnosis of puberty and in monitoring treatment for precocious puberty

Vincenza De Iorgi, Gianni Russo, Matilde Ferrario, Francesco De Cobelli, Pierluigi Paesano

IRCCS San Raffaele Hospital, Milan, (Italy)

Purpose: To define the role of PI as a diagnostic tool with particular attention to precocious puberty (PP); to evaluate PI as a parameter of hormonal therapy efficacy in PP.

Materials and methods: We retrospectively analyzed by sovrapubic ultrasound (US) 244 girls (age range: 1–17 yrs): 107 prepubertal and 137 pubertal girls [73 in physiological puberty (PHA) and 54 in precocious puberty (PP)] stage 3 according to Tanner scale and LH peak >5 UI/L after LHRH stimulation. All US were performed between September 2005 and January 2009 by the same expert paediatric radiologist, using convex and micro-convex arrays (5–8 MHz), correlating mean uterine length (cut-off for prepubertal girls ≤35 mm) with (PI value) (fixed >4.6 in prepubertal age). In a sub-population of 39/54 PP-girls, PI was measured before and during adequate inhibition of hypothalamus-pituitary-gonads axis through LHRH analog.

Results: We were able to calculate PI in all patients. In the 107 prepubertal group girls mean PI was 6.3 and mean uterine length was 33 mm. In the 137 pubertal girls, the 73 PHA girls had mean PI value of 3.2 and 3.5 in the remaining 54 PP girls; mean uterine length was 50 mm and 43 mm respectively. In 39/54 PP-girls subpopulation, PI mean value was 3.2 at baseline and raised to 5.7 after 3 months from LHRH analog therapy (p<0.001). Uterine mean length was 45 mm at baseline and 42 mm after therapy (p<0.003). The mean PI value was ≤4.6: our cut-off showed high sensitivity (93%), specificity (94%), PPV (96%) and NPV (91%) in recognizing pubertal girls.

Conclusion: In our experience a PI cut-off value of 4.6 could distinguish prepubertal from pubertal girls (both physiological puberty and PP). During hormonal therapy, PI value varies significantly and increase accordingly to the hormonal treatment efficacy, proving an effective additional parameter in follow-up.

GU-R2

Applying the updated transvaginal ultrasound criteria for polycystic ovarian syndrome (PCOS) to transabdominal ultrasound in overweight girls

Valerie Ward, Carol Barnewolt, S. Jean Emans, Amy DiVasta Children's Hospital Boston, Boston, United States

Purpose: Transvaginal ultrasound (US) findings are included in the recently updated PCOS diagnostic criteria, but girls usually undergo



transabdominal (TA) US instead. We aimed to determine whether TA US yields diagnostic images, especially in overweight girls, and whether androgen levels or body mass index (BMI) correlate with US findings.

Materials and methods: Two radiologists retrospectively reviewed TA US in girls with PCOS based on 1990 NIH criteria of menstrual irregularity and clinical/biochemical hyperandrogenism. Updated 2006 US criteria (ovarian volume ≥10 cc and/or >12 follicles/ovary), follicle distribution and endometrial thickness were assessed. Patients were excluded if on a medication affecting ovarian morphology or for a follicle diameter >10 mm. Associations between ovarian volume, androgens (free & total testosterone, dehydroepiandrosterone sulfate (DHEAS)) and BMI were evaluated by Pearson correlations.

Results: 78 females aged 15.8 \pm 2.3 years were identified. Mean BMI was 29.7 \pm 6.7 kg/m2 with 18 (29%) overweight and 32 (52%) obese. Despite their BMI, 96% of TA US images were usable, allowing evaluation of 65 right and 66 left ovaries after exclusions. Mean ovarian volume was: right 8.4 \pm 4.0 cc (range 2.5–19.7) & left 7.7 \pm 4.0 cc (1.6–16.0). Many met US criteria for PCOS: 34 patients had 1 ovary \geq 10 cc; 48 patients had either 1 ovary \geq 10 cc or >12 follicles/ovary; and 18 patients had both ovaries \geq 10 cc. The majority of follicles were distributed evenly; only a small percentage (2.7% right, 7.9% left) had a peripheral "string of pearls" follicle distribution. Endometrial thickness > 10 mm was seen in 16%. No correlations between ovarian volume and either androgen levels or BMI were found.

Conclusion: Between 27% and 73% of girls with a clinical diagnosis of PCOS also met updated US criteria, depending on the component of the definition used. Peripheral follicle distribution was surprisingly uncommon. Neither androgen levels nor BMI correlated with ovarian volume. TA US yielded diagnostic images in the vast majority of girls with PCOS, despite a high prevalence of obesity.

IR-1

Safety and efficacy of ethylene vinyl alcohol (EVOH) copolymer (Onyx) used in children

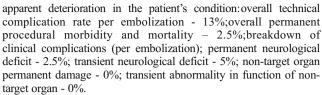
Ali Shaibani

Children's Memorial Hospital, Chicago (United States)

Purpose: Multiple articles have reported the increased efficacy of Onyx in the embolization of neurovascular lesions in the adult population, but there is a relative paucity of reported use in the pediatric population. In this submission we report a very large single center experience with Onyx embolization of pediatric neurovascular disease.

Materials and methods: All patients at a single institution treated with endovascular embolization using Onyx from August 2005 to July 2010 by a single operator were retrospectively reviewed. The following datapoints recorded included: lesion type, preembolization neurological status, efficacy/outcome of the embolization procedure, technical and clinical complications of the embolization, and neurological/functional outcome at follow-up. A total of 40 patients ranging in age from 4 weeks to 17 years of age were treated with a total of 82 embolizations (mean = 2.16 embolizations per patient).

Results: The angiographic efficacy of Onyx for embolization of pediatric vascular lesions is as below: brain pial AVM's-average final nidal reduction - 74%; spinal vascular malformations; average final nidal reduction - 100%; extracranial AVM's – average final nidal reduction- 80% vein Of Galen malformations – Average final nidal reduction – 80%. Technical complications were defined as unintended consequences of the treatment whether or not associated with clinically



Conclusion: Ethylene vinyl alcohol co-polymer can be used in pedicatric neurovascular procedures in a wide range of patient ages and conditions with very good efficacy and an excellent safety profile.

IR-2

Endovenous laser ablation (EVLA): usage in children with lower extremity vascular malformations

Philip John¹, Joao Amaral¹, Alex Barnacle²

¹The Hospital for Sick Children, Toronto (Canada) ²Great Ormond Street Hospital, London (United Kingdom)

Purpose: To describe a two-centre experience of EVLA in children with lower extremity vascular malformations. In adults, EVLA is considered the preferred treatment to close the long saphenous vein (LSV) in treating LSV reflux. Although EVLA usage in children is not widely reported, it offers a new treatment modality for children requiring closure of long venous channels.

Materials and methods: A retrospective review was undertaken on consecutive children undergoing EVLA from two tertiary care paediatric hospitals between 03/2007-11/2009. EVLA was performed under general anaesthesia with an 810 nm diode laser energy delivered via a 600 micron fiber.

Results: 18 consecutive patients (pts) (10 female), age range 3-17 yrs (mean=12.5 y) underwent 20 EVLAs (including bilateral in 1 & repeat in 1). 12 pts had venous malformations (VMs), 4 Klippel-Trenaunay Syndrome, 1 bilateral varicose veins, 1 an arteriovenous fistula (AVF). 16/18 pts had pain and 2/18 recurrent bleeding, all being difficult to control. Target venous channels lased (n=20) were 12 LSVs, 5 embryonic veins (EV) and 3 dysplastic veins. EVLA was done to provide outflow control for sclerotherapy of non-sequestrated VMs (8 pts), as a primary vein closure technique (7pts), to reduce skin lesion bleeding (2pts) and to reduce embolisation risk from gluing an AVF (1 pt). Initial technical success was achieved in 17/18 pts (18/19 lased channels). Length of follow-up = 1-26 mo (mean 12.6 mo). Clinical benefit was seen in 14/18 (78%) pts, in 1 a large dysplastic vein failed to close, in 2 despite EV vein closure there was no improvement and 1 LSV reopened after EVLA. Two minor and 1 major early procedural complications occurred (the major due to an IVC filter). One direct EVLA-related minor complication occurred (temporary sensory blunting).

Conclusion: Our results suggest that EVLA is well tolerated and can offer a safe, useful treatment adjunct in selected children with troublesome lower extremity vascular malformations. EVLA of large dysplastic veins may be difficult. EVLA of embryonic veins can be achieved though symptoms may persist.

IR-3

Is balloon burst pyeloplasty a useful alternative to open or laparoscopic pyeloplasty?

Boma Adikibi, Gordon A. MacKinlay, Alistair Graham Wilkinson Royal Hospital for Sick Children, Edinburgh (United Kingdom)

Purpose: In our institution 12.5% of patients who undergo surgical pyeloplasty require a subsequent procedure. We review our



experience of endoluminal balloon dilatation for pelvi-ureteric junction obstruction (PUJO) over 14 years.

Materials and methods: A retrospective review of all endoluminal balloon dilatations in one institution. A drainage score was derived from the MAG3 diuretic renography converting the T1/2 to a numerical value: 1- <15mins, 2-15-30 min, 3 30-55 min, 4-falling curve in 55 min too slow to calculate,5- level curve 55 min,6-rising curve. Ultrasonography measured the anterior posterior diameter of the pelvis (APD) and a scoring system was utilised:1-0-10 mm, 2-11-20 mm, 3-21-30 mm etc.

Results: 50 endoluminal balloon dilatations were performed in 44 patients. 31 M: 13 F. Age 5 months to 18.5 yrs (median 5 yrs). 31 primary procedures were performed on 29 patients. The pre median APD score was 4. The pre median MAG 3 score was 5. There was a reduction in the median post MAG 3 and APD score to 2. 39% of this cohort required further intervention. 19 dilatations were performed on 15 patients who had recurrent PUJO.The pre median APD score and MAG 3 score was 4 and 5 respectively.The median MAG 3 score fell to 3 after intervention. The median APD decreased to 2.53% required subsequent intervention. Half of the patients had redo balloon dilatation.Of the remaining 5 patients,1 had an open pyeloplasty and 2 had hemi/nephrectomies performed.

Conclusion: Balloon dilation for PUJO is effective with a decrease in the MAG3 drainage and APD score. 44% of all patients required further intervention. This is higher than the surgical pyeloplasty group in our institution. We postulate this is due to in part to 2 cases of unidentified crossing vessels and 3 patients who were completely obstructed requiring nephrostomy prior to intervention. Surgical results however appear better than balloon dilatation but the 2 groups of patients are extremely heterogenous with more patients with poor prognostic factors in the balloon group. We feel a randomised controlled trial is required to compare the two modes of treatment.

IR-4

Directed tumoral therapy of aneurysmal bone cysts in children William Shiels, James Murakami

Nationwide Children's Hospital, Columbus (United States)

Purpose: To evaluate clinical feasibility and efficacy of percutaneous imaging-directed therapy of aneurysmal bone cyst (ABC) with doxycycline as a multimodal (antitumoral, MMP inhibition, and osteoblastic stimulation) antineoplastic therapy.

Materials and methods: Thirty-eight children ages 2-18Y (Mean = 10.2Y) were treated for ABC. Doxycycline microfoam (10 mg/ml) was percutaneously injected into cystic and solid tumoral elements with US, CT, or fluoroscopic directed guidance (Mean dose = 300 mg/session). Bone graft substitute was injected into cystic spaces to facilitate osteoblastic ingrowth. The primary endpoint was boney healing of lytic foci, with stability during surveillance; follow-up 2–48 months.

Results: ABCs of the skull and spine (11), upper extremity (19), and lower extremity (8) were treated in 186 sessions. Four patients did not continue with the therapeutic protocol. Twenty-three patients completed therapy (11 continuing therapy) with mean number of sessions = 5.4, needle sizes 11–25 G, and mean number of needles per session = 4.8 (range = 1–16 needles). Doxycycline microfoam was visible with US in 92/92 cases targeting solid tumoral elements. Bony healing response was present in 34/34 patients; antitumoral response was biopsy proven in 4 cases; remodeling to normal or nearnormal morphology was documented in 71%, with visible bony scar in 81%. Normal bony morphology, including reconstitution of the medullary cavity was seen in 5 patients.

One case of focal skin necrosis was noted; no other complications.

Conclusion: Directed antitumoral therapy with Doxycycline microfoam is feasible, safe, and effective for percutaneous treatment of ABC in the axial and appendicular skeleton of children.

IR-5

Review of image-guided fine-needle aspirations of thyroid lesions in children

Sarah Deitch, Pauline Chou, Stanley Kim, Donald Zimmerman, James Donaldson

Children's Memorial Hospital/Northwestern University, Chicago (United States)

Purpose: The estimated prevalence of thyroid nodules in children is 0.05–1.8%, however up to one third are malignant. Fine needle aspiration (FNA) of thyroid lesions in adults is well established, but not in pediatrics. Few prior studies have focused on imageguided thyroid FNA in children, with biopsies relying heavily on the ability to palpate the lesion during biopsy. Here we describe our experience with ultrasound-guided FNA of thyroid lesions in children.

Materials and methods: Among 93 patients, ages 1–24 years, there were 101 ultrasound-guided thyroid FNA at our institution from January 1, 2005 to November 10, 2010. All were performed using a 25 gauge needle without suction aspiration and with either no sedation or light anxiolysis. Biopsies were done with the cytologist present. Additional passes were made until the cytologist determined that sufficient cells had been obtained. We reviewed the cytology reports as well as pathology reports for patients who went on to surgical resection.

Results: Cytopathology reports were available for 99 cases. Diagnoses included: 10 papillary carcinoma; 11 follicular neoplasm, 7 follicular lesions of undetermined significance, 34 benign nodules or collections of benign follicular cells, 13 lymphocytic thyroiditis, and 15 lymph nodes or lymphoid tissue. Surgical pathology results were available for 30 cases following thyroidectomy. The majority had concordant results with the FNA. Of the disconcordant results, two lesions that were suspicious for follicular neoplasm were diagnosed as papillary carcinoma following resection. An additional two were considered benign nodules by FNA and then diagnosed as adenomas following resection.

Conclusion: Ultrasound-guided fine needle aspiration is a reliable and minimally invasive method of evaluating thyroid lesions in children with thyroid nodules. A well-coordinated procedure with a pediatric cytopathologist is necessary for a successful program.

IR-R1

Delays in paediatric interventional radiology

Sam Stuart, Sam Chippington, Emma Stockton, Lonay Ridley, Toni Hall

Great Ormond Street Hospital, London (United Kingdom)

Purpose: To investigate the number and causes of delays in a paediatric interventional radiology department

Materials and methods: Data were collected prospectively for all patients booked for procedures in a paediatric radiology department of a children's hospital over a four week period. A specially designed proforma was used by the theatre list co-ordinator to collect data on the presence, timing and causes of delays. 170 patients from 24 different wards had procedures in the study period over 55 theatre sessions.



Results: Many patients and operating lists were delayed. 47% patients were ready for their procedure at the appropriate start time and 34/55 sessions had one or more patients not appropriately prepared for their procedure. 72% of delays occurred in morning lists. The majority of delays were a result of pre-theatre issues including the patients not being clerked or consented in time (50%), patients arriving late to the hospital (16%) and necessary blood results not being available (7%). There was a discrepancy in delays between individual wards with the largest referrers performing best and a poor performance from day wards

Conclusion: In these difficult economic times it is imperative that delays in our paediatric interventional radiology department are minimised to allow maximal utilisation of the operating rooms. Delays decrease efficiency and result in cancellations, patient complaints, longer waiting lists and poor staff moral with damage to the relationship between referrer and interventional radiology department. A high number of delays were identified in our study with nearly half of the patients not ready for their procedures at the appropriate start time with the majority of delays being pre-theatre delays. This needs addressing and possible interventions include educating staff on the importance of minimising delays or more wide sweeping changes to the system such as only allowing certain wards to prepare interventional radiology patients, the introduction of pre-clerking clinics or even the establishment of an interventional radiology day unit.

MI-1

Efficacy of two oral premedicants: midazolam or a low dose combination of midazolam-ketamine in children undergoing CT imaging

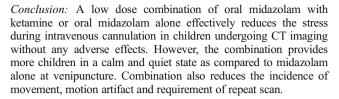
Babita Ghai, Kajal Jain, Akshay Saxena, Deepak Saini, Niranjan Khandelwal

Postgraduate Institute of Medical Education and Research, Chandigarh (India)

Purpose: To assess the efficacy and safety of oral midazolam and a low dose combination of midazolam and ketamine in children undergoing CT imaging.

Materials and methods: 92 ASA I/II children (1–5 years) scheduled for CT imaging under sedation were randomized to one of the three groups. Group M (n=29) received 0.5 mg/Kg midazolam in 5 ml honey, group MK (n=31) received 0.25 mg/Kg midazolam with 1 mg/Kg ketamine in 5 ml honey and group P (n=32) in Group P received 5 ml honey alone orally. 20–30 min after premedication, venipuncture was attempted at the site of EMLA cream. Sedation scores and venipuncture scores were recorded. The child then received IV ketamine to achieve a level of deep sedation for CT imaging. Any movement, motion artifact and repeat scan was noted. Primary outcome of the study was incidence of children crying at venipuncture.

Results: Significantly more children cried during venipuncture in placebo group compared to the other two groups i.e.19(59%) in group P versus 1 each in groups M and MK, p<0.001, (RR 2.37, 95% CI 1.55–3.63). 20–30 min after premedication more children were either crying or anxious in group P compared to the other two groups (p<0.05). However, group MK showed more children in calm and awake compared to group M (p=0.02). 14 children in group P and 5 in group M moved compared to none in group MK during scan (p<0.001). 10 children in group P and 2 in group M developed motion artifacts on CT imaging compare to none in group MK (p<0.001). 4 children, all in group P required repeat scan because of motion artifact hampering the diagnostic quality of image (p=0.015).



MI-2

The diagnostic value of radiology in invasive Panton–Valentine leucocidin (PVL) positive staphylococcus aureus (SA) infection. *Afshin Alavi*, Joanna Danin, Maria Nordlander, Mayai Seah, Linda Maruskova, Sam Walters

Imperial College Healthcare NHS Trust, St Marys HospitalLondon (United Kingdom)

Purpose: PVL is an exotoxin produced by some strains of SA which destroys leucocytes. PVL strains were recognized in the early 1990s in staphylococcal abscesses. There is an increasing number of PVL-SA isolates in the last decade, more than doubling each year since 2005. PVL-SA most commonly causes skin and soft tissue infections. It can also cause necrotizing pneumonia, complicated musculoskeletal (MSK) infections and deep abscesses. In this retrospective study we present 21 children with severe PVL-SA treated in our hospital since January 2006. The objective of this study was to describe systematically the radiological features of invasive PVL-SA, the correlation with the clinical and surgical results and to identify features which may allow early recognition of the disease in order to inform future management strategies.

Materials and methods: We retrospectively reviewed the imaging studies, medical records and risk factors of all children who had invasive PVL-SA infections since January 2006 and collected standardized data, to determine a correlation between specific radiological features and the presence of PVL.

Results: 21 children, 14 male and 7 female, median age 9 years had severe PVL-methicillin-sensitive staphylococcus aureus (MSSA) infections. 1 patient had massive retrophayngeal abscess, 3 had pneumonia, 2 had periorbital and intraorbital infections and 15 had MSK infections. Possible risk factors were identified in15 cases. 14 patients were admitted to a pediatric intensive care unit (PICU) with acute sepsis. 6 had DVT. All of the MSK cases showed radiological features of soft tissue and intraosseus abscesses. All of the pneumonia cases showed radiological characteristics of necrotizing pneumonia. The retropharyngeal and periorbital abscesses were diagnosed using imaging procedures. One child died and 9 have long-term morbidity.

Conclusion: Invasive PVL-SA can cause severe infections, sepsis and multi organ failure. The most common manifestation was severe MSK infections. The results of our study show the ability of imaging to provide important additional information that allow earlier diagnosis, and improve patient management and outcome.

MI-3

How and why an Australian children's hospital is planning for MR-PET in 2011

Timothy Cain¹, Rodney Hicks²

¹Royal Children's Hospital, Melbourne ²Peter McCallum Cancer Centre, Melbourne (Australia)

Purpose: MRI and PET/CT are important imaging technologies in paediatrics and are often complementary. Anticipating hybrid MR-PET poses design challenges that need to be considered.

Materials and methods: The hospital described is a specialist Children's Hospital that serves a population of about 6 million



people. It is affiliated with an independently funded Children's Research Institute and operates as a University Hospital. In 2005 the State Government decided to construct a new Children's Hospital in a different location as a Public-Private Partnership. The infrastructure of the new CH was therefore very clearly specified in the contract. This included a PET/CT and a need to "future proof" the design, but there was no specific mention of an MR/PET. The reasoning and methodologies applied in developing a new Medical Imaging Department for the Children's Hospital to accommodate MR/PET, which was not commercially available at the time of the design process, are discussed.

Results: An MR/PET was considered a desirable imaging tool for the CH due to the ability to eliminate the radiation associated with the CT component of a PET CT, the ability to perform MR and PET studies under the one anaesthetic, and the synergy of the excellent anatomical detail of MR with the unique functional properties of PET imaging agents. As well as the clinical advantages of an MR/PET scanner, there is also considerable potential to develop imaging paradigms that uniquely address the needs of childhood diseases that require a range of physiological tracers. The specific requirements for magnetic and radiation shielding, as well as support services that are MRI-compatible, informed the design process. These included access to patient preparation and tracer administration areas and consideration of radiotracer supply. The footprint of possible equipment configurations also required consideration.

Conclusion: The layout of the new CH has been configured to optimise the function of an MR/PET, but was physically built before commercial release. Forward planning has enabled the potential for early adoption of this technology.

MS1-1

Ultrasound of brachial plexus birth injury in infants: experience in a series of 80 patients

Maura Valle¹, Nunzio Catena¹, Filippo Senes¹, Maria Grazia Calevo¹, Carlo Martinoli²

¹Istituto Scientifico Giannina Gaslini, Genoa, ²Università di Genova, Genoa (Italy)

Purpose: To describe the diagnostic performance of ultrasound (US) in infants with a brachial plexus birth injury.

Materials and methods: From January 2002 to August 2010, a series of consecutive n=80 children (mean age 2.3 months; 54 males) with obstetrical palsy were examined with high-frequency 12-5 MHz and 17-5 MHz US transducers. All patients underwent cervical and brachial plexus MR imaging and MR myelography within 1 week of the US study. Then, 53/80 (66%) patients had surgery and underwent intraoperative electrophysiological studies. Analysis of US findings included nerve root injuries with or without pseudomeningoceles and posttraumatic neuromas.

Results: In patients who underwent surgery, the sensitivity and specificity of the US findings of posttraumatic neuromas in the interscalenic area were 89% and 95% respectively, using surgical findings and somatosensory evoked potentials as the standard of reference. Dividing the brachial plexus in an upper and lower part, US was able to establish the level of injury in 70% of cases. Paraforaminal nerve root injuries and pseudomeningoceles were identified with US in only 12% and 8% of surgically-proven root avulsions. In the group of infants who were managed conservatively, US was 92% sensitive and 100% specific to detect neuromas using MR imaging as the standard of reference. In this group, posttraumatic neuromas were smaller in size size (p<.0001) or absent (9 cases). Conclusion: US is promising for imaging brachial plexus birth injuries. The information provided has a prognostic value and is

useful for the surgeon in a preoperative setting.

MS1-2

Ultrasound of Poland syndrome

Maura Valle¹, Maria Grazia Calevo¹, Anwar Baban², Michele Torre¹, Carlo Martinoli¹

¹Istituto Scientifico Giannina Gaslini, Genoa, ²Ospedale Bambino Gesù, Rome (Italy)

Purpose: The aim of this paper is to describe the US scanning technique and the main ultrasound (US) findings in patients with Poland syndrome.

Materials and methods: We examined the pectoralis region of n=153 consecutive patients (age range, 8 months to 25 years; mean, 6 year) affected by Poland syndrome with 12-5 MHz and 17-5 MHz US. In each study, US provided information about: 1) status of any of the three heads (clavicular, sternocostal, abdominal) of the PMaj; 2) presence and size of the PMaj tendon; 3) status of the pectoralis minor (Pmin); 4) vessel size and blood flow characteristics from the ipsilateral subclavian, axillary and internal mammary arteries; 5) status of the latissimus dorsi. US data were matched with clinical phenotype findings.

Results: PMaj abnormalities were arbitrarily subdivided into three main types: type-I, complete agenesis of the PMaj; type-II, hypoplasia of the PMaj with presence of the clavicular head; type-III, hypoplasia of the PMaj with presence of the clavicular and part of the sternocostal heads. Complete agenesis of the PMaj was found in 83/153 cases. Associated agenesis of the latissimus dorsi was observed in 5% of them. In other 61/153 cases, the clavicular head of the muscle and a small tendon were present. The clavicular head associated with an underdeveloped stenocostal head was found in other 9 patients. The Pmin was found in only 7 cases (4.6%). All patients with destrocardia had partial agenesis of the PMaj muscle. No statistically side difference in blood vessel size and arterial blood flow was observed. Comparing the three types of anomaly, a higher incidence of upper limb abnormalities was found in type-I patients (p=0.01). None of the three types showed correlation with gender (p=0.39), rib (p=0.86), sternal (0.85) and nipple (0.61) abnormalities.

Conclusion: US can complement clinical examination to assess the abnormalities of the pectoralis complex in patients with Poland syndrome.

MS1-3

Variability of femoral condylar ossification on MRI: imaging features, frequency and age distribution

Lennart Jans¹, Jacob Jaremko², Michael Ditchfield², Koenraad Verstraete¹

¹Ghent University Hospital, Gent (Belgium) ²Royal Children's Hospital Melbourne (Australia)

Purpose: To determine how magnetic resonance (MR) signal of ossification variability of the distal femoral epiphysis in children varies with (a) age, (b) sex, (c) distribution to the medial or lateral condyles and (d) residual physeal cartilage.

Materials and methods: Ethics committee approval was obtained and informed consent was waived. Consecutive knee MR imaging studies of 910 children (457 boys and 453 girls; ages 0.7–16.9 years) were retrospectively reviewed for variability of ossification by two pediatric radiologists. The age, gender, site, configuration of the variability, residual physeal cartilage and presence of associated findings were analysed. Basic descriptive statistics, Student's t-tests for comparison of continuous variables and kappa statistics for interobserver agreement were performed where appropriate.



Results: In 202 (22%) patients (278 condyles), variability of ossification was present. Early ossification center (n=172, 18.9%), spiculated configuration of the secondary ossification center (n=50, 5.5%) were the most common variants. Puzzle piece (n=26, 2.9%), extra ossification center (n=9, 1.0%) and incomplete puzzle piece (n=2, 0.2%) configurations were seen less often. Ossification variability was more common in the medial condyle (n=169, 18.6%) than the lateral condyle (n=109, 12.0%), and was nearly always posteriorly located (99.6%). Ossification variability was more common in boys (n=135, 33.2%) than in girls (n=49, 10.9%). Ossification variability was less common with decreasing residual physeal cartilage. The peak age range of ossification variability was 2–12 yr (boys) and 2–10 yr (girls).

Conclusion: Ossification variability of the femoral condyles is common in children and should not be confused with pathologic processes.

MS1-4

Assessment of cortical bone loss with quantitative ultrasound, peripheral CT and micro-CT in post mortem knee specimens of a rabbit model of inflammatory arthritis

Afsaneh Amirabadi¹, Jackson Wang¹, Christopher Gordon¹, Christopher Tomlinson¹, Marc Grynpas², Rahim Moineddin³, *Andrea Doria*¹

¹The Hospital for Sick Children, Toronto, ²Mount Sinai Hospital, Toronto, ³University of Toronto, Toronto (Canada)

Purpose: The currently available methods for diagnosis of osteoporosis in children are varied. Micro-CT provides architecture bone information beyond bone densitometry, but it is invasive and bears radiation. Peripheral quantitative CT (pQCT) is capable of assessing trabecular and cortical bone geometry, but also bears radiation. Quantitative ultrasound (QUS) is a potentially valuable tool for assessing bone quality since it is low-cost, radiation free and readily-accessible. Our purpose was to correlate bone measurements of QUS, and pQCT of postmortem knee specimens of a juvenile rabbit model of inflammatory arthritis and bone loss using micro-CT as the reference standard.

Materials and methods: One of the knees of 7 juvenile white New Zealand rabbits was injected with 1% carrageenin solution (7 injected, 7 contralateral knees). Knees of 3 non-injected rabbits (6 knees) were used as controls. The animals were euthanized 28 days after induction of arthritis and their knee specimens kept frozen until 24 h prior to scans. Data acquisition and analysis of QUS (speed of sound), pQCT (bone mineral content and density, cortical bone thickness and area), and micro-CT were performed in the proximal medial and lateral tibiae of all post-mortem specimens. Results: No differences were noted in mean periosteal circumference

of arthritic (27.58 mm), contralateral (27.59 mm) and control (27.99 mm) specimens (P=0.94). In the lateral proximal tibiae of arthritic specimens substantial positive correlations were depicted between QUS and pQCT measurements of cortical bone mineral content (r=0.78, P=0.04), density (r=0.74, P=0.05) and area (r=0.78, P=0.04). In this location of control specimens excellent negative correlations were noted (cortical bone mineral content (r=0.93, P<0.05), density (r=0.99, P=0.07) and area (r=0.91, P<0.05). pQCT and micro-CT measurements correlated well.

Conclusion: Inverse QUS-cortical pQCT correlations were noted in lateral proximal tibiae of arthritic and control post-mortem specimens in our rabbit model of arthritis/bone loss. This could relate to differences in sound characteristics of bone integrity vs loss.



Avascular necrosis (AVN) of bone in adolescents with classical Hodgkin's Lymphoma—a single centre experience

Michael Steward, Peter Boavida, Joseph Cooney, Ananth Shankar, Stephen Daw, Paul Humphries University Hospital London (United Kingdom)

Purpose: To ascertain the incidence, site and extent of AVN/bone infarcts in adolescents with classical Hodgkin Lymphoma (cHL) treated with combination chemotherapy in our centre.

Materials and methods: Between April'05–April'10, 62 adolescents with cHL aged 12 to 18 years treated with OEPA-COPP-COPDAC chemotherapy were included. CT or MR imaging performed at staging, after 2 cycles of chemotherapy and at the end of chemotherapy was reviewed retrospectively by experienced radiologists for evidence of AVN.

Results: 8/62 patients (12.9%) developed imaging findings in keeping with AVN. 23/62 had CT imaging only, of these 2/23 had AVN. 7/62 had combination CT and MRI and no AVN was seen in this small group. 32/62 had serial MRI only and in these 6 had AVN. Of those patients scanned with MRI only, 6/32 (18.8%) developed AVN which was progressive on subsequent imaging. Pain and impaired joint function are the most common associated symptoms. A separate 3/32 developed early signs of AVN which resolved in follow up.

Conclusion: Avascular necrosis causes significant morbidity in adolescents with cHL which is best detected by MRI and may currently be under reported in this patient group.

MS1-6

Early assessment of the efficacy of digital infrared thermal imaging in pediatric extremity trauma

Cicero Silva, Nausheen Naveed, Syed Bokhari, Kenneth Baker, Lawrence Staib, Thomas Goodman

Yale University School of Medicine, New Haven (United States)

Purpose: This prospective, exploratory study, assessed the efficacy of Digital Infrared Thermal Images (DITI) in pediatric extremity trauma. Young children or those with intellectual disability are often unable to identify a precise site of injury and are subsequently subjected to multiple radiographs of a whole limb. We hypothesized that fractures would be associated with local hyperthermia detectable with DITI, which could then be used to direct focused radiographic examinations, minimizing radiation exposition.

Materials and methods: Patients seen over a 2-month period in the pediatric emergency department (ED) of a tertiary hospital following limb trauma were eligible for the study, and included if an extremity radiograph was taken on the day of ED visit. Patients were excluded if they were older than 18 years or had dressings or ice over the area of trauma. Enrolled patients had one thermal picture taken of the affected limb, and another from the contralateral limb, by a researcher blinded to the radiographs. The site of pain, when present and known, was recorded. DITI from all patients were pooled and presented in random order to three attending radiologists who, blinded to the radiographs, determined by consensus the warmest area on each image. Subsequently, the same radiologists evaluated the radiographs of each patient by consensus, blinded to the DITI findings, for the presence/absence/ location of fractures. The warmest area on the affected limb was correlated with the fracture site, when present, and with the site of pain. DITI data from contralateral, unaffected limbs were used to determine normal temperature distributions.

Results: 51 patients were enrolled in the study: 30 boys and 21 girls aged 9 m to 17y 10 m. The time interval between DITI and



radiographs was -614 to +127 min. A site of pain was unknown in 2 toddlers. DITI matched the pain site in 36 of the remaining 49 (73.5%) patients. Fractures were seen in 11 patients. DITI matched the fracture site in 7/11 (63.6%) patients. Unaffected limbs showed a fairly uniform DITI pattern.

Conclusion: DITI performance on this exploratory study seems encouraging for further evaluation with a larger cohort.

MS1-7

Lumbar back pain and the use of plain lumbar radiographs *Tom Watson*. Jeremy Jones. Annmarie Jeanes

Leeds Teaching Hospitals Trust, West Yorkshire Radiology Academy, Leeds General Infirmary, Leeds (United Kingdom)

Purpose: Paediatric lumbar back pain is a common complaint. Radiological investigation is variable according to institution, and no consensus exists with regards to imaging protocol. We attempt to identify common trends between children presenting to radiology with lower back pain with the aim of developing an imaging protocol for investigation of lower back pain.

Materials and methods: We conducted a retrospective review of all paediatric patients presenting to our institution for a lumbar X-ray in 2009. Those presenting with lumbar back pain but without history of trauma, scoliosis or raised intracranial pressure were included. X-ray reports and any subsequent relevant imaging such as MRI or Bone scintigraphy were reviewed. Normal and abnormal reports, clinical details and referring speciality were recorded and statistical analysis of the data were conducted using Microsoft Excel 2007.

Results: 116 patients were included with an average age of 13.6 yrs. 92 X-rays (79.3%) were normal, the majority of these 45 (48.9%) were performed following referral from General Practice. Of the 24 abnormal x-rays, 20 (83.3%) were in children over 10 years old. 36 MRIs were performed for children with normal and abnormal radiographs and 16 of them (44.4%) were abnormal. In 9 cases, the MRI demonstrated pathology that was not visible on the plain radiograph. 20 of the 22 patients with pathology (90.1%) presented with symptoms that were less than 1 year in duration (where clinical data were available).

Conclusion: This is a small dataset, but a number of conclusions may be drawn: Lumbar back pain is more common in older children. Pathology is more common in those patients with a shorter onset of symptoms(<1 year). A specialist assessment prior to imaging increases the positive diagnostic yield We recommend that those patients with a long symptom history (>2 yrs), a normal clinical assessment and X-ray need no further imaging. Further research is required to develop a protocol for those patients who do not fit these criteria.

MS1-R1

Mechanisms of injury in children younger than 3 years of age presenting to an emergency department

Amaka Offiah, Jessica Hume, Sally Gibbs, Alan Sprigg, Derek Burke

University of Sheffield, Sheffield Children's Hospital, Sheffield (United Kingdom)

Background: The diagnosis of child abuse is fraught with difficulties, not least being the relative absence of evidence regarding mechanisms of accidental injury in children of the appropriate age (less than 3 years). This is because detailed questioning of carers regarding mechanism of injury and correlation with fracture type is usually only performed when abuse is suspected.

Purpose: To improve our understanding of the mechanisms of accidental injury in children less than 3 years of age presenting to an Emergency Department (ED).

Materials and methods: We are prospectively interviewing consented carers accompanying children less than 3 years old to our ED, and collecting a wide range of information regarding family background, current and past medical history and mechanism of injury (including but not limited to whether the incident was witnessed and by whom, height of fall, number of stairs, nature of surface on which the child landed etc.). Results of any laboratory tests performed are also being recorded. Two consultant radiologists (experts in child abuse) are independently reviewing all images in order to allow correlation between mechanism of injury and resultant fracture(s) – if any. Local Research Ethics Committee approval has been obtained.

Results: We are on target to recruit 250 cases by the end of March 2011. We will correlate resultant injury with described mechanism and presence of an underlying pathological condition for each type of fracture (skull, long bone etc.). Interim data suggest that some fractures (e.g. ribs) will be under represented – this in itself is useful information, as it indicates the rarity of these types of fractures in the context of accidental trauma. We shall present the prevalence of particular fractures in three age groups (<1, 1 to 2 and 2 to 3 years) as well as the mechanisms by which they occur within the individual age categories.

Conclusion: Results will be useful to radiologists (from both clinical and medico-legal standpoints) when attempting to determine the veracity of mechanisms of injury put forward by parents/ carers in cases of suspected child physical abuse.

MS2-1

Prevalence of hip dysplasia in 18-vear-old Norwegians

Ingvild Engesæter, Trude G Lehmann, Lene B Laborie, Lars B Engesæter, Karen Rosendahl

Haukeland University Hospital, Bergen, (Norway)

Purpose: Developmental dysplasia of the hip (DDH) is the underlying cause of 8% of total hip replacements in Norway, thus representing a major health problem. While the reported prevalence of DDH as defined by the acetabular index in infants and young children is 2-3%, the prevalence at skeletal maturity as defined by "adult" markers for DDH such as the centre edge angle of Wiberg and femoral head coverage is unclear. We therefore examined such prevalences in a large, population based cohort of 18-year-olds.

Materials and methods: All subjects born in 1989 (n=4006) in our hospital were invited to participate in a follow-up hip trial, of which 2081 (1206 females) were included. During the period 2007–2009, all had a clinical examination, as well as two pelvic radiographs; one standing AP and one frog leg view. All radiographs were performed by one, particularly trained radiographer, using a low-dose DR technique. Markers for DDH were: Wiberg's center-edge (CE) angle <20°, femoral head coverage <75° and the acetabular shape as assessed subjectively by one experienced observer. The results for left hips are presented.

Results: A total of 2081 subjects, 1206 females (58%), were included. 35 (1.7%) had a CE angle below 20°, 25 females (2.1%) and 10 males (1.7%), while 55 (2.6%) had a pathological femoral head coverage (<75°), 35 females (2.9%) and 20 males (2.3%). 26 (1.2%) had a dysplastic acetabulum as assessed subjectively (1.7% females and 0.7% males). When classified as normal, borderline (1 of 3 markers for DDH) or dysplasia (2 markers for DDH), 1.6% (1.7% females, 1.2% males) had dysplasia and 2.0% were defined as borderline.

Conclusion: In a general 18-year-old Norwegian population, radographical dysplatic hips were found in 1.6% of the hips.



MS2-2

Long-term effects of different ultrasound screening strategies for developmental dysplasia of the hip (DDH)

Lene Bjerke Laborie¹, Ingvild Ø. Engesæter¹, Trude G. Lehmann¹, Lars B. Engesæter¹, Deborah M. Eastwood², Francesco Sera³, Carol Dezateux⁴, Karen Rosendahl¹

¹Institute of Surgical Sciences, University of Bergen, Haukeland University Hospital, Bergen (Norway), ²Department of Orthopaedics, Great Ormond Street Hospital for Children, London, ³Institute for child health, London/Arthritis Research UK (grant Ref 18196), ⁴MRC Centre of Epidemiology for Child Health, UCL Institute of Child Health, London (United Kingdom)

Purpose: To assess the long term effects of universal, selective or no ultrasound (US) screening on the femoral head coverage and on signs of undergone avascular necrosis (AVN) as a complication to treatment.

Materials and methods: During 1988–90, 11925 newborn infants were enrolled in a clinical trial designed to evaluate the effectiveness of 3 different screening strategies for DDH: a) universal, b) selective (risk factors or clinical indication) or c) no US (only clinical examination) screening. Those born in 1989 (n=4006) were invited to a follow-up at age 18/19. 2081(52%) were included. Femoral head coverage was measured using the CE angle of Wiberg. A medially flattened femoral head (yes/no) was defined as a marker for an undergone AVN. Differences between the three groups were examined using ANOVA tests for mean values and chi square statistics for grouping variables. A p-value (2-tailed)

Results: Radiographs of 2039 adolescents (58% females) were analysed, 560 from the universal US group, 782 from the selective US group and 697 from the no US group. For left hips and both sex together, mean CE angle at skeletal maturity was 31.9° (SD=5.8°) for the universal group, 31.8° (SD=6.0°) for the selective group and 32.5° (SD 6.0°) for the no US group (one-way between-groups ANOVA, p=0.031, posthoc p=0.032 between selective and no ultrasound group). When grouping into normal (CE>25°), borderline ($20^{\circ} \le CE \le 25^{\circ}$) or dysplastic (CE

Conclusion: Universal or selective ultrasound screening for DDH with treatment of those testing positive in the newborn period did not improve the femoral head coverage at skeletal maturity as compared to clinical screening alone, although treatment and follow-up rates were significantly higher for the two groups.

MS2-3

When should treatment for developmental delay of the neonatal hip be commenced?

Michael Jackson, Sally Wilkinson, Alastair Graham Wilkinson Royal Hospital for Sick Children, Edinburgh (United Kingdom)

Purpose: Supportive harness treatment for developmental dysplasia of the hip is a well-established therapy with a good evidence base. However, controversy exists concerning the optimum time to commence treatment. This study sought to clarify the optimum time to start harness therapy.

Materials and methods: Retrospective analysis of cases was conducted covering a 6-year period. 307 individuals recalled for a follow-up pelvic radiograph at 1 year of age were identified. This group included patients in whom harness treatment had been commenced in a range of different ages, together with individuals in which treatment had not been undertaken. Radiographs were anonymised and independently assessed for features of developmental dysplasia by two radiologists using a standardized

scoring proforma. Following scoring the treatment status of each individual was established and data analysis performed. Results and Conclusion: A much higher proportion of radiographically abnormal hips was found in individuals treated after 8 weeks of age with a further increase seen after 12 weeks. Our data suggest treatment should be commenced before 8 weeks of age when possible. Radiographic evidence of hip dysplasia was found in 13 of 92 untreated patients (14%) and in 25 of 166 patients in whom treatment had been commenced before 8 weeks of age (15%). In those treated after 8 weeks of age, abnormalities were found in 24 of 49 cases (49%), with abnormalities found in 82% of those treated after 12 weeks of age. Chi square analysis demonstrates significantly fewer abnormal radiographs in those treated before the following ages compared to after: 6 weeks (p<0.001), 8 weeks (p<0.0005) and 12 weeks (p<0.0005).

MS2-4

Relationship of acetabular and femoral head morphology to stability in ultrasound examination of neonatal hips

Alastair Wilkinson

Royal Hospital for Sick Children, Edinburgh (United Kingdom)

Purpose: to determine any relationship between visual examination of morphology and stability in neonatal hip ultrasound.

Materials and methods: The first US examinations performed by the author in 828 infants (1656 hips) referred to the hip assessment clinic were retrospectively reviewed to assess acetabular morphology. Acetabular angle, percentage femoral

head cover, the presence of femoral head flattening and notching of the acetabular margin and dynamic stability had been prospectively recorded.

Results: In 942 normally concave acetabula 5 hips were unstable (0.53%). Instability was more commonly observed in 17 of 395 (4.3%) hips with reduced concavity (chi2=24.5, p<0.0005), 80 of 238 (33.6%) hips with flat roofs (chi2=311, p<<0.0005) and 58 of 81(71.6%) hips with convexity of the acetabular roof (chi2=651, p<<0.0005). Notched acetabular margins has been noted in 53 hips and were associated with instability in 11 (20.7%), compared to 149 of 1603(9.2%) in hips with un-notched margins (chi2=7.72, p<0.001). Flattening of the articular surface of the cartilaginous femoral head was seen in 122 hips and was associated with instability in 53 (43.4%) compared to 107 (7%) of 1534 hips with round heads (chi2=172, p<<0.0005).

Conclusion: Observation of morphology may be equally or more important than measuring angles or calculating% femoral head cover in determining which babies should be treated. Observation of stability during spontaneous patient movement may be more important than stress testing.

MS2-5

Dynamic contrast-enhanced MRI of pediatric patients after reduction of dysplastic hips: quantitative MR perfusion analysis for predicting avascular necrosis

Ji Young Kim, Jung-Eun Cheon, Yun-Jung Lim, Woo Sun Kim, In-One Kim, Kyung Mo Yeon

Seoul National University Hospital (South Korea)

Purpose: To determine the relevant perfusion parameters in dynamic contrast enhanced MRI (DCE-MRI) for the prognostic factor of avascular necrosis (AVN) of the femoral head in the developmental dysplasia of the hip (DDH) pediatric patients after reduction of dysplastic hips.

Materials and methods: Nineteen unilateral DDH patients (six boys and thirteen girls; mean age, 12 months ± 6.5 ; age range, 4–



26 months) were taken the DCE MR perfusion imaging without 48 h of hip reduction. Quantitative perfusion parameters (Ktrans, Kep, Ve, and iAUC) of the cartilaginous portion of the bilateral femoral heads were calculated by using dedicated software, based on DCE-MR perfusion imaging. And then the parameter's ratio (DDH hip to normal hip) in the same patient, were calculated. The conventional post-contrast T1-weighted images were also reviewed for evaluation the gross perfusion status of femoral head. Hip plain radiographs taken at longer than 1 year follow-up were analyzed for the presence of the AVN by two radiologist and one orthopedic surgeon. Then the quantitative perfusion parameter's ratios were compared between AVN presence group and AVN absence group. Among these perfusion parameters, statistically significant values were determined using the independent ttest, the Mann-Whitney U test, and the receiver operating characteristic (ROC) curve analysis (to determine the optimal cut-off of Ktrans ratio and iAUC ratio).

Results: The Ktrans ratio (Ktrans_DDH hip/Ktrans_normal hip) and iAUC ratio (iAUC_DDH hip/iAUC_normal hip) in the AVN presence group were significantly lower than AVN absence group. According to ROC curve analyses, Ktrans ratio and iAUC ratio provided sensitive of 77.8%, 44.7% and specificity of 100%, 90% for the predicting factor of AVN at an optimum cut-off value of 0.95 and 0.9, respectively.

Conclusion: Ktrans ratio and iAUC ratio measured on DCE-MR perfusion imaging can be used as a prognostic factor for the AVN after reduction of dysplastic hips.

MS2-6

Frequencies of three longitudinal dysplasia phenotypes based on sonographic assessments in the newborn and radiological assessments at skeletal maturity

Trude Gundersen Lehmann¹, Lene Bjerke Laborie¹, Ingvild Øvstebø Engesæter¹, Lars Birger Engesæter¹, Fransesco Sera², Deborah Eastwood³, Carol Dezateux⁴, Karen Rosendahl¹

¹Haukeland University Hospital, Bergen (Norway), ²MRC Centre of Epidemiology for Child Health, UCL Institute of Child Health, London (United Kingdom) ³Great Ormond Street Hospital for Children, London (United Kingdom), ⁴MRC Centre of Epidemiology for Child Health, UCL Institute of Child Health, London (United Kingdom)

Purpose: To examine radiological outcomes at skeletal maturity of sonographically normal, immature and dysplastic hips in newborns.

Materials and methods: During 1988-90, 11925 newborn infants (>99.5% white) were enrolled in a clinical trial designed to evaluate the effectiveness of different screening strategies for developmental dysplasia of the hip (DDH). Approximately 35% were also examined by hip ultrasound performed in a standardised manner by a single observer. All with pathological ultrasound had standard treatment. In the present study we invited those born during 1989 (n=4006) and those born in 1988 and 1990 and in whom neonatal sonographic abnormalities were detected (n=503) to participate in a large clinical and radiological follow-up at 18/19 years of age. Radiographic markers for DDH were the centre-edge angle of Wiberg (>25° normal, 20–25° borderline, <20 pathological). Results: 915 out of 4509 participants had both a hip ultrasound as newborns and a hip-radiograph at age 18-19 years, of which 574 were females. For left hips, mean CE at skeletal maturity was 32.0° (SD=5.8°) for sonographically normal, 30.9° (SD=6.2°) for immature and 31.1° (SD 5.9°) for dysplastic hips (one-way between-groups ANOVA, p=0.037, thus, the effect size was small (eta sq.=0.007)). Of the 590 with sonographical normal hips at birth, 59 developed into borderline and 6 to dysplastic hips (11%), when grouping into normal (CE>25°), borderline ($20^{\circ} \le CE \le 25^{\circ}$) and dysplastic (CE<20°) hips based on an AP radiograph at skeletal maturity. This was the case for 40 and 4 of 235 immature at birth (18.7%) and 11 and 3 of 90 dysplastic hips (16%) (Pearson chiSq=0.024).

Conclusion: One in ten sonographically normal hip develops into a borderline or dysplastic hip at skeletal maturity, while this is the case for about one fifth of those with immature and one sixth of those with dysplastic hip in the neonatal period.

MS2-7

Radiographic and biologic assessment of cam-type femoroacetabular impingement morphology of developing hips in asymptomatic children and adolescents: a pilot study

Hal Dunlap¹, Sasha Carsen², Paul Beaule², Baxter Willis³, Leanne Ward³, Kawan Rakhra³, Paul Moroz¹

¹Children's Hospital of Eastern Ontario, Ottawa, ²The Ottawa Hospital, Ottowa, ³The Children's Hospital of Eastern Ontario, Ottowa (Canada)

Purpose: The importance of femoral head-neck morphology in the development of early hip osteoarthritis is recognized in femeroacetabular impingement (FAI); however no studies have examined FAI morphology in the developing hip. We developed an MR pilot project to study prevalence of CAM-type FAI hip morphology in both the pre- and post-closure proximal femoral physes of asymptomatic children.

Materials and methods: Recruitment included volunteers with asymptomatic lower extremities, and with either pre- or post-closure of the proximal femoral physis. Males were 10–12 years (pre-closure) or 15–18 years (post-closure); females were 8–10 years or 14–18 years. MR measurement of alpha angles at both the 3:00 (anterior head-neck junction) and 1:30 (antero-superior head-neck junction) radial image positions were obtained.

Results: Fifty-two recruits (32 boys, 20 girls) with 44 bilateral hips (88 hips) imaged. Radiographic analysis showed no CAM-type morphology in pre-closure hips and 14% in post-closure hips (alpha>50o). The difference between alpha angle measurements in 3:00 and 1:30 positions (5.16o) appears significant in developing hips.

Conclusion: Collected data found FAI in 14% of the closed-physes group and 0% in the open physes group suggesting possible physeal closure importance. Methodologically, the difference between 3:00 and 1:30 alpha angle measurements was significantly less than in published adult figures, suggesting a developmental role in CAM-Type FAI. This may be the first published attempt to assess CAM-type FAI morphology in the developing hip.

MS2-8

Osteonecrosis in children after allogenic bone marrow transplantation: study of prevalence, risk factors and longitudinal changes using MRI

Shelly Sharma, Wing-Hang Leung, Deqing Pei, Jie Yang, Shengping Yang, Richard Rochester, Lunetha Britton, Michael Neel, Kirsten Ness, *Sue Kaste*

St. Jude Children's Research Hospital, Memphis (United States)

Purpose: Osteonecrosis (ON) is a debilitating long-term complication of allogenic bone marrow transplantation (alloBMT) but this issue has seldom been addressed in pediatric population. Thus, we sought to estimate the prevalence and associated risk factors for ON after alloBMT.



Materials and methods: We retrospectively analyzed prospectively acquired magnetic resonance (MR) studies for children who underwent first alloBMT at our institution between December 2000 and September 2007. We described longitudinal changes of lesions for patients with both pre and post alloBMT MRs.

Results: Of the 149 consecutive patients {(84 males; median age at alloBMT 11 yrs (0.5-21 yrs)}, 116 had undergone alloBMT for malignant diseases; 33 for non malignant conditions. Median time to follow-up was 13.1 mo (0.03-84 mo). Amongst 149, 44(29.5%) were found to have ON either of hips or knees after alloBMT; 45% (20/44) had at least 30% epiphyseal involvement. Twenty three (52.3%) ON lesions were identified in the first yearly scan; 43 (97.7%) by third yearly scans. Knees were more frequently involved than were hips but severity of ON was greater in hips. Seventy-five children had both pre and post alloBMT MRs of hips and/or knees, out of these 44 remained negative, 10 remained stable, 17 progressed, 2 regressed and 4 resolved completely after alloBMT. Besides age at alloBMT (p=0.051) and race (p=0.043), the primary risk factor was ON identified on preBMT MRs (p=0.001).

Conclusion: For children with normal pre transplant and first 3 yearly post-alloBMT normal scans, further ON follow-up is not required. Preventive strategies for ON should focus on pre-alloBMT rather than transplant or post-alloBMT risk factors.

MS2-9

MRI of paediatric wrist and hand trauma—what gives?

Mary-Louise Greer, Michael Guandalini, Anubhav Sarikwal, David Lisle, Kieran Frawley, Trevor Gervais, Geoff Donald Royal Children's Hospital, Brisbane (Australia)

Purpose: To evaluate post-traumatic wrist and hand injuries in children detected by magnetic resonance imaging (MRI) and assess the impact of MRI on patient management.

Materials and methods: Institutional PACS audit identified children 16 years or under having a wrist or hand MRI for trauma on a 1.5 Tesla magnet at a tertiary paediatric hospital from September 2005 to August 2010. Clinical indications for MRI, injury mechanism and timing, and reviewed imaging findings were collated. MRI abnormalities were categorised relative to indication: expected injury, expected injury with additional abnormality, unexpected abnormality or normal. Two orthopaedic surgeons performed chart review to assess clinical outcome and relative impact of MRI on management.

Results: In total, 77 wrist and hand MRIs were performed in 35 boys and 42 girls aged 6 to 16 years (median age 11.8 years) over 5 years. Clinical indications and MRI abnormalities included scaphoid fractures, bone oedema, ulnar collateral ligament (UCL) and related thumb injuries, triangular fibrocartilage complex (TFCC) tears, scapholunate ligament injuries, ganglions and loose bodies. Timing of MRI scans was 27% within 4 weeks and 73% within 3 months of injury, however this varied with clinical indication, on average 4 weeks for suspected UCL injury, 8 weeks for suspected scaphoid fracture and 21 weeks for TFCC tears. MRI was normal in 25%, with treatment discontinued in 95%; had the expected abnormality in 25%, with management unchanged in 79%; additional abnormalities in 9%, 43% requiring a change in non-operative treatment; and had unexpected abnormalities in 41% with change in non-operative care in 72% and surgery in 6%. Clinically suspected scaphoid fractures, UCL injuries and TFCC tears were detected on MRI in only 30-50%.

Conclusion: Post-traumatic wrist and hand MRI were abnormal in 75% however common clinically suspected injuries were demonstrated on MRI in only 30–50%. MRI often showed other unsuspected injuries resulting in management change. The

negative predictive value of 94.7% suggests earlier MRI is better to avoid unnecessary immobilisation.

MS2-10

Ultrasound as an ALARA-alternative to fluoroscopy for shoulder injection

Tyler Ternes, Kamran Ali, John Knudtson, Debbie Desilet-Dobbs Univ of Kansas, School of Medicine, Wichita (United States)

Purpose: The purpose of this retrospective study was to review the utilization of ultrasound guided shoulder injections prior to MR arthrography as an ALARA (as low as reasonably achievable) alternative to fluoroscopic guidance. This is of particular importance with the increasing awareness of radiation doses in the pediatric population.

Materials and methods: A systematic review was per-formed of ultrasound guided shoulder injections for MR arthrography at our facility. Ultrasound guided joint injection via an anterior approach, utilizing the rotator interval, has been previously described. The procedure was performed in our imaging facility by two attending radiologists, KA with 3 years of experience, and JK with 3 years experience. The rotator interval was identified with ultrasound. After sterile prep, local anesthetic was administered. Then, a 20 gauge spinal needle was directed into the rotator interval with sonographic assistance. Once the needle was in place, position was confirmed with injection of a small amount of lidocaine into the rotator interval. After confirmation of position, a mixture of 0.1 ml gadolinium and 19 ml of sterile saline was injected into the joint space. Total injected volume ranged from 6 to 14 ml. Typically, a sonographic technologist also provided assisted in the procedure by holding the ultrasound probe in the appropriate location. Successful injection was characterized by distention of the shoulder joint. This was done with ultrasound.

Results: A total of 22 patients underwent ultrasound guided shoulder joint injections. Procedure times were not recorded. Ages ranged between 10 and 18 years. Average age was 15.7 years. A review of subsequent MR arthrograms was performed. All of the arthrograms demonstrated successful joint injection, and deemed subjectively adequate for arthrographic interpretation. No complications or adverse events were reported. Conclusion: Ultrasound as an ALARA alternative to fluoroscopy can be successfully utilized for contrast injection prior to MR arthrography as a means to eliminate radiation dose in the pediatric population.

MS2-11

Water-bath method for sonographic evaluation of superficial structures of the extremities in children

Rajesh Krishnamurthy¹, Hyun Yoo Jeong², Michael Callahan³
¹Texas Childrens's Hospital, Houston (United States) ²Mokdong Hospital, Ewha Women's University, Seoul (South Korea) ³Children's Hospital, Boston (United States)

Introduction: Sonography using gel or a stand-off pad is a useful method for evaluation of superficial structures of the extremities. However, there are several limitations because of small field of view (FOV), curved surface of the extremity resulting in poor transducer contact, compression of the structures by the transducer, non-cooperation related to patient discomfort, and patient motion.

Materials and methods: A water-bath technique was developed, in which the affected hand or foot is immersed in warm water with scanning performed without touching the skin. 20 pediatric patients (age range 2 months–10 years) with superficial extremity pathology were scanned by the standard technique using gel/stand-off pad, and the water-bath technique.



Results: The water-bath technique was found to be superior to the standard technique for depiction of depth of skin ulcers, subcutaneous masses, tendon pathology, osteomyelitis, effusions of small joints, foreign body and vascular lesions. Reduced compression of the superficial structures by the water-bath technique led to the diagnosis of a subcutaneous arteriovenous malformation (AVM) missed on the standard technique. In Raynaud's disease, varying temperature of the water-bath reproduced the skin changes of Raynaud's phenomenon. The lack of contact of the transducer with the skin resulted in reduced patient discomfort and improved co-operation.

Conclusion: The water-bath technique overcomes important limitations of standard sonography in the evaluation of superficial structures of the hands and feet in pediatric patients, thereby improving diagnostic accuracy, and has become the technique of choice for this indication in our institution.

MS2-12

Subtalar coalition with sparing of the middle facet: Is the abnormal morphology of the sustentaculum tali a clue to etiology?

Sarah Bixby, Delma Jarrett, Susan Mahan, Samantha Spencer, Paul Kleinman

Children's Hospital Boston, Boston (United States)

Purpose: To determine the prevalence and associated morphologic alterations of subtalar coalitions that lie exclusively posterior to the middle facet (MF).

Materials and methods: Radiology records from 1998 to 2010 were reviewed to identify CT studies with findings of subtalar coalition. 100 patients (50 male, 50 female, mean age 13.45 years) with subtalar coalition were identified. 50% (50/100) of patients had bilateral coalitions. CT images of 150 subtalar coalitions were reviewed to determine the site of coalition with respect to the MF. Patients with posteromedial subtalar coalitions that spared the MF were further studied using mutiplanar reformats. AP measurements of the MF and the portion of the sustentaculum tali (ST) extending posterior to the facet (posterior ST) were measured. A ratio of the MF to the posterior ST was calculated and compared to a control population undergoing CT for triplane fractures.

Results: 21% (32/150) of coalitions involved only the MF and 53% (79/150) involved both the MF and posterior ST. In the remaining 26% (39/150), the subtalar coalition spared the MF and involved only the posterior ST. In this group, the mean AP measurements of the MF and posterior ST were 11.5 mm and 14.1 mm, respectively, compared to 16.8 mm and 5.1 mm in the control population (p<0.001). The ratio of the MF to posterior ST was 0.86 for coalition patients versus 3.7 for controls (p<0001). Conclusion: Although it is often taught that subtalar coalitions involve the middle facet, our findings indicate that this is often not the case. Subtalar coalitions that spare the MF are common, and demonstrate altered morphology with hypoplasia of the MF and elongation of the ST posterior to the MF. These findings suggest that the etiology of subtalar coalions lies in a generalized developmental disturbance involving the posteromedial talocalcaneal interval, rather than a focal fusion defect of the middle facet.

MS2-14

Intramuscular hemangioma-small vessel type (IH-SVT): radiologic-pathologic correlation

Sabri Yilmaz, Harry Kozakewich, Steven Fishman, Ahmad Alomari, Gulraiz Chaudry

Children's Hospital Boston, Boston (United States)

Purpose: IH-SVT is a rare tumor of skeletal muscle that typically occurs in children. Histologically, it is comprised of small vessels of capillary size whose endothelium is immunonegative for GLUT-1. We evaluated the imaging of this tumor, with particular emphasis on features differentiating it from vascular malformations and sarcomas.

Materials and methods: A retrospective review was performed from 1990 to 2010 to identify patients diagnosed with IH-SVT. Patient demographics, tumor size, site and type of imaging were recorded. Lesions were evaluated for calcification, fat, outline, vascularity, enhancement and involvement of local structures.

Results: There were 22 patients with a biopsy-proven diagnosis, with adequate imaging in 11 (M:F, 4:7). The mean age was 9.8 yr (14 mo-17. 5 yr). Seven lesions involved muscles of the extremities, 3 of the trunk and 1 of the neck. MR studies had been performed in all 11, ultrasound in 7 and angiograms in 4. All lesions had flow voids on MRI consistent with high-flow, were heterogeneously hyperintense on T2, isointense to skeletal muscle on T1 and showed heterogeneous contrast enhancement. Ten were well-circumscribed and intralesional fat was seen in 4. US demonstrated a heterogeneous, predominantly isoechoic lesion with vascular channels showing arterial flow. Angiography showed inhomogeneous parenchymal staining, with no evidence of direct arteriovenous shunting. In 8, follow-up MRI imaging ranging from 3 mos to 10 yr showed the lesion either remained stable in size or enlarged in proportion to the child, with no change in imaging characteristics.

Conclusion: IH-SVT is rare benign tumor of skeletal muscle that can be distinguished from venous malformation by its high-flow nature. Features differentiating it from infantile hemangioma are age of the patient, location, heterogeneity on imaging, non-involution, and intralesional fat. However, as the main characteristic that distinguishes it from a sarcoma is its relatively stable appearance over time, imaging does not obviate the need for a biopsy.

MS2-R1

Magnetic resonance imaging and joint outcomes in boys with severe hemophilia A treated with tailored primary prophylaxis in a multicentric clinical trial in Canada

Andrea Doria¹, Jeanette Kraft², Paul Babyn², Christine Demers³, Sara Israelis⁴, Mohan Pai⁵, Man-Chiu Poon⁶, Georges Rivard⁷, John Wu⁸, Majorie McLimont¹, Victor Blanchette¹

¹The Hospital for Sick Children, Toronto ²The Hospital for Sick Children, Toronto ³L' Hôpital de l'Enfant-Jésus, Québec, ⁴University of Manitoba, Winnipeg ⁵McMaster University Health Sciences Centre, Hamilton, ⁶University of Calgary, Calgary, ⁷CHU Sainte-Justine, Montreal, ⁸University of British Columbia, Vancouver (Canada)

Purpose: Tailored primary prophylaxis (TPP) is a reducedintensity treatment program for hemophilic boys whose aim goal is to prevent arthropathy. Our purpose was to evaluate the joint outcomes of hemophilic boys treated with TPP using MRI and physical examination as outcome measures.

Materials and methods: Ankles, elbows and knees of 24 boys (median [range] age at start of therapy, 1.6 [1–2.5] years) with severe hemophilia A from 10 Canadian pediatric hemophilia treatment centers [Hamilton (5), Montreal (4), Toronto (4), Winnipeg (3), Calgary (2), Quebec City (2), Halifax (1), Ottawa (1), Thunder Bay (1), Vancouver (1)] were examined by 1.5T MRI, and physical examination at a median age of 8.8 years (range 6.2–11.5 years). Compatible MRI scale (progressive [P] and additive [A] scores) and Colorado Child Physical Examination scale were used to score joint changes.



Results: At a median age of 8.8 years 50% (12/24) of boys had evidence of osteochondral changes in index joints [ankles, 8/12; elbows, 5/12; and knees, 0/12] on MRI. Soft tissue changes were detected in 31% (20/65) of index joints with no history of clinically evident bleeding [ankles 75% (12/16); elbows 19% (6/32); and knees 12% (2/17)]. In these apparently "bleed free" index joints hemosiderin deposition was detected by MRI in 26% (17/65) of joints [ankles 63% (10/16); elbows 16% (5/32), and knees 12% (2/17)]. Boys with abnormal soft tissue scores on MRI had higher physical examination ioint scores as compared to boys with normal MRI scores (p=0.03). Joint scores demonstrated positive and moderate correlations with the two MRI scales in examinations of the elbows (soft tissue scores, r=0.47/r=0.5, p=0.001/p=0.004, P/A scores: osteochondral scores, r=0.58, p<0.0001, P/A scores), and borderline positive and weak correlations with soft tissue MRI scores of the 2 scales in ankle examinations only (r=0.28, p=0.05).

Conclusion: After a median follow-up of 7.1 years, in spite of TPP and the absence of clinical symptoms, 50% (12/24) of boys manifested MRI evidence of osteochondral changes. TPP does not completely avoid the development of structural joint damage in hemophilic boys.

MS2-R2

Whole-body MRI (WB-MRI) in the diagnostic work-up of patients with chronic recurrent multifocal osteomyelitis (CRMO)

*Tina Stuber*¹, Norbert Heim², Toni Hospach¹, Micha Langendörfer¹, Peter Winkler¹, Thekla von Kalle¹

¹Olgahospital, Stuttgart, ²Katharinenhospital Department of Traumatologic Surgery, Stuttgart (Germany)

Purpose: The purpose of this board-approved study was to investigate the number, localization and morphology of osseous lesions in CRMO by WB-MRI with the aim to describe a typical pattern of involvement.

Materials and methods: 53 patients (34 female, 19 male; median age 11.7 years) with CRMO underwent diagnostic WB-MRI (1.5T) between November 2004 and April 2010. CRMO was confirmed by histology (n=37) or by clinical diagnostic criteria according to Jansson et al. (n=15). Two experienced pediatric radiologists (>9 years of expertise in cross sectional imaging) reviewed coronal STIR images (4 mm).

Results: We found 513 lesions in 456 bones (1-27 lesions/ patient; median 8). Nearly all lesions were of high signal intensity (509). 263/509 (51.7%) (lesions showed parts with signal intensities as high as that of fluid. 4 lesions (0.8%) were hypointense. In 162/509 (31.8%) lesions the surrounding periost, joint and/or soft tissue showed increased signal intensity. In 33 out of 456 (7.2%) affected bones the shape of the bone had changed, 6 of these 33 (18.2%) were vertebrae planae. Lesions in long tubular bones were predominantly found adjacent to a growth plate (184/225 lesions; 81.8%). The most frequently affected tubular bones were tibia (n=65), femur (n=51), humerus (n=18) and fibula (n=17). Most frequent localizations of lesions according to anatomic regions were: pelvis/hip (41/53 patients), knee (33), ankle (28) foot (23).and shoulder (18). Bilateral lesions were found in 40 of 53 patients. 19/53 patients had spinal lesions (6 vertebrae planae).

Conclusion: Our study confirmed that WB-MRI can detect high numbers of lesions in patients with CRMO. Lesions detected by MRI, including deformed vertebral bodies, may be clinically asymptomatic. Typical localization and morphology of the lesions can help to support the diagnosis of CRMO and rule out other differential diagnoses.



NA_{-1}

Dating of fractures: an analysis of key radiological features of fracture healing in children aged 5 years and younger and inter-observer agreement

*Ingrid Prosser*¹, Alison Kemp², Alison Evans³, Sara Harrison³, Susan Morris³, Sabine Maguire², Zoe Lawson²

¹Cardiff and Vale University Health Board, University Hospital of Wales, Cardiff²Department of Paediatrics, Cardiff University, ³Department of Radiology, Cardiff and Vale University Health Board (United Kingdom)

Purpose: Fracture dating has significant bearing on child protection procedures, highlighting discrepancies in explanations offered, particularly for multiple fractures. There is a dearth of primary evidence to underpin the dating of fractures in children. Thus we aim to determine key radiological variables in fracture healing, their timeline and the level of agreement between reporting radiologists.

Materials and methods: We analysed digital x-rays of children, 5 years of age and under, who presented during 2008 with accidental fractures of known timing. X-rays were reviewed independently by three paediatric radiologists, blinded to clinical details. They evaluated six features of fracture healing; soft tissue swelling(STS), periosteal reaction, soft callus, hard callus, bridging, and remodelling. We used agreement on feature presence, between two or more radiologists, as a proxy for the gold standard of known presence. Kappa analysis was performed to assess the level of agreement between radiologists.

Results: Two hundred and fourteen films of 77 fractures from 63 children (mean age 3.9 years) were analysed. STS was seen in 60% of fractures in days 1–2, and then declined sharply. Periosteal reaction was first seen at day 5, and was seen in 70% of fractures at 21 days. Soft callus was first seen at day 12, and was seen in 46% of fractures at 21 days. Hard callus and bridging were both first seen at day 19, and were seen in 60% by 4 weeks. Remodelling was only found in fractures more than 30 days old. Kappa scores were between 0.52 and 0.79 overall and were greater still when a plaster cast was not present.

Conclusion: These data define the key features from which fracture dating can be estimated in young children. It is possible to date a fracture as acute (less than 1 week), recent (1–3 weeks), and old (more than 3–6 weeks) based on the presence or absence of five variables in combination. In addition, this study demonstrates good inter-observer agreement on the features of fracture healing assessed.

NA-2

Suspected non-accidental trauma—comparison between confirmed and indeterminate cases in a large 12-year review Eglal Shalaby-Rana, Allison Jackson, Tanya Hinds, Natalie Kissoon, Robert McCarter, Dorothy Bulas Children's National Medical Center, Washington (United States)

Purpose: To retrospectively review the distribution and prevalence of injuries in patients with suspected non-accidental trauma (NAT) and to compare the injuries in patients with proven NAT with those whose final outcome was indeterminate for abuse.

Materials and methods: From the radiology records of patients suspected of NAT, 653 children who had undergone radiographic skeletal surveys (SS) were identified. All radiological imaging results were recorded. The medical charts of 403 of these patients were retrospectively reviewed and the outcome, as determined by the child abuse pediatrician, was recorded. Final outcome was categorized as NAT 144 (36%), indeterminate (IND) 184 (45.5%), accidental trauma 68 (17%), medical 5 (1%) and unknown 2 (0.5%).

Results: Of 144 patients with confirmed NAT- 65 female, 79 male; age range birth-11.5 yrs, mean 17.4 mos. 50% had abnormal SS - 50% rib fractures (97% healing); 32% classic metaphyseal lesions (CML); 43% shaft fractures (32% healing, 55% acute, 13% both).; 26% skull fractures; 15% axial bone fractures and 4% spine fractures. 81% had head CT scans; 57% abnormal. 20% had abdomen CTs; 90% abnormal. Of 184 patients with IND; 81 female,103 male; age range birth-18 years, mean age 13.8 months. 54% had abnormal SS-18% rib fractures (83% healing); 10% CMLs; 44% shaft fractures (16% healing, 82% acute, 2% both), 30% skull fractures; 5% axial bone fractures and 4% spine fractures. 71% had head CT scans, 54% abnormal. 4% had abdomen CTs, 75% abnormal.

Conclusion: The types and prevalence of injuries parallel those in the literature except for a higher prevalence in abdominal injuries in this series. This probably reflects the increase in cross-sectional imaging in this population. Despite the fact that a number of children in the IND group had evidence of classic abuse injuries, including CMLs and healing rib fractures, proving NAT remains difficult.

NA-3

Validation of a CT based finite element bone model for investigating mechanisms of injury in child abuse

Amaka Offiah, Nick Emerson, Matt Carre, Gwen Reilly, Hayley Morris University of Sheffield, Sheffield (United Kingdom)

Background: Recently, finite element (FE) models based upon high resolution three-dimensional computed tomography (CT) images have been used to assess not only the mechanical properties of bone, but also the performance of its microarchitecture and even the effectiveness of treatments for bone fracture.

Purpose: To investigate whether the geometry and material properties of mid-shaft cortical bone calculated via CT imaging can be used to determine the location of fractures under prescribed test conditions in an FE model.

Materials and methods: Four porcine tibiae were imaged with a spiral CT (GE VCT 64 multi-slice) scanner. FE models were then created for each bone, allowing the correlation of specific geometry between FE and laboratory testing. Endplates were drawn in a CAD package and amalgamated with the cortical bone at the start of the metaphyseal region to replicate the constraints used in laboratory testing and to isolate the mid-shaft region. FE test results were validated by comparison with matched loading tests of each scanned bone within a laboratory setting. The loading tests were conducted by the application of torsional forces to each bone specimen until fracture occurred.

Results: Finite element model predictions of torsional rigidity correlated significantly with experimental torsional rigidity, validating the modelling process for future testing methods.

Conclusion: The use of FE analysis to determine failure mechanisms has great potential for use as a tool in fracture studies. Having validated the technique on a porcine model, we shall now conduct tests based on CT images of infants and children in order to improve our current understanding of mechanisms of injury in infants. In particular the technique may ultimately prove to be important for the validation of mechanisms of injury put forward by carers in the context of suspected child abuse, not only for shaft fractures, but also for fractures at other sites.

NA-4

Prevalence of rachitic changes in deceased infants: a radiologic and pathologic study

Jeannette Perez-Rossello¹, Anna G McDonald², Andrew E Rosenberg², Susan L Ivey¹, Joann M Richmond², Paul K Kleinman¹ Children's Hospital Boston, Boston, ²Massachusetts General Hospital, Boston (United States)

Purpose: Determine whether there are radiographic or pathologic changes of rickets in two groups of deceased infants, one group with inflicted skeletal injuries and a second group with sudden infant death syndrome (SIDS).

Materials and methods: 26 deceased infants (mean age 2.6 months) with fractures concerning abuse on skeletal imaging underwent osseous resection, detail specimen radiography and post mortem histopathologic assessment that included sections of the distal femurs. 108 infants (mean age 2.5 months) dying of SIDS underwent skeletal surveys as part of post mortem assessment by a State Medical Examiner. Two pediatric musculoskeletal radiologists reviewed the skeletal surveys for rachitic changes at the wrists and knees. The criteria for rachitic changes were physeal widening and/or cupping of the metaphysis, loss of the zone of provisional calcification and fraving of the metaphysis. A musculoskeletal pathologist and a pathology resident reviewed the distal femur specimens for histologic evidence of rickets. The criteria for rickets included osteoid alterations and disorderly accumulation of cartilage at the site of enchondral bone formation. Results: There were no radiographic rachitic changes in the SIDS cases. There were no radiographic changes of rickets in the 26 infants dying with inflicted skeletal injuries, and there were no pathologic features of rickets in the 88 distal femoral histology specimens examined in this group. The prevalence of rachitic changes in infants that died of SIDS was zero (95% CI: 0-0.04). The prevalence of radiographic or pathologic rachitic changes in infants that died with inflicted skeletal injuries was zero (95% CI: 0-0.16).

Conclusion: There were no rachitic changes in infant fatalities where inflicted injuries were present or where the cause of death was SIDS. Although vitamin D insufficiency/deficiency is common in infants, it is unlikely to manifest as rickets in the general population or in infants with inflicted skeletal trauma.

NA-5

Long bone fracture detection in suspected child abuse: contribution of lateral views

Boaz Karmazyn, Ryan Duhn, S. Gregory Jennings, Matthew Wanner, Bilal Tahir, Roberta Hibbard, Ralph Hicks

Indiana University School of Medicine, Riley Hospital for Children, Indianapolis²Kalamazoo Division – ARS, Kalamazoo (United States)

Purpose: Evaluate if adding lateral radiographs for long bones changes frequency and confidence of fracture detection in skeletal survey radiographs for suspected abuse.

Materials and methods: From the radiology archives of a tertiary care children's hospital (1/2003-7/2008), we identified 100 patients less than 2 years of age who underwent skeletal survey for child abuse, including 56 consecutive patients with multiple long bone fractures, 22 patients with a single fracture, and 22 patients with no fractures. Our routine skeletal survey includes frontal and lateral radiographs of the long bones. Two separate randomized study series were created. The first group included only frontal radiographs and the second group included both frontal and lateral radiographs of the long bones. Four radiologists (two pediatric radiologists, one pediatric radiology fellow, and one general radiologist) evaluated the two study series for metaphyseal and diaphyseal fractures.

Results: For combined readers, significantly more metaphyseal fractures (p=0.01) were detected with the two views series radiographs compared with the frontal only view; there was no difference for diaphyseal fractures. Sensitivity of the frontal view for metaphyseal fractures was 72%. Confidence was also significantly higher for the two views series. Kappa was 0.64-0.71 for



diaphyseal fractures for both series and 0.34 for metaphyseal fractures in the frontal view only. The kappa improved when lateral views were added (0.46).

Conclusion: ACR recommends frontal only radiographs of the long bones in skeletal surveys for child abuse. Adding lateral radiographs resulted in significant improved confidence in fracture detection and increased detection of metaphyseal fractures.

NA-6

Upper and lower limb fractures in non-ambulatory children: are we doing enough skeletal surveys?

Raj Das, Mark Ingram, Samantha Negus St George's Hospital, London (United Kingdom)

Purpose: There are well recognised fracture patterns that hold a high specificity for non-accidental injury (NAI) however a long bone fracture sustained in a non-ambulatory child is the commonest radiological mode of NAI presentation. Following recent high-profile UK cases of child physical abuse, and despite the efforts of paediatricians and paediatric radiologists, it is still felt that NAI presentations are under-recognised. We have analysed the practice within a London teaching hospital, to assess standards of NAI recognition.

Materials and methods: Retrospective review was conducted of children presenting over a 5-year period (2005–2010) undergoing a full NAI skeletal survey. Injuries were categorised into: cranial, upper and lower limb, rib injuries and assessment of highly specific NAI patterns and multiple injuries. Further sub-assessment of all non-ambulatory children (<1 year of age) presenting with an upper or lower limb fracture May 2008–2010 was also performed.

Results: 81 skeletal surveys for NAI were performed 2005–2010. 52 (64%) skeletal surveys were performed in those under 1 year, and the remaining 29 (35.8%) were >1 year of age. Of those under 1 year of age: 69.2% had no bony injuries, 11.5% had an upper limb fracture, 9.6% had a lower limb fracture. 11.5% demonstrated injuries with high specificity for NAI and 5.8% had multiple fractures. In the 2-year substudy of all non-ambulatory patients, 61 children sustained an upper or lower limb fracture. 9% of patients went on to a skeletal survey for upper limb fracture and 6.8% for lower limb fracture.

Conclusion: Non-ambulatory children (<1 year) sustaining humeral or femoral fractures represent a small proportion of skeletal surveys performed for NAI. Our study demonstrated that only 9% of upper and 6.8% of lower limb fractures sustained in non-ambulatory children proceeded to skeletal survey. We suggest increased vigilance in the assessment of long bone fractures in non-ambulatory children, as a significant number of these may be related to NAI, and current data suggest that these may be under-reported.

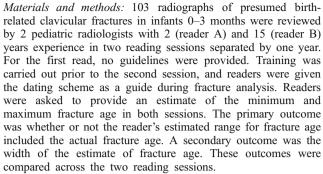
NA-R1

Fracture dating in infant abuse: a scientific system to improve radiologist performance

Michele Walters, Peter Forbes, Sarah Bixby, Carlo Buonomo, Paul Kleinman

Children's Hospital Boston, Boston, United States

Purpose: Dating fractures is critical in cases of suspected infant abuse, but there are little scientific data to guide radiologists, and dating is generally based on personal experience and conventional wisdom. We previously reported a scientific scheme for dating fractures in infants based on an analysis of subperiosteal new bone and callus formation in birth-related clavicular fractures. We hypothesize that when used as a guide this system can significantly improve the ability of radiologists to accurately date fractures in young infants.



Results: The rate of correct response significantly increased after training for each reader (reader A: 66% to 89%, p<.0001; reader B: 76% to 86%, p=.041). The width of estimated fracture age after training was significantly smaller for each reader (reader A: mean width 17 days to 13 days, p<.0001; reader B: 25 days to 15 days, p=.001).

Conclusion: Our results suggest that the ability of a radiologist to accurately date fractures can improve significantly when provided with a scientifically based system outlining patterns of fracture healing. This scheme can be applied in radiologic practice and may prove particularly useful in cases of suspected abuse, where fracture dating often has forensic implications.

NE1-1

3-tesla intraoperative MRI in the management of paediatric cranial tumours—initial experience

Shivaram Avula, Laurence Abernethy, Barry Pizer, Conor Mallucci Alder Hey Children's Hospital NHS Foundation trust, Liverpool, (United Kingdom)

Purpose: To review the initial experience of a dedicated paediatric 3T intraoperative MRI (IoMRI) unit in the management of paediatric cranial tumours.

Materials and methods: 37 Children (Mean age 10.9 years; range 0.2–17.6 years) underwent IoMRI during cranial tumour resection using a 3T MR scanner located adjacent to the neurosurgical operating theatre that is equipped with neuronavigation facility. IoMRI was performed either to assess the extent of tumour resection after surgical impression of complete/intended tumour resection or to update neuronavigation. The IoMRI findings were reviewed with the patient records, pathology reports and follow up imaging where available.

Results: Of the 37 children, complete resection was intended in 25. IoMRI confirmed complete resection in 15. Residual tumour was seen in 5 of these children, 2 (5%)of whom underwent further surgery and complete resection was achieved. Of the remaining 3 children with residual tumour, resection was extended in 1(2%) child but complete resection was not achieved, second look surgery in the 2nd child did not reveal residual tumour on direct visualisation and resection biopsy of a small residual abnormality revealed tumour tissue in the 3rd child. Among 5 children in the complete resection group, the findings were equivocal for the presence of residual tumour. In 3 of these children, it was not possible to distinguish surgically induced contrast enhancement from possible residual tumour along the surgical margin. Follow up imaging in these children revealed gradual reduction in the degree of enhancement. In 12 of the 37 children, the surgical aim was to debulk the tumour. In 7(19%) children surgical resection was extended following IoMRI. There were no procedure related complications.

Conclusion: In our initial experience 3T IoMRI has increased the rate of complete resection and the extent of tumour debulk with



surgical strategy being modified in 26% of children undergoing cranial tumour resection. It is important to be mindful of potential pitfalls in image interpretation and collaborative analysis of IoMRI by the radiologist and neurosurgeon is vital to avoid errors.

NE1-2

An MR system for imaging neonates in the NICU

Jean Tkach, Jean Tkach, Randy Giaquinto, Wolfgang Loew, Ronald Pratt, Barret Daniels, Blaise Jones, Lane Donnelly, Charles Dumoulin

Cincinnati Childrens Hospital Medical Center, Cincinnati (United States)

Purpose: The current practice of transferring neonates to radiology departments and imaging in full-sized MR scanners is associated with significant safety and image quality issues. To overcome these issues, we are converting a low-cost, small-bore (28 cm) single channel 1.5 Tesla MRI scanner intended for adult orthopedic use (GE Healthcare, Waukesha, WI) into a dedicated neonatal MRI system designed for pre-clinical and clinical use. This small system can be easily sited and installed in a Neonatal Intensive Care Unit (NICU), mitigating many of the logistical limitations. We present the capabilities of our system, and review the steps necessary in the development of such a project. Materials and methods: We have installed a prototype scanner for technological development and preclinical research in a Biosafety Level 2 (BSL-2) research laboratory. A second scanner will be installed in our NICU for clinical use in approximately 9 months. The MR imaging performance of the gradient system (70 mT/M max amplitude; 200 T/m/s slew rate) exceeds that found on fullsized MR systems, permitting us to optimize the most advanced MRI techniques (e.g. ASL, DCE, DTI) for neonate size and anatomy. Modifications to the original system include the addition of multiple receiver channels and the development of dedicated phase array surface and volume coils.

Results: The modified system enables state-of-the-art imaging of the neonatal brain, chest and abdomen with a high degree of safety and diagnostic imaging quality. S/N enhancements and parallel imaging enabled by these changes result in improved image quality and/or reductions in scan time, beyond what is currently possible on conventional MRI scanners. The advanced techniques and resulting image data from our research laboratory unit will be presented.

Conclusion: The development of new RF coils, parallel imaging techniques and advanced MR acquisition strategies optimized for the neonate enables high-performance neonatal MRI on a small-size 1.5 Tesla MRI scanner within the NICU and creates new research tools to advance the study of early human development. The adult orthopedic MR system is a product of GE Healthcare, Waukesha, WI.

NE1-3

Diffusion tension imaging (DTI) and 1H in-vivo MRS in normally developing children, and in children with hypoxic-ischemic encephalopathy

Zinayida Rozhkova, Elena Dolia Medical Clinic "BORIS", Kiev (Ukraine)

Purpose: We propose fractional anisotropy (FA) and apparent diffusion coefficeint (ADC) values, and the ratios of the main cerebral metabolites as quantitative indicators for the characteristics of regional and age peculiarities of the brain microstructure and metabolism in normally developing children and in children with hypoxic-ischemic encephalopathy.

Materials and methods: 56 children were examined by 1H MRS using 1.5T Signa EXCITE HD (GE). The 1st group (NG)

consisted of 10 healthy children (in the age from 1 month to 16 years). The 2nd group (PG) included 46 developmentally delayed children (2 weeks -16 y). The subjects of both groups were divided into 5 age groups: less than 1 mo, 1 mo- 1 y, 1 y- 3 y, 3 y-8 y, and older than 8 y. 1H spectra were recorded with STEAM:TR/TE=1500/144 ms.

Results: We analyzed alteration of the FA, and ADC values during neurodevelopment: in the neonates of the NG they were higher than in adult brain. In the NG during first 3 years, the mean ADC values in WM are (1.13×10-3 mm2/s) and in GM (1.02×10-3 mm2/s), and in children older than 3 v. decreasing ADC values with maturation of the brain were observed. In the PG, there was a significant reduction of FA values in the anterior part of corpus callosum, the posterior limb of the right, and left internal capsule, the left superior cerebellar peduncle and the right and left middle cerebellar peduncle. In PG (for all age groups) FA was elevated in the left putamen. In the PG (for all age groups) a significant decrease of NAA/Cr, increase of Cho/ Cr, and mIns/Cr in anterior cingulate and left striatum in comparison with NG was obtained. In WM in the NG in the 1-3 months age group, the Glu/Cr increased rapidly from (0.23+ -0.02), peaking at 6 months (0.34+-0.02), and thereafter decreasing moderately to adults level (0.30+-0.02) for the age

Conclusion: DTI and MRS of the fetal, neonatal and adolescent human brain gives us a unique possibility for monitoring neurodevelopment and provide a baseline for age-related differences in the normal human brain and in the brain under pathology.

NE1-4

Perinatal brain injury assessed by dynamic FDG-PET in newborn piglets

Charlotte de Lange, Eirik Malinen, Hong Qu, Berit H Munkeby Oslo University Hospital Rikshospitalet, Oslo (Norway)

Purpose: Changes in cerebral glucose metabolism may be an early prognostic indicator of hypoxic ischemic injury. The aim of this study was to use a piglet model to evaluate dynamic FDG-PET changes immediately after global hypoxia and the influence of the oxygen content during resuscitation.

Materials and methods: 16 anesthesized piglets were subjected to global hypoxia using FiO2 8% for 40 min followed by resuscitation with FiO2 21 or 100% for 30 min and reoxygenation. Dynamic PET was performed by injection of 18F Fluoro-2-deoxyglucose (18F FDG), before and after hypoxia and resuscitation. T2 weighted MR images were acquired for anatomic imaging and coregistered with the FDG-PET images. Regions of interest (ROIs) were traced around the basal ganglia, cerebrum, cerebellum, cortex and white matter. Global and regional cerebral metabolic rates of glucose (CMRgl) before and after hypoxia and resuscitation was assessed by Patlak analysis. The two resuscitation groups (room air and 100% O2) were compared. Statistical analysis was performed with paired t-test with a significance level of p=0.05.

Results: Global CMRgl was significantly reduced from a mean baseline level (± 1 SD) of 21.3 ± 1.9 to $12.3\pm 0.9~\mu$ mol/min/100 g after hypoxia and resuscitation, for all piglets (p<0.01). There was no significant difference between the 21 and 100% group or between different regions, but the basal ganglia, cerebellum and cortex showed the greatest decrease in CMRgl.

Conclusion: Global hypoxia causes immediate decrease of cerebral glucose metabolism in newborn pigs independent of resuscitation with 21 or 100% of O2. Early regional and global cell death or a down-regulation of glucose metabolism are likely mechanisms.



NE1-5

Neurodevelopmental outcomes in preterm infants with diffuse excessive high signal intensity seen on MRI at near term-equivalent age

Ji Hye Kim, Tae Yeon Jeon, So-Young Yoo, Hong Eo, Jung Yi Kwon, Jee Hoon Lee, Yoon Sil Chang, Won Soon Park Sungkyunkwan University, Samsung Medical Center, Seoul (South Korea)

Purpose: Diffuse excessive high signal intensity (DEHSI) in the white matter (WM) is commonly seen on brain MRI in preterm infants. However, it is unclear whether DEHSI represents overt white matter abnormality causing any neurodevelopmental deficit. This study was performed to compare the neurodevelopmental outcomes between preterm infants with DEHSI and those without DEHSI.

Materials and methods: High risk preterm infants (n=126) who underwent brain MRI at the time of discharge (mean corrected gestational age of 36.6 ± 1.9 weeks) were classified into 2 groups (infants with DEHSI and those without DEHSI) and the neuro-developmental outcomes including Bayley scales, presence of cerebral palsy, and neurosensory impairment at 2 years of age were compared. The association of other WM lesions (non-cavitary lesion, cystic encephalomalacia, loss of volume, ventriculomegaly, and myelination) and neurodevelopmental outcomes were also evaluated. In addition, apparent diffusion coefficients (ADCs) in the frontal, central, and posterior WM at the level of centrum semiovale were analyzed.

Results: Ninety five infants (75%) were classified into a group with DEHSI while there were 31 controls without DEHSI. Severe cognitive delay, severe motor delay, and cerebral palsy were not significantly different in two groups. Severe motor delay and cerebral palsy were more common in infants with DEHSI and other WM abnormalities compared with infants without WM lesions (p=.001 and p<.0001, respectively). Of WM abnormalities, non-cavitary lesion and cystic periventricular leukomalacia were significant univariate predictors for severe motor delay (9.3; 1.56–52.63, 7.9; 1.09–55.56) and cerebral palsy (32.3; 5.02–250, 13.3; 1.61–100). In preterm infants with DEHSI, ADC was higher in all WM regions than in those without DEHSI (p<.0001), with posterior white matter ADC being higher than central or frontal white matter ADC.

Conclusion: Although the incidence of DEHSI was high in highrisk preterm infants at near term MRI, DEHSI alone does not predict adverse neurodevelopmental outcomes.

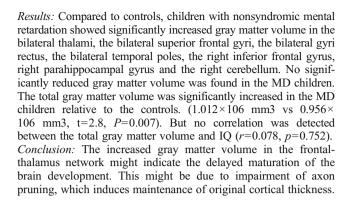
NE1-6

The alteration of gray matter volume in children with mental retardation: an optimal voxel-based morphometry study

Xinyu Yuan¹, Sheng Xie², Jiangxi Xiao², Chunhua Jin¹ Capital Institute of Pediatrics, Beijing (China), ²The Peking University Hospital, Peking (China)

Purpose: To detect brain structural difference in children with nonsyndromic mental retardation compared to children with typically normal development.

Materials and methods: Magnetic resonance imaging was obtained from 21 children with nonsyndromic mental retardation and 30 agematched control children without intellectual disabilities on a 1.5T scanner. Voxel-based morphometry analysis with an optimization of spatial segmentation and normalization procedures was applied to compare the two groups in order to find differences in gray matter. The total gray matter volume was compared between the two groups, and correlation was conducted to analyze the relationship between the total gray matter volume and Intelligence Quotient (IQ).



NE1-7

Functional connectivity evaluation of mesial temporal lobes in epilepsy, potential replacement of Wada memory tests; preliminary studies.

Dennis Shaw, Andrew Poliakov, Edward Novotny, Khanna Paritosh, Gisele Ishak, Jeffrey Ojemann

Seattle Children's Hospital, Univ. of Washington Seattle (United States)

Purpose: Functional MRI (fMRI) has increasingly supplanted the Wada test in presurgical evaluation of epilepsy, in particular for language lateralization. Clinical evaluation of mesial temporal lobe function in memory with fMRI has been more difficult, and is particularly problematic in children who are unable to cooperate with the Wada. We have begun investigation of resting state fMRI for evaluation of mesial temporal lobe function.

Materials and methods: Imaging was performed on a Siemens (Erlangen, Germany) 3T (Trio) (EPIBOLD sequence, TE=30 ms, flip angle = 90°). Analysis was performed using 1000 Functional Connectomes Project scripts based on AFNI and FSL software packages. We retrospectively analyzed connectivity patterns in 5 healthy control subjects (ages 11–15) and compared to 2 patients (age 17 and 6) with epilepsy due to hippocampal sclerosis and 3 patients (ages 5, 3 and 20) with epilepsy without hipppocampal sclerosis including two under propofol anesthesia. Resting state data were analyzed for connectivity with seed points in ventral precuneus and retro-splenial cortex.

Results: Robust connectivity with seed points was seen in fusiform gyri, parahippocampus and hippocampus in individual subjects. Connectivity pattern was found to be bilateral and symmetric in control subjects (in agreement with the literature), and in the patients with epilepsy without hippocampal sclerosis. In contrast the epileptic patients with hippocampal sclerosis exhibited an asymmetric pattern of connectivity with decrease in the hippocampal and parahippocampal regions ipsilateral to their sclerosis.

Conclusion: Epilepsy patients with hippocampal sclerosis revealed a deviation from typical connectivity pattern in controls with diminished connectivity on the side ipsilateral to seizure onset, also not seen in patients with extra temporal epilepsy. This connectivity in memory networks revealed with fcMRI analysis appears to be sufficiently robust, to be clinically applicable in assessment of both adult and pediatric subjects with epilepsy, warranting further study to correlate with Wada and neuropsychiatric testing.

NE1-8

Utilization of diffusion tensor imaging (DTI) fiber tractography in children undergoing corpus callosotomy

Susan Palasis, Robert Flamini, Laura Hayes, Richard Jones, Damien Grattan-Smith

Children's Healthcare of Atlanta (United States)



Purpose: To correlate the extent of corpus callosotomy when comparing anatomical and electrical findings utilizing MRI, DTI/Fiber Tractography and electroencephalography (EEG).

Materials and methods: A total of 13 children underwent corpus callosotomy at our institution over the past 5 years. These children had intractable epilepsy and no focal localizing area of ictal onset. Of this group of children, 5 underwent DTI/Fiber tractography. The extent of the callosotomy was determined by the ictal and interictal features, imaging findings, and patient developmental profile. Post operative MRI volumetric imaging was performed on 1.5T and 3.0T scanners. CISS/SPACE imaging sequences were analyzed by a neuroradiologist blinded to the findings of MR tractography or patient's clinical outcome. DTI was performed in 12–35 directions and was coregistered to the 3D imaging data sets utilizing Siemens Neuro3D software for seed points and fiber tractography. EEG reports and patient outcomes were analyzed and compared to imaging data in regards to the degree of EEG asynchrony, seizure frequency, and severity.

Results: The analysis of the conventional MRI data disclosed full callosotomy in only one of the patients in the group. When fiber tractography was analyzed, there was an excellent correlation between the techniques. The visualization of the connecting fibers was far superior utilizing DTI. Conversely, the degree of electrical asynchrony did not correlate with the extent of the disconnection. Seizure outcome showed significant improvement on 2 out of 3 patients following complete callosotomy, one of whom still had posterior connection fibers on tractography.

Conclusion: We recommend the performance of fiber tractography and CISS/SPACE imaging for patients status post corpus callosotomy for proper visualization of the degree of callosal disconnection. According to seizure outcome, these high resolution images can be used to define the need for further surgical intervention in patients with suboptimal seizure outcome. The electrical correlation appears to be poor. Remaining connecting fibers across the corpus callosum can be missed by conventional MRI analysis.

NE1-9

Role of diffusion tensor imaging in the post-surgical MR of pediatric patients with pharmacologically resistant epilepsy undergoing hemispherotomy

Carlo Cosimo Quattrocchi, Daniela Longo, Luciana Nogueira Delfino, Olivier Delalande, Elisabetta Genovese, Nicola Specchio, Lucia Fusco, Federico Vigevano, Vittorio Cannatà, Bruno Bernardi, Francesco Randisi

Ospedale Pediatrico Bambino Gesù, Rome, (Italy)

Purpose: Pharmacologically refractory seizures from monolateral brain lesions in pediatric patients are responsive to surgical disconnection of the affected hemisphere. The aim of our study was to correlate residual epileptic activity after functional hemispherotomy with conventional magnetic resonance imaging (MRI) findings and Diffusion Tensor Imaging (DTI) including tractography. Materials and methods: Four patients have been studied: two males and two females, mean age 6 years and 2 months. The etiologies of monolateral refractory seizures were hemimegalencephaly, Rasmussen encephalitis, hemispheric dysplasia and prenatal middle cerebral artery infarction. All patients underwent hemispherotomy as treatment for refractory epilepsy: two patients underwent a vertical parasagittal hemispherotomy and the other two underwent a peri-insular hemispherotomy. MRI studies were performed using a 1.5 T Magnet (Achieva PHILIPS Nova Dual 66 mT/m, slew rate 160T/m/sec), applying a protocol of conventional MRI (FLAIR and Turbo-Spin-Echo T1/T2 weighted imaging), isotropic voxel MPRAGE T1 weighted imaging, followed by DTI with SE-EPI images acquired at b0 and b1000 (6 gradient directions applied). Analysis of images was performed off-line on an EWS (Extended MR workspace, PHILIPS) workstation.

Results: Soon after hemispherotomy all patients had seizures remission. In the patient with Rasmussen encephalitis, seizures recurred after a few months. Tractography revealed an anterior interhemispheric residual bundle of corpus callosum connecting the two cerebral hemispheres. Fiber Tractography of the three patients with 1 year follow-up seizure free showed a complete interruption of interemispheric connections, which is a prerequisite of a good clinical outcome.

Conclusion: Our study suggests that DTI can be used in the post surgical evaluation of hemispherotomies for drug resistant epilepsy to demonstrate residual inter-hemispheric connections and their anatomical location. Further studies in larger patient cohorts should validate DTI with Tractography as a useful technique to evaluate the anatomical results of hemispherectomy.

NE1-11

Blunt head trauma in a community health care setting: a description of patients and use of computed tomography

Jane McMillan, MD¹, Patrick Van Winkle Van Winkle, MD¹, Casey Vibbard, MD, MsPH², Ngoc Ho, PhD³, Laura Sirikulvadhana, MPH³

¹Kaiser Permanente Medical Center, Anaheim, United States, ²Department of Family Medicine, Kaiser Permanente, Orange County ³Research and Evaluation, Southern California Permanente Medical Group,

Purpose: Describe the characteristics of pediatric patients presenting with minor blunt head trauma in a community health care setting and identify factors associated with the use of computed tomography (CT).

Materials and methods: Retrospective cohort study of consecutive patients zero to 18 years of age presenting to community clinics or general emergency departments in our Health Maintenance Organization over a 12 month period. Logistic regression models were used to compare differences in characteristics between patients who received and did not receive CT scans.

Results: One thousand and seven patients were included in the study, 62% male, age range from 14 days to 18 years. Thirty-three percent were seen in a primary care clinic, 34% in urgent care, and 33% in the emergency department. The majority of patients presented with trivial mechanisms of injury and 99% by private transportation. Thirteen (1.3%) patients were hospitalized, and none required Neurosurgical intervention or died. One hundred eighty-nine (18%) had CT scans, 2 (0.2%) showed evidence of ciTBI. One of these patients was an adolescent that presented to the emergency department after a fall off a skateboard, with a nondisplaced skull fracture and a small subdural hematoma. The second patient was an infant who presented 3 days after a poorly described event to urgent care with evidence of nonaccidental trauma, and had subdural and subarachnoid hemorrhage. Also, for the patients that did not receive CT scans, none subsequently had scans or were found at a later time to have ciTBI related to this event. Patients were more likely to have a CT scan if treated in the emergency department compared to the clinic (OR 7.78, 95%CI 3.01-20.15). Time to presentation was not found to be a significant variable, with patients that presented after 48 h just as likely to be scanned as those that presented at 2 h (OR 1.46; 95% CI 0.84-2.53).

Conclusion: This is a distinct, previously unstudied group of patients that appears to be at low risk for ciTBI. There is a potential for overuse of CT in this population.



NE1-12

Brain perfusion in trigonocephaly: arterial spin labelling in children *Francis Brunelle*, David Grevent, Federico di Rocco, Christian Sainte-Rose, Nathalie Boddaert

Hopital Necker Enfants-Malades, Paris (France)

Purpose: Craniosysnostosis in children leads to an absence of growth of the cranium leading to increased intracranial pressure. The purpose of this study is to evaluate the brain perfusion pre and post operatively in children with trigonocephaly.

Materials and methods: Brain perfusion was evaluated in children with trigonocephaly pre and post operatively (day three and after three months) with MRI and arterial spin labelling. Mean age was 9 months. Values were compared to a control group matched for age.

Results: preliminary results (6 patients on a 3 months period) shows a preoperative 26% global diminution of brain perfusion. Post operatively brain perfusion increases by 9% but is still inferior to normal (-17%).

Conclusion: ASL demonstrate a global diminution of brain perfusion in children with trogonocephaly. In May 2011 results on a series of 12 to 16 patients will be presented.

NE1-13

Spinal drop metastases revealed with (RS) EPI diffusion tensor imaging (DTI)

Laura Hayes, Richard A Jones, Damien J Grattan-Smith, Susan Palasis, Dolly Aguilera, Claire Mazewski

¹Children's Healthcare of Atlanta and Emory University, Atlanta (United States)

Purpose: To evaluate readout segmented (RS) EPI as a method for diffusion imaging of the spine to detect drop metastases from hypercellular brain tumors.

Materials and methods: Readout segmented DTI was performed on a 1.5T Avanto & a 3T Trio scanner with 7 segments, a parallel imaging factor of 2, a b factor of 500 s/mm2 and an in-plane resolution of 1.25 mm². The b factor was chosen to be lower than that used for studies of the brain to compensate for reduced SNR due to the smaller voxel dimensions and for a reasonable acquisition time of approx. 5 min. A sagittal slice orientation was chosen. In initial studies of the C-spine, both gated and nongated versions of the sequence were evaluated, however artifacts were high when gating was not used. Thus, only gated C-spine imaging was used, performed with a single slice acquired on every 3rd heartbeat and a delay for the peripheral trigger of approx. 1/3 of the cardiac cycle. Gating was not used for the T/L spine. This sequence was added to standard protocols for imaging pediatric spines to evaluate for drop metastases from hypercellular brain tumors. 44 studies were performed, and the studies were reviewed independently by 3 pediatric neuroradiologists.

Results: (RS) EPI produced excellent image quality, nearly free from the artifacts plaguing other types of spine diffusion imaging. Traditional artifacts from the vertebra and motion of CSF, breathing, and arterial pulsations were drastically reduced, providing good spatial resolution and strong signal, allowing identification of hypercellular drop metastases. These were identified in 5 patients where no lesions were identified on post-contrast T1-weighted images. Moreover, DWI was helpful in confirming a lack of metastases when conventional sequences were negative.

Conclusion: (RS) EPI is a powerful method for diffusion imaging of the spine. This technique is exquisitely helpful in identifying

drop metastases to the spine from hypercellular brain tumors. Diffusion imaging of the spine should be used routinely in the evaluation for drop metastases.

NE1-14

Feasibility of non-invasive quantitative MRI measurements of cerebral vascular reactivity using a computer controlled stimulus in children with sickle cell disease

Andrea Kassner, Jackie Leung, Fatima Nathoo, Manohar Shroff, Gabrielle deVeber, Suzan Williams

Hospital for Sick Children, Toronto (Canada)

Purpose: Sickle cell disease (SCD) is the major cause of stroke in children leading to mortality or long-term disability. A noninvasive means of measuring cerebral blood flow (CBF) reserve would facilitate assessment and clinical management of these patients. Cerebrovascular reactivity (CVR), an indirect measure of CBF reserve, is defined as the CBF response to a vasodilatory stimulus. BOLD MRI has been used as a surrogate for CBF changes in response to partial pressure of CO2 (PCO₂). The aim of this study was to 1) introduce this technique to a pediatric population with SCD, 2) demonstrate the type of information that can be derived; and 3) discuss advantages and disadvantages over existing CVR methods. For this purpose we report our experience with CVR studies in 11 pediatric SCD patients.

Materials and methods: 11 pediatric SCD patients were imaged on a 1.5 T MRI. PCO₂ and O₂ targets were achieved using a model-driven perspective end-tidal targeting (MPET) system with a custom built breathing circuit. MRI was performed in synchrony with the MPET using a standard BOLD sequence. These data were assessed by correlating the BOLD signal change in time with the measured PET CO₂ values of each subject, and then normalizing over the mean signal to produce a voxel-wise map of CVR. Structural MRI, MRA and CVR maps were assessed visually by an experienced neuroradiologist (MS) as well as an imaging scientist (AK).

Results: There was a strong concordance between CVR and angiographic findings. All patients in this study had ischemic changes in the brain parenchyma as identified with structural MR imaging. Nine of the 11 patients demonstrated mapped reductions in CVR extending beyond the ischemic lesions (as identified with MR structural imaging) into normal appearing brain parenchyma.

Conclusion: The combined application of tightly controlled reproducible changes in PCO2 and BOLD MRI for generating whole brain maps of CVR is a promising method for imaging the distribution of vasodilatory reserve in children with SCD.

NE1-R1

Evaluating the number of acquisitions for non-fiber tracking diffusion-weighted imaging (DTI) applications in pediatric neuroimaging

Salil Soman¹, Samantha Holdsworth¹, Stefan Skare², Jalal Andre¹, Murat Aksoy¹, Roland Bammer¹, Patrick Barnes¹, Kristen Yeom¹ Stanford University, Stanford (United States),²Clinical Neuroscience, Karolinska Institute, Stockholm (Sweden)

Purpose: At our pediatric hospital, routine clinical DTI entails averaging 3 separate acquisitions to obtain high SNR DTI and optimize fiber-tracking. We hypothesized that clinically useful fractional anisotropy (FA) and eigenvector-color-coded FA (EV) maps could be derived from DTI using NEX = 1 or 2.

Materials and methods: 15 children with various brain pathologies were imaged at 3T with a twice-refocused GRAPPA DT-EPI



sequence (matrix size = 1282, acceleration factor = 3, 25 directions with b=1000 s/mm2, 5 b=0) and retrospectively reviewed. Three datasets (NEX=1, 2, 3) were generated from the original 3 NEX DTI data, each containing the isotropic diffusion weighted image (DWI), isotropic apparent diffusion coefficient (ADC), FA, and FA (EV). Two neuroradiologists independently reviewed these 3 datasets for each patient in a blinded fashion. A modified Likert scale (1 = poor, 2 = below average, 3 = average, 4 = above average, 5 = excellent) was used to grade SNR, lesion conspicuity, and diagnostic confidence. Additionally, FA and ADC values of the pathologic lesions were obtained for NEX = 1, 2, and 3. The difference between measured average and standard deviation (SD) of the FA and ADC values for |NEX1-NEX2|, |NEX2-NEX3|, and |NEX1-NEX3| were calculated.

Results: The score for all 3 datasets was near or above average. For all 4 parameters, NEX=1 scored lower than NEX=2. As expected, the score for SNR and lesion conspicuity increased with NEX, except on DWI where NEX=2 scored the highest. The average FA showed least difference between NEX=2 and NEX=3 and greatest between NEX=1 and NEX=2 (Figure 1B). The average ADC showed greatest difference between NEX=1 and NEX=2, followed by NEX=1 and NEX=3. The FA SD stayed constant amongst groups, while the ADC SD showed greatest difference between NEX=1 and NEX=3.

Conclusion: Our findings suggest that NEX=2 represents an appropriate balance between scan time (time reduction by 1/3) and diagnostic confidence for non fiber-tracking applications. Future work will evaluate the impact of NEX on fiber-tracking in our clinical setting.

NE1-R2

Spectrum and evolution of MRI findings in children with cerebral palsy

Charuta Dagia¹, Susan Reid¹, Michael Ditchfield², Dinah Reddihough¹

¹The Royal Children's Hospital & Murdoch Children's Research Institute, Melbourne, ²Monash Childrens, Clayton (Australia)

Background: Cerebral palsy (CP) encompasses a group of non-progressive motor impairment syndromes secondary to lesions or anomalies of the brain, arising in the early stages of brain development. It is the most common physical disability in childhood, occurring in about 2/1000 live births, with significant financial and emotional implications. Despite this, the etiologic factors remain uncertain in a large percentage of cases.

Purpose: To investigate the frequency, spectrum and evolution of MRI abnormalities in a population of children with CP born between 1999 and 2005 in Victoria, Australia.

Materials and methods: 870 patients (59.5% males), mean age at assessed scan 2.5y, (sd 2.2y, range 1d to 10.2 y) were identified through the Victorian Cerebral Palsy Register. Their medical records were systematically reviewed. MRI was available for 641 (74%). 20% MRI scans were comprehensively evaluated by two Paediatric Radiologists to assess correlation, the rest by one of these two readers. Abnormalities were identified on 87% scans. Of these, 12.2% patients were excluded (10.6% with only neonatal MRI, 1.6% with metabolic MRI features). Of the 10% with both neonatal and late scans, the pattern of MRI findings was separately recorded, and assessed for discordance. MRI abnormalities were also correlated with the type of CP.

Results: The most common abnormalities on MRI were periventricular white matter injury (PWMI, 44.5%), grey matter injury (14.3%), focal vascular insult (9.8%) and malformations (10.2%). Non-specific findings in 8.5% patients. Of the patients with neonatal and delayed scans, 29% with PWMI, 7.1% with grey

matter injury had discordant interpretation on assessing only one of the two scans. The interpretation was concordant for all focal vascular lesions and malformations.

Conclusion: Periventricular white matter injury, followed by grey matter injury were the most common MRI findings. Interpretation for likely etiology in both these groups was optimal when assessing neonatal and later scans in conjunction.

NE2-1

Difference in shape and relative alignment of semicircular canals in adolescent idiopathic scoliosis (AIS) compared with normal controls: high-resolution MRI and morphometry study

Winnie CW Chu, Defeng Wang, Lin Shi, Darshana D Rasalkar, Pa Heng, Jack CY Cheng

The Chinese University of Hong Kong, Hong Kong (China)

Purpose: Adolescent idiopathic scoliosis (AIS) is a complex threedimensional deformity of the spine with unknown cause. Abnormal vestibular function has been reported to be a contributing factor to the observed impaired balance control of AIS, which could be linked to the initiation and progression of spinal deformity. This study sought to investigate any morphometric difference in the semicircular canals between AIS subjects and normal controls.

Materials and methods: 19 AIS girls (mean age 13) with Cobb's angle (mean 24° +/- S.D. 6°) were compared with 12 matched normal controls. All subjects underwent high resolution T2 weighted imaging of the vestibular system using 3T MRI. The 3D vestibular system surfaces were segmented by automatic computational pipeline. A best-fit circle was calculated using quadratic optimization to fit each of the three semicircular canals. The shape of each canal was reflected by the radius of its circle while spatial relationship among the three canals was reflected by the length and angle formed between the corresponding lines connecting the centers of each pair of circles. Orientation asymmetry between left and right vestibular systems was measured by the Euler angles calculated from 3D rotational matrix. Statistical analysis was performed using one-way ANOVA.

Results: There was significant difference in the shape and relative alignment of the LEFT-sided semicircular canals between the AIS and controls, as follows: (1) distance between the centers of the lateral and superior canals (p=0.007); (2) angle with the vertex at the center of posterior canal (p=0.05); (3) radius of the posterior semicircular canal (p=0.01); however no significance group difference was found in the right vestibular system. In general, AIS girls had a greater orientation asymmetry between the left and right vestibular systems along the z axis (p=0.0067).

Conclusion: Morphological difference of the semicircular canals may be one of the factors affecting vestibular function and hence postural mechanism in AIS. Whether this anatomical change has any prognostic effect on curve progression warrants further longitudinal investigation.

NE2-2

Establishment of normative neurosonographic indices, including resistive index, based on a longitudinal study of newborns followed through infancy with normal neurodevelopmental outcomes

Don Soboleski, Maya Leitner, Cody Li, Safeeq Salahudeen, Jessica Beiderman, Maxine Clarke, Ian Silver, Michael Flavin, Elizabeth VanDenKerkhof

Queens University, Kingston (Canada)

Background: Normative values for resistive index (RI), delta RI and ventricular size are well established in the neonatal



population. Neurosonograms (NS) of infants up to 9 months of age are routinely requested in the following scenarios at our institute: i) follow-up of preterm/term infants visiting the neurodevelopmental (N/D) center, ii)an enlarging cranium, iii) and as a preliminary workup of an infant with possible increased intracranial pressure (ICP). There are few longitudinal studies and minimal data available regarding the expected values in this older age group. Normative indices/ranges are required to help predict and enable prognosis of N/ D deficiencies and to determine which patients need further workup Purpose: To develop normative reference data regarding RI, delta RI with fontanelle compression and ventricular size in the infant population. Materials and methods: A longitudinal cohort study of 420 NS performed on 131 newborns (n=73 male) ranging in gestation from 26 weeks to 42 weeks. Timing of the NS was from day 1 of birth thru to ~9 months of age. Routine NS was performed with inclusion of RI and delta RI of the ACA with fontanelle compression. Infants underwent neurodevelopmental testing between 18 and 24 months of age.

Results: All infants had normal N/D exams. Mean RI values increased up to 6 months of age (0.7--0.79) then showed a decreasing trend. Mean delta RI decreased with age (0.6--0.0) apart from a small peak at \sim 3 months. All ventricular measurements increased with increasing age(frontal horn width mean 1.5 mm-7.2 mm).

Conclusion: Delta RI values can be expected to decrease with age with a possible small peak at ~3 months. These findings suggest delta RI could be used to predict the presence of increased ICP in infants presenting with ventriculomegaly or enlarging cranium, using the method previously described by Taylor et al. Increasing ventricular size with age should be expected when interpreting NS in infants. The normative values used in the newborn and neonatal intensive care unit (NICU) patients should not be used in infants >3 months of age.

NE2-3

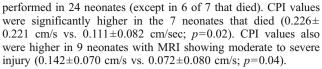
Cerebral perfusion measurements using dynamic color Doppler sonography in neonates with hypoxic ischemic encephalopathy (HIE) treated with therapeutic hypothermia *Ricardo Faingold*, Guilherme Cassia, Christine Saint-Martin, Linda

Morneault, Guilherme Sant'Anna Montreal Children's Hospital, Montreal (Canada)

Purpose: The objective of this study was to evaluate the cerebral perfusion intensity (CPI) of the basal ganglia with dynamic color Doppler sonography (CDS) in hypoxic ischemic encephalopathy (HIE) neonates treated with hypothermia and to investigate the correlation between CPI measurements and survival.

Materials and methods: A head ultrasound (HUS) was performed with a 9S4 MHz sector transducer in all HIE neonates submitted to hypothermia, as part of their routine care. CDS was performed with an 11LW4 MHz linear transducer to obtain DICOM color Doppler videos of the blood flow in the basal ganglia. Three videos of 3 s each were obtained for the regions of interest (ROIs), in the coronal plane, and used to calculate the CPI. Measurements of CPI were evaluated retrospectively by 2 radiologists using Pixelflux Chameleon software. It allows automatic quantification of color Doppler data from a region of interest (ROI) by dynamically assessing color pixels and flow velocity during the heart cycle. CPI is expressed in cm/sec and is calculated by multiplying the mean velocity of all pixels by the area divided by the ROI. Clinical and radiological data were evaluated retrospectively. Data are presented as mean \pm SEM or median (quartiles).

Results: A total of 30 neonates, that underwent HUS, were included in this study: 18 male, 12 female, BW= 3.469 ± 607 g, GA= 39 ± 2 weeks, age at time of exam 27.9 ± 13.1 h. MRI



Conclusion: Increased cerebral perfusion intensity to the basal ganglia in neonates with HIE treated with hypothermia was associated with poor outcome. CPI quantification with dynamic CDS opens a window to better understand reperfusion injury in HII. The software Pixelflux Chameleon was acquired with a grant from Canadian Heads of Academic Radiology (CHAR-GE Development Award).

NE2-4

Trilateral retinoblastoma: neuroimaging characteristics and the potential value of brain MRI screening on admission *Firazia Rodjan*¹, Pim de Graaf¹, Annette C. Moll¹, Paolo Galluzzi², Philippe Maeder³, Sophia Göricke⁴, Hervé Brisse⁵, Jonas A. Castelijns¹

¹VU University Medical Center, Amsterdam, the Netherlands, ²Azienda Ospedaliera e Universitaria Santa Maria alle Scotte Siena, (Italy) ³CHUV, Lausanne (Switzerland) ⁴University Hospital Essen (Germany), ⁵Institut Curie, Paris (France)

Purpose: Trilateral retinoblastoma (TRb) is a rare syndrome associating hereditary retinoblastoma with an intracranial neuroblastic tumor. Treatment is difficult and prognosis is poor. The purpose of this European multicenter study was to evaluate imaging features of TRb and assess the potential value of brain MRI on admission to detect early stage TRb.

Materials and methods: Data of 17 patients (16 TRb- and 1 quadrilateral Rb-patients) were reviewed for clinical data including time-intervals between Rb- and TRb-diagnosis and presence of baseline brain imaging (BBI). Two reviewers reviewed all images and 1 reviewer from each participating center evaluated images of patients of their center. Consensus was reached during a joint scoring session. Studies were reviewed for tumorlocation, size and imaging characteristics (signal intensity (SI) on T1- and T2-weighted images, enhancement pattern and presence of cystic component). Short-term follow-up imaging was needed to distinguish pineoblastoma from a pinealcyst in small tumors.

Results: Mean interval between the detection of Rb and TRb was 17mo (median 12 mo, range 0–54 mo). Ten patients (all without BBI) showed metachronous TRb (mean interval 28mo [range 5–54 mo]), whereas synchronous TRb showedin 7 (41%) patients. Tumor size was smaller in patients with BBI (mean MAD 15 mm [range 9–21 mm]) compared to patients without BBI (mean MAD 35 mm [range 13–45 mm]) (P=0.05). Of the 18 intracranial tumors, 78% was located in the pineal gland and 22% suprasellar. All tumors showed well-defined borders with mostly heterogenous enhancement (72%) and mainly isointense SI on T1 (78%) and T2 (72%)-weighted images with respect to grey-matter. The majority of pineal TRb showed a cystic component (57%).

Conclusion: TRb mainly develops in the pineal gland with a cyst-like appearance that may cause confusion in diagnosis of small tumors. TRb with BBI were diagnosed in an earlier and potentially curable stage of disease.

NE2-R1

Skeletal Features in Cerebroretinal Microangiopathy with Calcifications and Cysts

Sanna Toiviainen-Salo, Tarja Linnankivi, Anne Saarinen, Mervi Mäyränpää, Riitta Karikoski, Outi Mäkitie Helsinki University Hospital, (Finland)



Purpose: Cerebral cysts and calcifications with leukoencephalopathy and retinal vascular abnormalities are diagnostic hallmarks of cerebroretinal microangiopathy with calcifications and cysts (CRMCC). Previous studies have suggested that skeletal involvement is common, but its characteristics are unknown. This study aimed to assess the skeletal features of CRMCC.

Materials and methods: All recognized patients in the country with features consistent with CRMCC and for whom radiographs were available were included. Clinical information pertinent to the skeletal phenotype was collected from hospital records, and all plain radiographs were reviewed for skeletal features. Bone mineral density (BMD) was measured by dualemission X-ray absorptiometry (DXA). In one patient, bone biopsies were obtained for bone histology and histomorphometric analyses.

Results: The skeletal features of CRMCC include 1) compromised longitudinal growth pre- and postnatally, 2) generalized osteopenia or early-onset low turnover osteoporosis with fragility fractures, and 3) metaphyseal abnormalities that may lead to limb deformities such as short femoral neck or genua valga. DXA measurements in three patients showed low BMD, and bone biopsies in the fourth patient with pathological fractures and impaired fracture healing showed low-turnover osteoporosis, with reduced osteoclast and osteoblast activity.

Conclusion: The CRMCC-associated bone disease is characterized by low BMD and pathological fractures with delayed healing, metaphyseal changes, and short stature pre- and postnatally.

ON-1

Can preoperative MR imaging predict optic nerve invasion of retinoblastoma?

Hong Eo¹, Ji Hye Kim², So-Young Yoo², Tae Yeon Jeon²
¹Samaung Medical Center, Seoul, ²Samsung Medical Center, Seoul (South Korea)

Purpose: To assess the accuracy of preoperative MRI for the detection of optic nerve invasion in histopathologically proved retinoblastoma.

Materials and methods: The institutional review boards approved this study and waived the requirement for informed consent. A total of 41 patients (21 girls, 20 boys; mean ages: 21 months) who underwent MR imaging within 30 days before enucleated for retinoblastoma were included. Two radiologists retrospectively reviewed MR images without the knowledge of the pathologic result. Optic nerve enhancement and optic nerve sheath enhancement were determined independently by two readers. Kappa value was calculated to assess interobserver agreement. Other MR findings such as tumor size, growth pattern, and intraocular location were evaluated and compared with pathologic findings of optic nerve invasion by using a Fisher's exact test and t-test.

Results: Optic nerve invasion was confirmed histopathologically in 20% (8/41). The Kappa value for interobserver agreement for optic nerve enhancement was 0.616. Sensitivity, specificity, and accuracy of reader 1 were 25%, 61%, and 54% respectively. Sensitivity, specificity, and accuracy of reader 2 were 25%, 70%, and 56% respectively. The Kappa value for interobserver agreement for optic nerve sheath enhancement was 0.552. Sensitivity, specificity, and accuracy of reader 1 and reader 2 were 38%, 76%, 68% and 38%, 79%, 71% respectively. Tumor sizes were 16.0 mm (SD: 1.9 mm) and 15.1 mm (SD: 3.2 mm) in patients with and without optic nerve involvement respectively (P = 0.422) and only one patient (2%) demonstrated endophytic growth pattern. Tumor location was not statistically associated with optic nerve invasion (P = 0.592).

Conclusion: Findings of MRI including optic nerve and sheath enhancement, size, growth pattern, and location the intraocular tumor could not preoperatively predict presence of the optic nerve invasion in retinoblastoma.

ON-2

CT- and MR-imaging characteristics of second primary tumors after irradiation in retinoblastoma patients

Firazia Rodjan¹, Pim de Graaf¹, Esther Sanchez¹, Jonathan I.M.L. Verbeke¹, Annette C. Moll¹, Paolo Galluzzi², Philippe Maeder³, Sophia Göricke⁴, Hervé Brisse⁵, Jonas A. Castelijns¹

¹VU University Medical Center, Amsterdam, the Netherlands, ²Azienda Ospedaliera e Universitaria Santa Maria alle Scotte Siena (Italy) ³CHUV, Lausanne (Switzerland) ⁴University Hospital Essen (Germany) ⁵Institut Curie, Paris (France)

Purpose: Second primary tumors (SPTs) are now the leading cause of death in patients with heritable retinoblastoma (Rb), especially in irradiated patients. In this study, CT and MRI parameters of primary tumours (PTs) in the irradiated area are evaluated to understand the location and pattern of tumorspread per tumortype.

Materials and methods: Data of 42 Rb-patients with radiation therapy (RT) (40 with SPTs and 2 patients with third PTs) obtained from 5 different European retinoblastoma Centers were reviewed. Clinical data included heredity, Rb-treatment, age of irradiation, time-intervals between irradiation and SPT-diagnosis and histological type. Observed imaging parameters included tumor location, spread and imaging characteristics. Consensus was reached during a joint scoring session.

Results: All patients had hereditary Rb and were treated with RT (29 patients in the 1st year [group1] and 13 patients after the 1st year [group 2]). Mean interval between RT and SPT was 14 years (range 3–37 years). Histological type was subdivided into osteosarcomas (41%), rhabdomyosarcomas (23%), other sarcomas (18%), carcinomas (11%) and miscellanous tumors (7%). All 44 PT were divided into 5 predilection sites (PS) from which the tumor originated and/or the largest part of the tumor was located: temporal muscle/bone (TMB, 39%), ethmoid sinus (ES, 23%), orbit (18%), maxillary sinus (MS, 16%) and intracranial (IC, 4%). Osteosarcoma mostly occured in group 1 (78%) and mainly in the orbit (33%) and TMB (39%). In 80% of the patients, rhabdomyosarcoma developed in group 1 with PS in the TMB (50%) and ES (40%). Other sarcomas (71% in group 1) and carcinomas (60% in group 2) had a wide variety of PS. All miscellaneous tumors were located IC and developed in group 2. All SPTs showed characteristic imaging findings.

Conclusion: Osteosarcomas and rhambdomyosarcomas are most common SPTs and frequently develop in patients treated by RT before one year of age. Evaluation of the orbit, temporal muscle/bone and ethmoidal sinus are most important locations for screening.

ON-3

Incidence of abdominal tumors in syndromic and idiopathic hemihypertrophy/isolated hemihyperplasia—a retrospective review *Molly Dempsey-Robertson*, David Wilkes, Alec Stall, Patricia Bush, Edward Batista

Texas Scottish Rite Hospital, Dallas (United States)

Purpose: To review the incidence of associated abdominal neoplasms in our patient population of both syndromic and isolated hemihyperplasia and identify the specific clinical information used for diagnosis.

Materials and methods: We reviewed 285 patients diagnosed with hemihypertrophy by 8 pediatric orthopaedists over a 10-year period.



The results and frequency of patients' abdominal imaging were recorded

Results: Of the 285 patients, 39 had syndromes associated with asymmetric tissue overgrowth such as Klippel–Trenaunay and Beckwith–Wiedemann (BWS). 239 children had non-syndromic hemihyperplasia. The overgrowth involved the upper extremity in 17, the lower extremity in 179, and both in 23. 13 patients also had facial asymmetry. There were 7 with partial limb involvement. 80% of patients underwent at least one ultrasound. Only 7% were not imaged at least once and were under the age of 7 years at presentation. Screening intervals ranged from 3 to 24 months. 4 patients had abdominal tumors. One was diagnosed with adrenal carcinoma on the first US, one with Wilms after a normal US one year prior and another diagnosed with Wilms 11 months after a normal US when the child went to the ER for fever and abdominal pain. The other child had hepatoblastoma and BWS.

Conclusion: There was a range of diagnostic criteria for hemi-hypertrophy. The US screening frequency was quite variable and likely due to multiple factors. There was a 1.3% incidence of tumors in patients with nonsyndromic hemihyperplasia.. 162 of these patients were over the age of 7 and 132 over the age of 10 years at last visit. This differs from the 5.9% incidence previously reported. Two of three patients with non-syndromic isolated hemihyperplasia were diagnosed with tumor by screening exams. One Wilms' tumor was found through screening and the other in the ER despite screening. In both a normal scan had been done 1 year prior. This rapid growth of Wilms' has been reported in the literature, specifically with BWS. This makes the utilization of ultrasound screening alone difficult and has led to the suggestion of the use of US and parental abdominal exams.

ON-4

Imaging studies in multi-center trial of Hodgkin lymphoma: importance of central review in assuring consistent response assessment

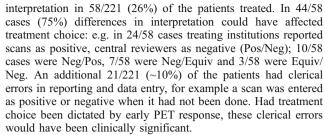
Stephan Voss¹, Frank Keller², Kathleen McCarten³, Lu Chen⁴, Steven Cho⁵, James Nachman⁶, Tj Fitzgerald⁷, Louis Constine⁸, Cindy Schwartz⁹

¹Children's Hospital Boston: Boston, ²Emory University and Aflac Cancer Center, Atlanta, ³Hasbro Children's Hospital, Brown University, Rhode Island, ⁴Children's Oncology Group Data Center, ⁵Johns Hopkins University Medical School, Baltimore, ⁶University of Chicago School of Medicine, Chicago, ⁷Quality Assurance Review Center, University of Massachusetts, ⁸University of Rochester Medical Center, ⁹Hasbro Children's Hospital, Brown University (United States)

Purpose: Patients with favorable risk HL were enrolled in COG AHOD0431, designed to investigate the prognostic significance of very early response as measured by FDG-PET after the first course of chemotherapy. The purpose of this study was to determine whether central review of the early response data would impact treatment stratification.

Materials and methods: 287 subjects with non-bulky IA and IIA HL were enrolled. 221 pts had evaluable fludeoxyglucose (FDG)-PET results after 1 cycle of chemotherapy. CR was defined after 3 cycles as ≥80% shrinkage of the primary nodal mass with a negative PET. Images were centrally reviewed by a team of 2 radiologists and 1 radiation oncologist experienced in interpreting CT and PET response data in patients (pts) being treated for HL. Treatment stratification was dictated by the institutional interpretation; central review served as a quality control measure, only over-turning institutional interpretation when a discrepancy was unequivocal.

Results: Central review of early response assessment data as reported by the treating institutions revealed discrepancies in



Conclusion: Central review of imaging studies performed in multi-center clinical trials plays an important role in assuring consistent interpretations in response assessment, and can have a significant impact on treatment stratification. Clearly defined response criteria are needed with improved guidelines for interpreting complex multi-modality imaging studies.

ON-5

Pre-treatment nodal apparent diffusion coefficient (ADC) histographic centile measurements — predictors of early response in adolescent and paediatric lymphoma?

Paul Humphries, Alan Bainbridge, Stephen Daw, Ananth Shankar, Shonit Punwani

University College London Hospital, London (United Kingdom)

Purpose: Assess pre-treatment nodal 25th, 50th and 75th centile ADC for predicting post chemotherapy residual nodal volume at early response assessment [ERA] of lymphoma.

Materials and methods: Sixteen patients with biopsy proven lymphoma underwent 1.5 T MRI at initial staging (pre-treatment), and after two cycles of chemotherapy (ERA). A pre-treatment anatomical MRI defined 9 cm tissue block (containing lymphadenopathy) was interrogated with trace diffusion weighted imaging [DWI] (Short TI Inversion Recovery - Echo Planar Imaging [STIR-EPI] with b=0, 300 and 500). ERA DWI was matched to the same anatomical region as at initial staging of each patient. Regions of interest [ROI] were drawn on the pre-treatment and ERA b500 images precisely around the borders of nodal tissue within the imaged volume (Jim 5.0, Xinapse Systems Ltd., Northants, UK). Total ROI volume was recorded and percentage residual nodal volume at ERA derived. Pre-treatment ROIs were exported to the corresponding apparent diffusion coefficient (ADC) map and a histogram of ADC values for ROI pixels produced. Twenty-fifth centile, 50th and 75th centile ADC values were recorded for each patient. Correlation between ADC centiles and percentage residual volume was assessed with Spearman statistics. Area under ROC curves [AUC] for discrimination between complete response (<25% residual) and incomplete response (>=25%) was determined.

Results: Pre-treatment 25th, 50th and 75th centile ADC ranged from $0.71\text{-}1.53\times10\text{-}3$, $0.85\text{-}1.4\times10\text{-}3$ and $1.1\text{-}2.42\times10\text{-}3$ mm2/s respectively. Percentage residual nodal volume varied between 6% and 66%. Pre-treatment 25th centile ADC approached statistical significant correlation with% residual nodal volume (r=0.44, p=0.08); 50th and 75th centile ADC did not (r=0.21 and 0.31 respectively). AUC was 0.87, 0.83 and 0.81 for 25th, 50th and 75th centile ADC measurements.

Conclusion: Pre-treatment 25th centile ADC shows promise as a predictor of early response to chemotherapy of paediatric and adolescent lymphoma. Recruitment is ongoing and full series data will be presented.

ON-6

The value of whole-body MRI on Hodgkin lymphoma in pediatrics *Henrique Lederman*, Jose Schiavon, Rodrigo Regacini, Flavio Luisi Graacc/Federal University of Sao Paulo, Sao Paulo (Brazil)



Background: Computed tomography (CT) and positron emission tomography (PET) have been used as gold standard for staging and evaluating therapy on Hodgkin lymphoma. The development of whole-body MR imaging (WBMRI) with short tau inversion recovery (STIR) technique brought a new angle of assessment regarding "as low as reasonably achieved" (ALARA) principles. Purpose: Evaluation by WBMRI of IOP-GRAACC-UNIFESP, Sao Paulo, Brazil patients with Hodgkin lymphoma comparing with CT, PET or scintigraphy findings when available.

Materials and methods: 15 patients from the last 2 years with Hodgkin lymphoma with a medium age of 16.0 years (range 6–21) that could perform a WBMRI along with CT, PET or scintigraphy. Image findings were compared with Bone Marrow Biopsy (BMB) and clinical findings.

Results: WBMRI agreed with clinical findings on most patients (86.7%). A substantial agreement between WBMRI and BMB was found. WBMRI disagreed with clinical findings in only two patients due to remaining high T2 lesions after treatment. One WBMRI positive finding with negative BMB was treated as positive according to clinical findings, considering, as described in the literature, that the biopsy site did not reach the ill bone marrow. Scintigraphy, less sensitive, could not find secondary lesions in one patient. The disagreement along with CT was about residual masses that lost its signal on MR studies and could be found on CT, considered negative. This study has significant findings helping determinate its value as part of the diagnostic and follow-up of Hodgkin lymphoma following ALARA principles.

ON-7

Are the RECIST criteria useful in assessing response in paediatric rhabdomyosarcoma?

Reineke A. Schoot¹, Rick R. van Rijn¹, Kieran McHugh², Johannes H.M. Merks¹

¹Emma Children's Hospital – Academic Medical Centre, Amsterdam, (Netherlands) ²Great Ormond Street Hospital, London (United Kingdom)

Purpose: Volume (3D) measurements are routine in paediatric oncology trials. Unidimensional (1D) measurements (RECIST) have been validated in adult tumours but not with paediatric malignancies. The purpose of this study is to compare volume and RECIST response evaluation in paediatric rhabdomyosarcoma. Materials and methods: We evaluated a consecutive cohort of children with rhabdomyosarcoma treated at two children's institute.

children with rhabdomyosarcoma treated at two children's institutions (GOSH and EKZ-AMC) between 1998 and 2008. Tumour measurements in 1D and 3D with CT or MRI were assessed at diagnosis and after 2–3 cycles of chemotherapy. Partial Response (PR) as defined by volume measurements is a decrease in tumour volume of <66%, by RECIST a decrease in largest diameter of <30%. Progressive disease (PD) as defined by volume measurements is an increase in volume of >40%, by RECIST an increase in largest diameter of >20%.

Results: 64 patients were identified with the relevant imaging over 10 years. 32 Patients were excluded (primary surgery at diagnosis, ultrasound follow-up, transfer elsewhere, films missing). There were 36 males and 28 females. Median age was 3.9 years (range 0.2–16.0 years). Median interval between studies was 9.0 weeks (interquartile range 8.4–11.9 weeks). PR was seen in 49 patients with 3D measurements and in 38 with 1D. Stable disease was seen in 10 with 3D and in 22 with 1D. Progressive disease was observed in 2 patients when measured with 3D and in 1 with 1D. Three patients achieved complete remission (CR).

Conclusion: We observed 12 discrepancies (18.8%). 11 cases classified as PR by 3D had SD on 1D assessment and 1 case showed PD on 3D and SD on 1D. In 11 of these cases this would have meant a different treatment decision. Based on this study we

feel that implementation of RECIST in paediatric soft-tissue sarcoma trials is not warranted as it may lead to a significant misclassification of patients.

ON-8

Off-therapy CT monitoring of patients with Wilms tumor: is pelvic CT necessary?

Sue Kaste, Samuel Brady, Brian Yee, Valerie McPherson, Yimei Li, Najat Daw, Robert Kaufman, Alberto Pappo St. Jude Children's Research Hospital, Memphis (United States)

Background: We sought to assess the utility of pelvic CT examination as a component of follow-up CT studies in detecting pelvic relapse in patients treated for Wilms Tumor (WT).

Materials and methods: We retrospectively identified patients treated between January 1999 and December 2009, recorded number of CTs that included pelvis, patient demographics, disease stage, treatment regimen, disease relapse and location, and estimated dose length product (DLP) by age groups. Patient Effective Dose (ED), a merit of relative risk from radiation, was calculated from DLP. We differentiated patient dose from chest-abdominal-pelvic (CAP) and chest-abdominal (CA) only CT exams, using MOSFET dosimeters and selected age-specific anthropomorphic phantoms to measure organ specific doses. CT scanning of phantoms used identical scan parameters from age and weight groups they represented.

Results: Of the 168 patients, 73 were males, 112 white, 47 African-American, 9 other. Median age at diagnosis, 3 y (range, 4 m–19 y). At diagnosis, 26 had Stage I, 42 Stage II, 32 Stage III, 33 Stage IV, 31 Stage V, 4 not coded. 35 had bilateral WT, 2 had extension, 1 was extrarenal. 32 developed relapse 4–59 m from diagnosis; none pelvic. Average patient ED for CAP CT exams across all ages/genders was (23.2±27.7) mSv (range, 2.9–171.4 mSv). Average patient received 5.5±5.4 CAP studies (range, 1–28). When comparing patient equivalent ED measured on anthropomorphic phantom an average estimated dose savings from chest-abdomen only CT scan was 29% across all ages/genders (range, 21–36%).

Conclusion: Omitting pelvic CT in routine surveillance of WT patients saves an average 29% ED without compromising disease detection and reduces ultimate lifetime risk from needless gonadal and marrow radiation exposure.

ON-9

Propranolol for treatment of infantile hemangiomas: utility of US for therapeutic effects

Jaroslaw Madzik, Maria Uliasz, Monika Bekesinska-Figatowska, Katarzyna Bilska, Wojciech Wozniak⁴, Hanna Bragoszewska Institute of Mother and Child, Warsaw (Poland)

Background: Over the last 3 years some reports have been published in the literature of effective treatment of infantile hemangiomas with orally administered Propranolol. The program of infantile hemangiomas treatment with use of propranolol was implemented at the Institute of Mother and Child in Warsaw in March 2010.

Purpose: To determine whether ultrasonography (US) is useful for assessment of therapeutic effects in children with hemangiomas treated with Propranolol.

Materials and methods: Since March till November 2010 thirty patients with infantile hemangiomas have been admitted to our Institute and qualified to start therapy with Propranolol (median age at onset of treatment: 5,6 months). The inclusion criteria are as follows: age up to 12 months, big lesions that are life-threatening or disabling important organs (localization – close to the eyes, nostrils, ears, anus, urethra), narrowing respiratory pathways or giving



feeding difficulties. Sonography has been performed in all the patients before treatment and during therapy at 4–6 weeks intervals. In certain cases MRI (or angio-MRI) has been performed.

Results: Immediate effects of therapy were noted in 93,3% of children (28/30). In two of them (6,7%) therapy was stopped after 4 months without effect. In next two children hemangiomas resolved totally after 3–5 months therapy. 26 children are still treated and observed. In US effects on growth (decrease of size of hemangioma), morphology (increase of echogenicity) and flow parameters in hemagioma's vessels (slowness of flow, increase of resistive index, RI) were observed. Almost no side effects were noted (in one child transient bradycardia was observed after first dose of Propranolol).

Conclusion: US is useful to distinguish hemangioma from other vascular abnormalities and is the method of choice in evaluation of therapeutic effect.

ON-10

Incidence and etiology of new liver lesions in pediatric patients previously treated for malignancy

Ethan A. Smith, Shelia Salisbury, Rose Martin, Alexander J. Towbin

Cincinnati Children's Hospital Medical Center, Cincinnati (United States)

Purpose: New liver lesions in patients with a prior malignancy represent a diagnostic dilemma. Prior reports have shown an increased incidence of focal nodular hyperplasia (FNH) in these patients. The purpose of this study was to examine the time course, etiology, and imaging characteristics of new liver lesions in pediatric patients with a previously treated malignancy.

Materials and methods: The hospital cancer registry was used to identify all patients diagnosed with cancer between 1980 and 2005 who met the following criteria: history of solid tumor, survival >2 years after diagnosis, no liver lesions at a post-treatment baseline, and imaging follow-up of >2 years. Three hundred randomized patients were selected. All available cross-sectional imaging reports that included the abdomen were obtained and reviewed for the mention of new liver lesions. Positive reports were followed by consensus review of the images as well as a review of each patient's medical records.

Results: A total of 79 patients met the inclusion criteria and had adequate imaging follow-up. Of these patients, 16 developed liver lesions (20.3%). The frequency of confirmed or suspected FNH was 6.3% (5/79) overall, and 31.2% (5/16) in patients with liver lesions. The frequency of confirmed or suspected liver metastasis was 5.1% (4/79) overall, and 25% (4/16) in patients with liver lesions. The mean time from initial cancer diagnosis to the development of FNH was 85.6 months, while the mean time to the development of metastasis was 31 months. FNH demonstrated hyper-enhancement on early postcontrast imaging while metastases were hypo-enhancing on postcontrast imaging.

Conclusion: The most common liver lesions occurring in patients with a treated pediatric malignancy were FNH and metastasis. FNH tended to occur farther from the time of diagnosis and appeared hyper-enhancing on early postcontrast imaging, while metastases occurred closer to the time of diagnosis and appeared hypo-enhancing after contrast. These characteristics may allow more confident differentiation of metastatic disease from FNH.

ON-11

Pancreatic neuroblastoma: imaging features of a rare entity *Eithne DeLappe*, Sara Abramson

Memorial Sloan Kettering Cancer Center, New York (United States)



Purpose: Neuroblastoma is the most common extracranial solid tumor of childhood, and metastasis to distant organs such as bone, bone marrow and liver is well documented. Pancreatic involvement however has only rarely been reported. We present the largest documented case series of pancreatic neuroblastoma and describe the radiological features. We review the radiographic findings with emphasis on the use of metaiodobenzylguanidine (MIBG) and computed tomography (CT). Imaging findings are correlated with clinical and pathological features.

Materials and methods: We reviewed the clinical findings, radiology and pathology of all neuroblastoma patients with a diagnosis of pancreatic involvement by neuroblastoma presenting to our institution. Specifically we correlated CT with MIBG imaging findings and confirmed these with surgery and pathology where available.

Results: Seven patients with a diagnosis of neuroblastoma developed pancreatic involvment. Mean age at development of pancreatic disease was 4 years (range 1–9 y). All patients had stage 3 or 4 disease with 5/7 having stage 4 disease. One patient had pancreatic involvement at initial presentation and the remaining 6 developed pancreatic disease at later relapse. 5 of 7 patients had intrinsic pancreatic lesions while 2 had pancreatic involvement by a local mass. All 7 patients had unfavorable histology at initial disease diagnosis. Pancreatic metastases were initially diagnosed with the aid of MIBG and CT imaging. Other imaging studies reviewed included gadolinium enhanced MRI, fluorodeoxyglucose (FDG) PET CT and ultrasonography.

Conclusion: The diagnosis of pancreatic neuroblastoma can be facilitated by an understanding of characteristic appearances seen on MIBG and CT. Through our institutional experience we provide an informative pictorial review of the radiological features allowing confident diagnosis and institution of appropriate management. Pancreatic metastasis should be considered in patients found to have pancreatic nodules and calcification concurrent with neuroblastoma.

ON-R1

Suprarenal masses in newborns and infants: imaging characteristics, clinical correlation and follow-up

Nina Rodrigues Stein, Alan Daneman, Oscar Navarro The Hospital for Sick Children, Toronto (Canada)

Purpose: With increasing use of sonography (US), suprarenal masses (SRM) are more commonly detected ante- and post-natally. In this clinical setting, the main issue is to differentiate neuroblastoma from other entities, usually benign. The aim was to review spectrum of US appearances of SRM in infants (<1 year), to determine whether CT or MR added useful information regarding character and local extent of disease and to correlate imaging findings with final diagnosis as determined by clinical progress, histopathology and urine catecholamines.

Materials and methods: Retrospective analysis of clinical, imaging, histopathology and urine catecholamine levels in 87 infants with SRM detected on ante- or post-natal US in a tertiary care hospital between March 1999 and December 2009.

Results: SRM were diagnosed antenatally in 29, in neonatal period in 33 and in infants in 25. Based on imaging findings, SRM were considered to be adrenal in 61, extra-adrenal in 19, indeterminate in 5 and a pseudomass in 2. The initial US findings were highly suggestive of neuroblastoma in 24 and of other pathologies in 63. Histopathology was obtained in 31/61 adrenal lesions and 11/19 extra-adrenal lesions. Neuroblastoma was pathologically confirmed in 26 patients. Two cystic neuroblastoma cases had initial features indistinguishable from adrenal hemorrhage. CT and MR were helpful

in confirming the diagnosis of SRM or in decision making in only 23/50 (46%) who had CT and 2/10(20%) who had MR. Only one case of proven neuroblastoma had normal urine catecholamines. Clinical and US follow up was available in 85 patients, showing that 33 adrenal and 6 extra-adrenal cases decreased in size or disappeared.

Conclusion: At presentation, the main difficulty is differentiating cystic neuroblastoma from adrenal hemorrhage. US follow up was the most helpful tool for decisions regarding clinical management. CT and MR were helpful mainly for staging neuroblastoma and other large solid neoplasms. Urine cathecolamines are useful in most cases.

ON-R2

Investigation of ultrasonographic findings of infantile hepatoblastoma compared with surgical and pathological presentations

Yingzi Su, Xinyu Yuan Capital Institute of Pediatrics, Beijing (China)

Purpose: To investigate the value of color Dopplar Ultrasonography (US) in exhibiting the characteristics of infantile hepatoblastoma compared with the findings of surgery and pathological examination. Materials and methods: 8 infants with hepatoblastoma confirmed pathologically were enrolled in the study. There were 3 boys and 5 girls, aged from $9{\sim}48$ (18.75±12.68) months. The patients were examined in two-dimension scanning and situation of vessels in/around the tumors with color Doppler Ultrasomography. The findings of US were compared with the manifestations of surgery and pathology statistically by the paired-temple t test and/or the paired-temple Kappa test ($P{<}0.05$)

Results: Comparing with findings at surgery and pathology, the correct rate of US to localize the tumor was 87.5%. US were consistent significantly with surgery and pathology examination in detecting the shape of mass, calcification or/and ossification and cyst in tumors, statistically (κ =1.000, κ =0.714 and κ =0.750 in turn, P=0.05). The specificity of revealing the shape of mass, calcification or/and ossification and cyst in tumors was 100% and the sensitivities of which were 100%, 80% and 66.7%, respectively. Conclusion: US is an effective tool for illustrating the localization and shape of the hepatoblstoma as well as the calcification and/or ossification and cysts in the tumors accurately with significant sensitivity and specificity. It would be helpful in determining the strategy of treatment and evaluating the prognosis.

RS-1

Quality Improvement Registry in CT Scans in Children (QuIRCC): use of a new pediatric CT dose estimate (CTPD) to develop diagnostic reference levels (DRL) for abdominal CT Marilyn Goske¹, Keith Strauss², Laura Coombs³, Keith Mandel¹, Michael Callahan², Kassa Darge³, Donald Frush⁴, David Larson¹, Daniel Podberesky-Alexander Towbin¹, Jeffrey Prince⁵, Sjirk Westra⁶

¹Cincinnati Children's Hospital Medical Center, Cincinnati, ²Boston Children's Hospital, Boston, ³American College of Radiology, ⁴Duke University Medical Center, ⁵Primary Children's Hospital, ⁶Massachusetts General Hospital (United States)

Purpose: Radiation doses associated with CT scans in the pediatric population are poorly understood. We started the first US pediatric CT dose registry to establish baseline values of typical scan technique and estimates of radiation dose using a new measure (CTPD) for the purpose of developing DRL.

Materials and methods: 6 children's hospitals participated in a 3 month retrospective review of abdominal CT scans on

patients <18 years of age. We recorded: study indication, age, weight, size, contrast, scanner information, scan technique, FOV, CTDIvol and DLP. A new CT dose estimate (CTPD), which accounts for body width (BW), was adopted since CTDIvol is a poor indicator of radiation dose of pediatric patients with varying BW. CTPD was calculated by applying a correction factor to CTDIvol as a function of patient size. The correction factors were derived from measured attenuation data on CT scanners of the 4 major CT manufacturers. CTDIvol and CTPD data were compared as a function of BW.

Results: 555 exams (55% males) were entered into a registry in the American College of Radiology's National Radiology Data Registry. The most common indication was pain (46%). The kVP increased significantly with age. For ages 0–2, 39% of exams were <120 kVp; 18% were <120 kVp for ages 15–18 (*p*<.0001). Mean mGy (95% CI) for CTDIvol were 2.9 (2.0–3.9); 4.8 (4.1–5.5); 5.3 (5.0–5.7); 7.6 (6.9–8.2); and 12.2 (10.5–13.9) for body widths <15 cm; 15–19 cm; 20–24 cm; 25–29 cm; and >=30 cm. Mean mGy (95% CI) for CTPD were 7.3 (4.9–9.7); 10.5 (8.9–12.1); 10.3 (9.7–11.0); 12.2 (11.2–13.3); and 14.8 (12.8–16.8) for body widths <15 cm; 15–19 cm; 20–24 cm; 25–29 cm; and >=30 cm.

Conclusion: This registry represents a critical quality improvement strategy for evaluating, optimizing and monitoring CT radiation dose. CTPD values are substantially higher than CTDIvol, especially in younger children. CTPD is a more accurate pediatric radiation dose descriptor for the purpose of developing DRLs and guiding improvement.

RS-2

Conversion of the dose-length product to effective dose for different voltages and anatomic regions for pediatric CT examinations

Yulia Smal, Willi A. Kalender Institute of Medical Physics, Friedrich-Alexander-University, Erlangen-Nuremberg (Germany)

Purpose: The dose-length product (DLP), a technical dose descriptor, is provided on the scanner console for each CT examination. The fastest and most practical way to estimate the effective dose (E) for the respective exam is applying conversion factors (CF) from DLP to E. There is a lack of published CFs, however, reflecting their dependence on voltage and on patient age and gender for the different body regions. Moreover, the new ICRP tissue weighting have to be taken into account.

Materials and methods: We therefore determined CFs for pediatric CT using a validated Monte Carlo dose calculation tool (ImpactMC, CT Imaging GmbH, Erlangen, Germany) and determined organ and effective dose values for a family of anthropomorphic pediatric phantoms mimicking 0, 1, 5, 10, and 15 year-old patients. Five anatomical regions were considered corresponding to head, neck, chest, abdomen, and pelvis. For each phantom and anatomical region we determined CFs at 60, 70, 80, 100, 120, and 140 kV for both tissue weighting factors recommended by reports ICRP60 and ICRP103.

Results: CF values and thereby also E estimates vary notably depending on age and gender and differ significantly from the values published for adults. E.g., for thorax examinations of a newborn and a 15 year-old patient CFs decreases from 0.095 to 0.018 with increasing age. The highest gender-related differences were observed for pelvis examinations using ICRP60 and thorax examinations using ICRP103; the CF for a 5 year-old child can vary by 47% (thorax region applying ICRP103) or 56% (pelvis region applying ICRP60). An energy dependence which was not considered for CFs so far was observed for younger patients.



Conclusion: We conclude that new age-, gender-, and energy-specific conversion factors from DLP to E should be established for pediatric CT to allow for more accurate estimates of effective dose.

RS-3

New conversion coefficients for reconstruction of radiation doses applied during paediatric computer-tomographic (CT) examinations

Michael Seidenbusch, Karl Schneider Kinderspital, Klinikum der Universität München, Munich (Germany)

Purpose: Previously published conversion coefficients for CT were calculated assuming single slice examinations with slice thicknesses of more than 5 mm and neglected fan beam bowtie filtration. As the old conversion coefficients may not be longer appropriate for dose reconstruction in paediatric CT, new conversion coefficients were calculated for different paediatric age groups.

Materials and methods: Calculations of new conversion coefficients were performed by Monte Carlo simulations using the commercially available computer programme PCXMC developed by the Finnish Radiation and Nuclear Safety Authority STUK and the CTX algorithm developed by the authors simulating spiral and high resolution CT examinations considering angle resolutions of 1° and slice thicknesses of 1 mm. Fan beam bowtie filtration was formally taken into consideration.

Results: New conversion coefficients for dose reconstruction considering angle resolutions of 1° and slice thicknesses of 1 mm and different fan beam bowtie filtrations are presented for body CT of newborns, 1 and 5 year old children. It can be shown that, depending of slice position, spatially radiation dose distribution in high radiation risk organs and tissues can be significantly higher than described by the conversion coefficients published so far

Conclusion: After including real bowtie filter data, the new conversion coefficients presented here shall allow realistic reconstructions of radiation doses applied to children of any age group during high-resolution and spiral computer-tomographic examinations. The embedding of the factors in a commercially available computer program is planned.

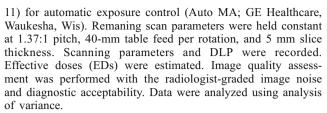
RS-4

Adaptive statistical iterative reconstruction technique of the children: radiation dose reduction of computed tomography

Hong Eo, So-Young Yoo, Ji Hye Kim, Tae Yeon Jeon Samaung Medical Center, Seoul (South Korea)

Purpose: To assess radiation dose reduction and image quality for computed tomography (CT) using adaptive statistical iterative reconstruction (ASIR) technique in the children

Materials and methods: The institutional review boards approved this study and waived the requirement for informed consent. From December, 2009 to February, 2010, chest and abdomen CT examinations were performed using ASIR in 78 patients (42 girls, 36 boys; mean ages: 6.4±2.8 yrs) with the CT examinations not using ASIR within 1 year on the same 64-slice multidetector CT (Lightspeed VCT, GE Healthcare, Waukesha, Wis). CT was performed with weighted-based adjustment of kilovolt (peak) (Chest CT with 80 kVp at 20 kg or less; 100 kVp at 21 kg or more, Abdomen CT with 80kVp at 10 kg or less; 100 kVp at 11 kg to 40 kg; 120 kVp at 40 kg or more) and noise indices (Chest CT: 12, Abdomen CT:



Results: Compared with non-ASIR, ASIR was associated with an overall mean (SD) decrease of 44% in ED (ASIR, 0.63 (0.29) mSv; non-ASIR, 1.12 (0.42); P<0.001). With the use of ASIR, the ED values were 0.79 (0.38) mSv (38% decrease), 0.42 (0.10) mSv (53% decrease) for the chest and abdomen CT, respectively, compared with 1.28 (0.53) mSv, 0.93 (0.24) mSv with non-ASIR (P<0.001). Despite dose reduction, there was no decrease of the image quality.

Conclusion: Significant radiation dose reduction and diagnostically acceptable image are achieved in the CT using ASIR technique in the children.

RS-5

Clinical validation of optimized mutidetector computed tomography (MDCT) paediatric abdomen protocols with iterative reconstruction: radiation dose and image quality assessment

Antonio Ciccarone¹, Philippe Coulon², Marco Esposito³, Silvia Mazzocchi³, Giovanna Zatelli³, Claudio Fonda¹ Meyer's Children University Hospital, Florence (Italy) ²Philips Healthcare, (United States), ³Florence Healthcare

Purpose: Optimization of X-ray dose in paediatric CT is a major concern due to children sensitivity to radiation. The purpose of our study is to assess the image quality and radiation dose of new MDCT paediatric abdomen protocols with an automatic mAs selection (DoseRight), dose modulation and a innovative iterative reconstruction technique iDose4 (Philips Healthcare), and to compare with our previous protocols with mAs adjusted according to a table based on patient weight and size resulting from an internal phantom study.

Materials and methods: 50 consecutive paediatric abdomen CT without contrast injection and 50 with contrast injection acquired on a 64 MDCT scanner (Brilliance 64, Philips Healthcare) with the new protocols and reconstructed with iDose4, were mixed with 100 paediatric abdomen CT (50 without and 50 with contrast) extracted from our picture archiving and communications systems (PACS), acquired with the previous protocols and reconstructed with a conventional Filtered Back Projection (FBP) method, for a blind reading. For each dataset, 2 experienced radiologists graded the perceived image noise, low contrast separation between muscle and fat, small structures visibility and diagnostic confidence. Objective noise measurements were also performed in the liver and muscles. Aligned rank and Wilcoxon's signed rank tests were used for statistical analysis.

Results: A reduction in average CTDI of 30% has been reached in our new scanning protocols with automatic mAs selection, dose modulation and iterative reconstruction as compared to our previous protocols with FBP, without any significant reduction of the detection in low-visibility structures like fat, muscle, liver, small vessels or diagnostic confidence.

Conclusion: An Automatic Exposure Control technique optimized for paediatric CT combined with new iterative reconstruction techniques can significantly reduce the radiation dose to children compared to already optimized low dose protocols based on patient weight and size mAs selection and FBP without compromise on image quality and diagnostic confidence.



RS-6

Automatic exposure control in pediatric CT—does it really work? Erich Sorantin, Dennis Boysen

Medical University Graz (Austria)

Background: Children are considerable more sensitive to radiation than adults. Besides cardiac catherization, Computed Tomography (CT) represents one of the most widely used and dose burdened type of examination in children. Several possibilities for dose reduction exists, automated exposure control (AEC) being one of many.

Purpose: Efficiency assessment of AEC in CT examinations of traumatized children.

Materials and methods: CT examinations in 52 pediatric trauma patients (mean age 13.4+-4.2y). All patients were investigated by a AquilionOne (Toshiba Medical Systems Inc.). AEC z-modulation with fixed noise values were used, all other parameters were kept constant. Patients demographic data, including, age (as a marker of body composition) weight, height, body mass index (BMI), type of examination (head-cervical, chest, abdomen-pelvis), scan length for every individual organ region as well as the corresponding dose length products (DLP) and Computed Tomography Dose Index (CTDIv) were stored in the database. Finally the DLP and the CTDIv was compared to BMI and age by regression analysis and both factors were combined in an multiple regression model.

Results: The 54 ct examinations consisted the following regions head-neck: 14, thorax: 19, abdomen-pelvis: 19. Therefore only the regions head-neck, thorax and abdomen-pelvis were used for analysis. Regression analysis yielded no statistical correlation between DLP and CTDIv with BMI and age for head-neck even in a combined model. For thorax an R2 of 0.643 (p<<0.0001) was found for BMI, and for age a R^2 of 0.566 (p<0.00012), respectively. The corresponding values for CTDIv were R² of 0.69 (p<<0.00001) for BMI and R² of 0.611 (p<<0.0001) for age. Using a combined model of BMI and age for DLP and CTDIv only BMI reached statistical significance for both variables but R2 squared increased only minimally. Analysis of the abdomen-pelvis values yielded same results: R² of 0.79 (p<<0.0001) for BMI versus DLP, R² of 0.524 (p<0.00028) for DLP versus age, R² of 0.68 (p<0.0001) for BMI vs CTDIv and R² of 0.547 (p<0.00018) for CTDIv versus age. Using a combined model of age and BMI there was only a minimal change of R2 in DLP and CTDIv.

Conclusion: Automated exposure control is statistically significant dependent on BMI for chest, abdomen-pelvis - as can be expected. But the BMI effect accounts only for about 2/3 of all effects. Combining with age does not increase the correlation. Of all CT imaging protocols using Z-modulation, which rely on simple data like weight, height and BMI, maybe only 2/3 meet the target. More reseach will be done using other available AEC systems (XY-Modulation, 4D-Modulation) but more importantly, the interaction between children's growth and dose requirements need further study.

RS-7

Combining organ-based dose modulation technology and innovative dosimetry: refining our ability to practically estimate patient- and age-specific cancer risk in children from chest mutidetector computed tomography (MDCT)

Brett Bartz¹, Donald P. Frush¹, Terry T. Yoshizumi¹, Ehsan Samei¹, Xiang Li¹, Greta Toncheva¹, Lynne Hurwitz¹, William Paul Segars¹, Xiaodong Zhou²

¹Duke University Medical Center, Durham, ²Siemens (United States)

Purpose: To assess the effect of new organ-based dose modulation (OBDM: mA reduced in a 1200 arc over anterior structures such

as breasts with posteriorly increased mA) on effective dose (ED), organ dose, and age and gender specific total cancer risk estimates in pediatric chest MDCT.

Materials and methods: (1) MOSFET dosimetry data were obtained in a 5-yr-old anthropomorphic phantom for 64-slice MDCT (120 kVp, 47 effmAs, 64×0.6, 0.6 pitch) with OBDM (Siemens X-CARE) on and off. Doses averaged in 20 organs were used for ED estimation (ICRP 103). (2) A validated Monte Carlo MDCT dose study determined correlative relationships between organ dose and chest diameters. Organ doses for a 15.4 cm chest diameter equivalent to the 5-yr phantom were used to calculate ED and to estimate the total cancer risk (lifetime attributable risks: cancer incidence/10,000 exposed males and females; BEIR VII). The Monte Carlo-predicted breast, esophageal and lung doses were modified by applying the% dose changes from OBDM MOSFET on vs off for these same organs and effect on total cancer risk determined.

Results: MOSFET ED (mSv) was 3.0 OBDM on and 3.2 OBDM off, similar to Monte Carlo (3.1). Monte Carlo organ doses closely agreed (differed by 7.2% for breast, 17.7% for esophagus, and 0.7% lung) with MOSFET. Using OBDM, MOSFET data demonstrated that dose decreased 12% in the breast, increased 2% in the esophagus, and decreased 5% in the lung. Using these% changes, Monte Carlo simulation-predicted total cancer risk was lower for a 5-yr-old girl with OBDM on (12.3 cases) versus OBDM off (13.0) but similar for a 5-yr-old boy with OBDM on (4.3) and off (4.4). Conclusion: Phantom and MOSFET provide for system- atic evaluation of new OBDM technology, and MOSFET agrees with Monte Carlo. Use of OBDM decreased breast dose without changing ED. Based on this investigation, there was a decrease in total cancer risk using OBDM for a 5-yr-old girl not seen in boys. Combining MOSFET dose data with Monte Carlo simulation can provide gender and age specific total cancer risk unavailable with dose measurement changes alone and may guide clinical use of dose reduction strategies for pediatric CT.

RS-8

Comparison of radiation dose estimates and scan performance time in pediatric head and neck imaging using volumetric 320-row detector CT and helical 64

John Egelhoff¹, Alan Brody¹, Daniel Podberesky¹, Terry Yoshizumi², Erin Angel³, Greta Toncheva², Colin Anderson-Evans², A Barelli³, Chris Alsip¹, Sheila Salisbury¹, Donald Frush²
¹Cincinnati Children's Hospital Medical Center, Cincinnati, ²Duke Medical Center, ³Toshiba Medical Systems (United States)

Purpose: Determine and compare effective radiation dose (ED) estimates and scan time for pediatric temporal bone, orbit, and sinus exams using volume acquisition mode on a 320-row MDCT scanner and helical acquisition mode on a 64 row MDCT scanner. Materials and methods: Using a 5 year-old pediatric anthropomorphic phantom organ doses were measured using twenty metal oxide semiconductor field effect transistors (MOSFET) dosimeters for volumetric temporal bone, orbit, and sinus exams on a 320 MDCT scanner and compared to helically acquired exams on a 64 row MDCT scanner using clinical pediatric acquisition parameters. Three scans for each protocol were averaged to calculate a mean ED using a weighted average of measured absorbed organ doses (ICRP 103). Computed tomography dose index (CTDI)/dose length produuct (DLP) values and scan times were recorded. Image quality was not directly evaluated. The protocols are used clinically and image quality was considered diagnostic by a consistent group of pediatric radiologists.

Results: ED for volumetric studies (320 row) MDCT compared to helical studies (64 row) MDCT are: temporal bone - 0.17 mSv vs



0.44 mSv; orbit - 0.41 mSv vs 2.24 mSv; sinus - 0.20 mSv vs 1.09 mSv. Use of volume acquisition on a 320 row MDCT resulted in decrease in ED of 60.8%, 81.8%, and 80.6% (average 74.4%) respectively for temporal bone, orbit, and sinus studies compared to 64 row MDCT. CTDI and DLP values were consistently lower on the 320 row MDCT. Scan time was 0.5 sec (volume) vs 3.33 sec (helical). Conclusion: The combination of MOSFET and anthropomorphic phantoms provides an opportunity to study dose changes with new CT technology in the pediatric age group. Using clinical pediatric acquisition parameters, volumetric temporal bone, orbit, and sinus studies on a 320 row MDCT scanner resulted in a substantial decrease in effective dose (2.6 - 5.5 fold) compared to helically acquired studies on a 64 row MDCT scanner. Reduced scan time with volumetric studies may decrease motion artifact and the need for sedation.

RS-9

Bismuth shielding and automatic tube current modulation during pediatric head CT

Maria Raissaki, Antonis Papadakis, Kostas Perisinakis, John Damilakis

University Hospital of Heraklion, Heraklion (Greece)

Background: Automatic tube current modulation (ATCM) reduces dose during pediatric CT. Bismuth shielding reduces low-energy photons; this effect cannot be equivalently achieved by reducing tube current alone. ATCM combined with bismuth shielding during pediatric head CT and its effect on tube current and image quality have not been investigated.

Purpose: To study the effect of orbital bismuth shielding combined with ATCM on tube current and image noise.

Materials and methods: Four anthropomorphic phantoms (ATOM phantoms, CIRS Inc., Norfolk), representing the average head of newborn, 1, 5, and 10-year-old were scanned on a Siemens Somatom Sensation 16 scanner a) with fixed tube current b) with ATCM c) with ATCM and a shield on orbits before scout acquisition and d) with ATCM and a shield on orbits after scout acquisition. Noise was measured in Hounsfield units (HU)by drawing 0.5 cm3 regions of interest (ROIs) in homogeneous-appearing areas at both orbits, temporal, frontal and parietal lobes for each scan. Results: CDTIs were 20.21 mGy/100mAs in all scans. DLPs were

303, 430, 485 and 515 mGy x cm for the neonate, 1, 5 and 10-year equivalent, respectively. Tube current was 110 mA when fixed and 59–87 mA (mean 74.56) with ATCM. Current reduction over the eyes was 5–43.5% (mean 22.5%) and overall 20.9–46.4% (mean 32.2) with the neonate-equivalent scans benefiting the most from ATCM. Current over the eyes was 62–100 mA (mean 83.2) and 63–104.5 mA (mean 86.1) when ATCM was combined with bismuth shield placement before and after the scout acquisition, respectively. Mean orbital values were 34.44 HU without shields and 43.73 HU with shields. Mean brain values were 27 in the neonate (24.8 without, 28.5 with shields) and 46.54 in other age phantoms (46.4 without, 46.6 with shields).

Conclusion: ATCM is a requisite during pediatric head CT. Tube current is not affected by bismuth shield placement. Shields cause increase in image density over the eyes especially in neonates, irrespectively of fixed or reduced current. Brain density is minimally affected by shield placement.

RS-10

Breast dose reduction utilizing breast shield in pediatric cardiac gated and non-gated CT angiography

Beverley Newman¹, Juan Plata², Arundhuti Ganguly², Frandics Chan¹Lucile Packard Children's Hospital, Stanford, ²Stanford University, Stanford (United States)



Purpose: CT angiography (CTA) of the chest incurs the highest organ dose to the breasts. Childhood exposure increases the cumulative risk of developing breast cancer later in life. We examine the effectiveness of breast shield in reducing radiation exposure to the breasts during non-gated CTA and cardiac gated CTA studies in children.

Materials and methods: A tissue-equivalent anthropomorphic phantom (Model 705D, CIRS) was used to simulate a 5-year old child. Five MOSFET detectors were imbedded to measure radiation dose at the breasts, heart, liver, and thyroid gland. The phantom was scanned in a 64-slice multi-detector row CT scanner (Definition, Siemens) using non-gated CTA and retrospectively electrocardiography (ECG)-gated CTA protocols, at 80 and 100 kVp, and with and without a breast shield (AttenuRad, F&L Medical Products) in place. Each scan was repeated. The breast shield was deployed after the scout view to prevent the automatic tube current software (CareDose4D, Siemens) from adjusting for the breast shield attenuation. Shielded and non-shielded radiation doses were compared for statistical significance using Student t-test.

Results: For all ECG-gated protocols and the non-gated protocol at 100 kVp, the breast shield achieved a statistically significant (p< 0.004) reduction of breast dose by an average of 25%. For the non-gated protocol at 80 kVp, there was a 10% reduction that was not statistically significant (p=0.13). For other organs, the change in average organ dose ranges from -13% to +11%, none statistically significant. Without breast shield, a drop in tube voltage from 100 to 80 kVp reduces breast dose by 44% for gated study and 49% for non-gated study. A change from gated to non-gated study lowers the breast dose by 60% for 100 kVp and 63% for 80 kVp.

Conclusion: Breast shield reduces breast dose by 25% in pediatric non-gated and retrospectively ECG-gated CTA studies while having little impact on other organs. Decrease in tube voltage and conversion to non-gated scan achieve greater dose reduction and remain important dose reduction techniques.

RS-11

Radiation doses from CT-guided abdominal and pelvic interventional procedures in children at a tertiary care general hospital: Is there opportunity for improvement?

Shauna Duigenan, Shauna Duigenan, Debra Gervais, Bob Liu, Xinhua Li, Mueller Peter

Massachusetts General Hospital, Boston (United States)

Purpose: Given the currently accepted linear non-threshold model for radiation-induced cancer, radiation doses in children are under intense scrutiny. The purpose of our study is to review historic radiation doses from CT guided abdominal and pelvic procedures in children in a single tertiary care general hospital setting and to compare to historic radiation doses from the adult literature on similar procedures.

Materials and methods: All patients up to 18 years of age who underwent a CT guided abdominal or pelvic interventional procedure from 1995 to 2010 were retrospectively identified from an institutional interventional radiology database. Medical records and images were retrospectively reviewed with IRB permission. Data collected included, dose length product (DLP) and scanning parameters such as kVP, mA, pitch, gantry rotation time, length of scan, slice thickness, and total number of slices. For studies lacking dose reports, DLP was calculated from scan data and converted to effective dose using published pediatric DLP to effective dose conversion coefficients. Mean values of effective dose for this cohort was compared to literature values obtained for cohorts of adult patients who underwent similar interventional procedures.

Results: Data were obtained for 43 CT guided abdominal or pelvic interventional procedures performed in children from 1995 to 2010. Mean effective dose dose was 13 mSv with an interquartile range of 5.5 to 13.8 mSv and total range of 1.4 to 94 mSv. This is compared to values in the literature for adult CT guided cases [mean of 18 mSv and ranges of 10.9 to 31.5 mSv]. Only 5 cases employed tube current modulation to reduce dose.

Conclusion: In a tertiary general hospital setting, historic radiation doses for CT guided abdominal and pelvic interventional procedures in children vary widely and mean radiation doses in children have approached those for adult patients. Comparable historic radiation doses in children and adults for CT guided procedures at a tertiary care general hospital provides a baseline and impetus for implementation of dosereduction strategies.

RS-12

Comparing radiation dose from 3D O-arm imaging (3D-Oarm) with that of traditional CT and 2D imaging

Xiaowei Zhu¹, Marc Felice²

¹The Children's Hospital of Phialdelphia, 34th and Civic Center Blvd., Philadelphia, ²University of Pennsylvania (United States)

Purpose: Portable fluoroscopic imaging systems with CT-like imaging capabilities enable the orthopedic surgeon to confirm the precision of surgical procedures without transferring patients out of the operating room (OR) for conventional CT imaging. However, it is important to ascertain the radiation dose consequence of this practice. This study compares the radiation dose from 3D O-arm imaging (3D-Oarm) in the OR suite with that of traditional CT and 2D imaging.

Materials and methods: 2D and 3D scans were performed utilizing an O-arm with a multidimensional surgical imaging platform on a 5-y old anthropomorphic phantom. Scans were performed of cervical(C), thoracic(T), and lumbar(L) spines in 2D and 3D modes. The CTDIw was measured on the anthropomorphic phantom for the 3D scans on the O-arm, and on a traditional CT scanner utilizing clinical scan protocols. Entrance Skin Exposure Rates from 2D fluoroscopic studies were also measured. The effective radiation dose was evaluated with PCXMC software and compared for the 2D, 3D and CT studies. Results Utilizing the routine clinical settings during our phantom studies, we determined that the effective doses from one-minute of 2D-Oarm, a 3D-Oarm image, and a conventional CT of the C-spine are 1.1 mSv, 2.9 mSv and 1.6 mSv; while those of the T-spine are 0.3 mSv, 7.4 mSv and 6.1 mSv; and of the L-spine are 1.1 mSv, 6.0 mSv, 10.9 mSv, respectively.

Conclusion: The Effective Dose from 3D-Oarm studies are 20% to 70% higher than traditional CT for C- and T-spine studies, and 40% lower for L-spine. The dose from a single 3D-Oarm study is equivalent to 2.5 to 25 min of 2D-Oarm fluoroscopy, depending of the anatomical region. It was also observed that 2D-Oarm fluoroscopy provides higher doses than conventional C-arm fluoroscopy, since only a fixed 30 pulse per second mode is available. This phantom study provided practical dose references to clinicians regarding 2D and 3D imaging modalities for orthopedic surgery and dose comparison with traditional CT.

RS-13

Quantitative assessment of overexposure in pediatric digital chest radiographs based on European guidelines

Argiend Imeri, Erich Sorantin, Sabine Weissensteiner Medical University Graz, Austria *Purpose:* Quantitative Assessment of Overexposure in pediatric digital chest x-rays based on "European Guidelines on Quality Criteria for Diagnostic Radiograpic Images in Pediatrics".

Materials and methods: 89 pediatric chest x-rays (age 5.63± 5.3 y, range from 0.08 to 17.9 y) were selected randomly in the x-ray unit and reseted to unprocessed state. On these images the following rectangles were drawn by digital image processing: the minimal exposed area (MEA), the area above and below MEA in full width of the unexposed image, as well as on both lateral sides between the upper and lower area. According to the guidelines 2.0 cm above and below the MEA was accepted. Afterwards all areas were expressed as percentages of MEA in order to normalize them and all results refer to this normalization. It must be taken into account that the rectangles above MEA and on the lateral side do not reflect the overexposed body surface area, as the body surface represents only part of that are. This is particularly important for the rectangle above MEA (cervical region). The normalized rectangle represents an indicator of overexposure. For image processing and statistical analysis the following open source software: ImageJ (http://rsbweb.nih.gov/ij/) and R-Project (http:// www.r-project.org/)

Results: Overall overexposure was $42\pm18.9\%$ of MEA, individual analysis yielded the following results: rectangle above MEA (cervical region) $15.6\pm13.9\%$, rectangle below MEA (upper abdomen) $14.3\pm10.5\%$, right lateral rectangle $6.5\pm4.9\%$ and left rectangle $7.5\pm4.6\%$. There was trend that overexposer decreased with age.

Conclusion: Improper use of the shutter results in overexposure and degrades image quality. An electronic shutter allows radiographers to fine tune the image. Even in a dedicated pediatric division, overexposure can happen in about 40% of cases, this figure could be even higher in units not dealing with children on a daily basis. The trend to reduce by age reflects the complexity of estimating the correct anatomic landmarks for exposure. The proposed method is easy to perform and can be used as a quality assurance tool.

RS-14

Assessment of pediatric radiation exposure during ureteroscopy *Jeanne Chow*, Paul Kokorowski, Keith Strauss, Melanie Pennison, Caleb Nelson

Children's Hospital Boston, Boston, (United States)

Purpose: The "as low as reasonably achievable" (ALARA) principle requires efforts to minimize exposure to the patient. Little is known about radiation exposure during urologic procedures in children, including ureteroscopy (URS) for urolithiasis. Our goal is to measure radiation exposure during pediatric URS and identify opportunities for improvement.

Materials and methods: We performed a prospective direct observation of URS as part of a quality improvement initiative. Pre-operative patient characteristics, operative factors, fluoroscopy settings and radiation exposure were recorded. Primary outcomes were total fluoroscopy time (min) and patient skin entrance dose (SED, mGy). Specific modifiable factors were identified as targets for quality improvement. Univariate tests of association were used to identify specific patient and operative factors associated with primary outcomes.

Results: Direct observation was performed on 48 consecutive URS procedures at a single hospital. 34 procedures were included in our analysis, excluding 2 procedures for arteriovenous malformations, 1 terminated procedure, and 11 adults (≥21 years of age). Median patient age was 16.5 years (range 7.4–19.2). 21% of procedures resulted in failure to treat a stone due to spontaneous passage or difficult access. Median total



fluoroscopy time was 2.85 min (range 0.4–6.7) and median SED was 42.7 mGy (range 2.23–223.4). There was considerable variability across multiple examined factors and thus no single factor was significantly associated with fluoroscopy time and only source to skin distance (SSD) was associated with skin entrance dose (p=0.02). However, several other modifiable factors (eg. fluoroscopic image rate and field of view) are opportunities for dose reduction.

Conclusion: Pediatric patients receive considerable radiation exposure during ureteroscopic procedures. Multiple potential methods for potential radiation reduction were identified and future efforts will focus on implementing dose reduction strategies consistent with the ALARA principle.

RS-R1

Pediatric mutidetector computed tomography (MDCT) of the abdomen: evaluation of image quality with automated tube modulation for dose reduction

Zebedin Doris, Barbara Oberdabernig, Katrin Dorr, Erich Sorantin, Michael Riccabona

University Hospital of Radiology, Graz, (Austria)

Purpose: To evaluate image quality and diagnostic confidence in pediatric abdominal MDCT by using a z-axis modulation technique and age-adapted CT settings (reference tube current,

standard deviation = SD) with adopted reconstruction algorithms to reduce radiation dose while maintaining constant image quality. Materials and methods: 50 children aged 2 to 17 years (22 girls, 28 boys) were referred for abdominal CT. Indications were acute abdominal pain with unclear abdominal ultrasound findings. CTs were performed on a Aquilion One (TMSE Inc) scanner applying a z-axis modulation technique. In all protocols age-adapted settings for mA and kV ranged from 50 to 90 and 80-120, respectively. Rotation time was fixed to 0.5 sek. In 15 patients a SD of 10, in 10 children of 20 and in the remaining 25patients a SD of 15 was used. All CT settings including dose (CTDIvol) were recorded on a summary sheet. All studies were assessed using a three point scale from excellent image quality (no artifacts, clear delineation of organ borders and pathology), fair image quality (acceptable artifacts, organs contours and pathology acceptable depicted) to non-diagnostic image quality.

Results: 24 abdominal CTs had excellent image quality, 26 cases a fair image quality, and no CT was non-diagnostic. Reconstructed slice thickness varied from 3 to 5 mm – consecutively the CTDIvol decreased from 10.82 to 7.14 mGy (reduction of 34%) for a SD range of 10–15, from 7.14 to 5.12 mGy (28%) for a SD range of 15–20.

Conclusion: Dose reduction of around 30% can be achieved in abdominal pediatric CT by using automated tube modulation in combination with dedicated post-processing methods without significant loss of image quality or diagnostic confidence.

